COMBINED HEAT AND MOISTURE TRANSFER IN BUILDING CONSTRUCTIONS

Carsten Rode Pedersen

Thermal Insulation Laboratory
Technical University of Denmark

Report no. 214, September 1990

COMBINED HEAT AND MOISTURE TRANSFER IN BUILDING CONSTRUCTIONS

Carsten Rode Pedersen

Thermal Insulation Laboratory
Technical University of Denmark

PREFACE

This report forms the main documentation of the work conducted in my study for the Danish Ph.D. degree "Licentiatus Technices" at the Thermal Insulation Laboratory of the Technical University of Denmark. Several reports in Danish on separate subjects and international papers have led to this concluding presentation.

February 28, 1990   Carsten Rode Pedersen

Minor changes and corrections have been added in the second edition when the thesis was prepared for print.

September, 1990   Carsten Rode Pedersen

CONTENTS

SUMMARY

The report is divided into three chapters.

The first chapter summarizes the theory for combined heat and moisture transport needed for calculations of the hygrothermal behavior of composite building constructions. The description of the theory takes advantage of the similarities between the governing equations for transient transfer of heat, vapor and liquid moisture.

A computer program, MATCH – Moisture and Temperature Calculations for Constructions of Hygroscopic Materials, has been developed on the basis of this theory. The second chapter describes the algorithms in the computer program. The numerical procedures are described to the extent they differ from regular schemes for finite difference techniques. A special procedure called "Alternating Parameters Implicit method" (API) was used to handle the coupled equations efficiently.

MATCH is a 1–dimensional model that accounts for moisture transport by vapor diffusion and liquid suction. The moisture retention properties have also been accounted for. The program runs on a PC and an attempt has been made to make the user interface easily accessible by supplying a small preprocessor and by presenting results graphically as the calculations proceed. The intention is that MATCH and similar models should one day be regular items in the toolbox of the building designer.

The third chapter deals with applications of the model. One application, mostly of theoretical interest, takes advantage of the ability of the numerical model, in an empirical way, to account for the hysteresis in the sorption and suction curves for the materials. It turns out that the accurate description of hysteresis is without important effect on the results for constructions exposed to a naturally varying climate.

Another research oriented application is the simulation of drying experiments

performed in the laboratory on initially vacuum saturated specimens of aerated concrete. The ability of the model to predict moisture distributions accurately was verified for moisture contents in and above the hygroscopic region.

More practical applications are given in the last two sections of the third chapter. Various problems with diffusive moisture intrusion into the cavity of flat roofs are analyzed after it has been concluded that ventilation of air spaces in the roof cavity should be avoided. A special kind of vapor retarder, the Hygro Diode, is described and calculations show how it may help preventing moisture problems. A few calculations were done to investigate the problem of moisture accumulation due to vapor diffusion through EPDM roofing membranes in hot, humid climates. These calculations did not indicate that such accumulation takes place.

The modes of heat transfer in wet, permeable insulation are discussed in the last section. Analyses concentrate on the effect of the release or uptake of enthalpy when the moisture changes phase. The latent heat transfer may, for shorter periods, contribute to the total heat transfer by the same amount as the heat conducted through the insulation. In a southern climate, the annual sum of inwards heat flow was increased by as much as 40%.

RESUME

Rapporten er inddelt i tre kapitler.

I det første kapitel gennemgås kortfattet den nødvendige teori for beregning af koblet fugt– og varmetransport for sammensatte bygningskonstruktioner. I beskrivelsen af teorien er der gjort nytte af den analoge måde hvorpå ligningerne for instationær transport af varme, damp og væske kan opstilles.

Et EDB–program, MATCH – Moisture and Temperature Calculations for Constructions of Hygroscopic Materials (Beregning af fugt– og varmetransport i konstruktioner af hygroskopiske materialer), er blevet udviklet med anvendelse af den beskrevne teori. Det andet kapitel beskriver algoritmer i EDB–programmet. Beskrivelsen omfatter også numeriske procedurer i det omfang disse adskiller sig fra gængse fremgangsmåder ved endelige differensers metode. En sådan speciel procedure, kaldet "API" (Alternerende parametres implicitte metode), er brugt, der effektivt håndterer de koblede transportligninger.

MATCH er en 1–dimensional model, der regner fugttransport under hensyntagen til såvel damp– som væsketransport. Der er også taget hensyn til materialernes evne til at akkumulere fugt. Programmet, der kører på en PC, er udviklet med henblik på at opnå høj grad af brugervenlighed. Der hører således et lille program til, der hjælper opstillingen af input til modellen, ligesom hovedresultaterne præsenteres grafisk under beregningsforløbet. Intentionen med MATCH er at den og lignende modeller skal blive daglige værktøjer for den projekterende af bygninger og bygningskonstruktioner.

Det tredie kapitel viser en række anvendelser af modellen. En sådan anvendelse, der mest har teoretisk interesse, udnytter modellens mulighed for, på en empirisk måde, at tage hensyn til hysteresen i materialernes sorptions– og suctionkurver. Det viser sig, at den nøjagtige beskrivelse af hysteresen ikke har nogen stor betydning, når der regnes på konstruktioner, der udsættes for et naturligt varierende klima.

En anden forskningsorienteret anvendelse af modellen er simuleringen af et udtørringseksperiment, der er udført i laboratoriet på en til start vaccuum-vandmættet prøve af gasbeton. Modellens evne til nøjagtigt at forudsige fugtfordelinger blev verificeret for fugtindhold såvel i som over det hygroskopiske område.

Mere praktiske anvendelser af modellen er gjort i de sidste to afsnit af det tredie kapitel. En række problemer med diffusive indtrængniner af fugt i hulrummet af et fladt tag analyseres, efter det er konkluderet, at hulrummet ikke bør ventileres. En nyudviklet type dampspærre, Hygrodioden, beskrives, og i beregninger vises hvorledes, den er i stand til at afhjælpe fugtproblemer i flade tage. Nogle få beregninger analyserer en problemstilling med fugtophobning på grund af dampdiffusion gennem tagmembraner af EPDM–gummi i varme, fugtige klimaer. Disse beregninger indikerer ikke at en sådan ophobning skulle finde sted.

Sidste afsnit behandler de forskellige måder, hvorpå varmen transporteres i våde, permeable isoleringsmaterialer. Analysen koncentrerer sig om betydningen af entalpioverførsler når fugten undergår faseændringer. Transporten af sådan latent varme kan i visse tilfælde være af samme størelsesorden som den varme, der transporteres ved ledning (inklusiv stråling og konvektion) i isoleringsmaterialet. For et sydligt klima vises, at den årlige sum af indadrettet varmetransport kan blive forøget med op til 40% på grund af den latente varme.

NOMENCLATURE

A	Area	m^2
c_p	Specific heat capacity	J/kg K
D_Θ	Moisture diffusivity	m^2/s
E	Irradiance	W/m^2
g	Moisture flux	kg/m^2 s
g	Acceleration of gravity	m/s^2
h	Heat transfer coefficient	W/m^2 K
h	Mass specific enthalpy	J/kg
h	Room height	m
I	Source of moisture by phase change	kg/m^3 s
K	Hydraulic conductivity	kg/Pa m s
k	Thermal conductivity	W/m K
m	Mass	kg
P	Pressure	Pa
p	Partial water vapor pressure	Pa
q	Heat flux	W/m^2
R	Gas constant	J/kg K
R	Thermal resistance	m^2 K/W
S	Source of moisture	kg/m^3 s
S_q	Source of enthalpy	W/m^3
T	Temperature	K
t	Time	s
u	Moisture content	kg/kg
x	General 1–dimensional space coordinate	m
z	Vertical coordinate	m
z	Vapor resistance	Pa m^2 s/kg
α	Absorptance	—
β_p	Mass transfer coefficient	kg/m^2 s Pa
δ_p	Water vapor permeability	kg/Pa m s
ϵ	Emissivity	—
θ	Surface tilt angle	0
Ξ	Moisture capacity in the suction diagram	kg/kg Pa
ξ	Moisture capacity in the sorption diagram	kg/kg
ρ	Density	kg/m^3
σ_r	Stefan–Boltzmann constant	W/m^2 K^4
φ	Relative humidity (RH)	—

INDICES:

a	Absorption
a	Air
c	Convection
cap	Capillary saturation
cr	Critical (moisture content)
d	Desorption
h	Hydraulic (pressure compared to one atmosphere)

hys	Hysteresis
i	Phase of moisture (= ice, liquid water or vapor)
liq	Liquid
p	With vapor pressure as potential
p	Isobaric
r	Radiation
s	Saturation
suc	Suction (negative pressure)
t	Temperature
vac	Vacuum saturation
v	Vapor
w	Water
0	Dry
98	Maximum hygroscopic

NUMERICAL HELPING FUNCTIONS AND VARIABLES:

A	Variable in analytical expression for sorption isotherm
A_{des}	Variable in analytical expression for suction curve
A_{dry}	Variable in analytical expression for suction curve
A_{ipt}	Variable in analytical expression for suction curve
A_k	Variable in expression for hydraulic conductivity
A_{wet}	Variable in analytical expression for suction curve
B_{des}	Variable in analytical expression for suction curve
B_{dry}	Variable in analytical expression for suction curve
B_{ipt}	Variable in analytical expression for suction curve
B_k	Variable in expression for hydraulic conductivity
B_{wet}	Variable in analytical expression for suction curve
exp	Variable in analytical expression for suction curve
f	Displacement factor of node
f_k	Moisture and temperature coefficients for the thermal conductivity
h	Heat transfer function
h0	Transfer function for heat storage
hz	Vapor transfer function
hz0	Transfer function for vapor storing capacity
hzliq	Liquid transfer function
hzliq0	Transfer function for liquid storing capacity
i	Node number
lnP	Natural logarithm of suction pressure
lnP_0	Variable in analytical expression for suction curve
n	Variable in analytical expression for sorption isotherm
Rx	Thermal resistance between layers
u_h	Variable in analytical expression for sorption isotherm
u_0	Variable in analytical expression for suction curve
zliq	Hydraulic resistance
zx	Vapor resistance between layers
zxliq	Liquid resistance between layers

INTRODUCTION

Keeping building constructions dry is a problem that extends over practically all kinds of climates. Human activities and comfort requirements will almost always expose constructions to gradients in temperature and moisture concentration. The energy crises of the seventies and the following requirements for higher insulation standards may have accelerated some of the processes that lead to condensation.

The implications of such condensation are damage to the constructions such as decay of wood, corrosion of metals, degradation of binders and adhesives, swelling of materials, reduced frost resistance, etc. The list is endless, as moisture is a catalyst in most of the processes that make materials disintegrate. Wet, or even humid, constructions have a noticeably larger heat loss than they would have had if they were dry. Aspects of human health in humid, mold tormented indoor climates further add to the list of harm done by moisture in building constructions.

The concern for the environment is increasing these years. It may therefore be worth mentioning the harmful effects seen when the construction materials are not cherished the way they should be. The energy aspects of increased heat loss throughout the lifetime of wet constructions have already been mentioned but the energy consumption involved in manufacture and handling of building materials will increase with decreasing lifetime. Other than energy related environmental aspects are those concerning the waste of raw materials and the eventual problems of deposition of the large volumes of scrapped materials. Such materials may not always go easily back into their original cycles of nature when they have been modified to fulfill the requirements as structural components.

Thus, even without mentioning the economic aspects, the reasons are numerous as to why building constructions should be kept dry. The final goal for research in the field is to develop building codes that accurately describe the necessary precautions against moisture build–up. Current Danish codes vaguely indicate that actions should be taken to avoid condensation and give a few practical examples of how this could be done. The basic physical background that would make it possible to extrapolate the precautions to include new types of

constructions and materials is not incorporated in the codes. The reason is that the means for calculating hygrothermal behavior have been limited so far, unlike the case when other requirements of constructions, such as structural durability, were designed for.

The most common way to calculate moisture distributions has been the one developed by Glaser, 1959. This method only accounts for diffusion as the transporting process and it assumes stationary conditions that practically never occur in real constructions. The easy access to microcomputers and their increasing speed make it possible to base improved dimensioning tools on such machines. Computer based tools may easily cope with other transport phenomena than diffusion and they will usually include a description of the moisture retention properties of materials. These properties cause time lags in the development of moisture distributions that are considerably larger than seen in the heat transfer.

Aspects of moisture transport that have not been studied in detail in this project are those of defining material parameters and of investigating the effects of convection in constructions of porous materials. Though models as the one developed in this project will improve on the existing means of moisture dimensioning it must be realized that such models are no better than the material parameters fed into them. An evaluation would also be necessary to determine if convection or multidimensional effects are important for each of the constructions being analyzed.

CHAPTER 1
MOISTURE PHYSICS

This chapter describes the most important laws involved in calculating migration of moisture as vapor and liquid water in porous materials. Moisture migration is a process that is dependent on the temperature distribution in the construction of investigation, and the basics of heat transfer are therefore also presented. The migration of heat is a phenomenon which in turn is dependent on both moisture content and flux. This interaction is taken into consideration as well. The theory of combined heat and mass transfer has been described in numerous textbooks, some of which are mentioned in this report. For a more thorough investigation of the details of this field, the reader is referred to these textbooks (for instance Luikov, 1966 and Krischer, 1978) and to an earlier report by this author (Pedersen, 1989a).

1.1 MIGRATION OF MOISTURE

The migration of moisture can roughly be divided up into two types of transfer which take place in the gaseous and in the liquid phase. It turns out that the laws describing the migration in each phase will look very similar. Describing and understanding the combined transfer of heat and moisture, however, is easier when the two moisture migration phenomena are dealt with separately. Transient calculation of moisture transfer requires knowledge of the moisture storing capabilities of the materials. This is described by the sorption and suction curves for vapor and liquid moisture, respectively. "Retention curves" is the general expression used to describe both of these curves.

1.1.1 RETENTION AND TRANSPORT OF VAPOR

SORPTION ISOTHERMS:

Porous materials have the capability of absorbing moisture from an environment of air that may seem dry to us human beings. This is mainly due to adsorption forces, with which the solid parts of the material, even at very low vapor pressures, attract molecules of vapor internally in the porous system, and due to the depression of vapor pressure over the curved menisci of the water filled capillaries. It has been verified experimentally that there is a close connection between the relative humidity of the surrounding air and the amount of moisture taken up by the material. The relative humidity is defined as the ratio between the actual vapor pressure and the vapor pressure when the air is saturated with vapor.

$$\varphi = \frac{p}{p_s} \qquad\qquad (1.1.1)$$

where

φ	=	Relative humidity (RH)	$(-, \%)$
p	=	Partial pressure of vapor	(Pa)
p_s	=	Partial vapor pressure at saturation	(Pa)

It is worthwhile mentioning that the saturation vapor pressure is a very rapidly increasing function of temperature. This is a fact that becomes crucial when moisture migration under thermal gradients is studied.

Moisture content of a material is often plotted versus the relative humidity of the surrounding air, as is shown by the typical S-shaped curves in figure 1.1. The symbol used here for moisture content is, "u", which designates the ratio of the weight of absorbed moisture compared with the dry weight of the material (kg/kg or weight-%). Such curves are called sorption curves, or more correctly sorption isotherms, since the moisture content is dependent on temperature. A higher temperature level results in a lower moisture content for the same relative humidity. Or, the relative humidity increases with increasing temperature if the moisture content is fixed. This effect is in agreement with the Le Chatelier principle and the fact that moisture adsorption is an exothermic process.
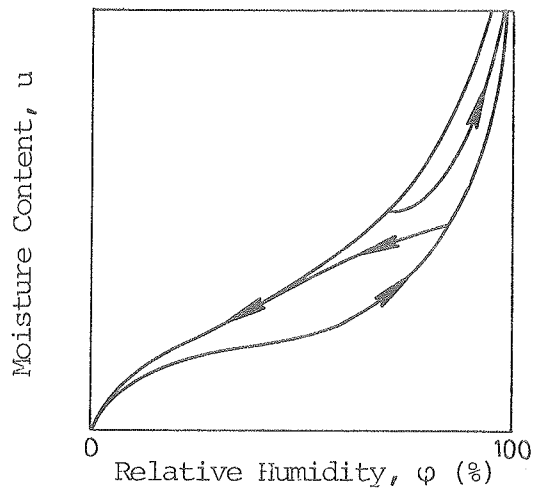
Figure 1.1   Sorption curves during absorption, desorption and scanning (Ahlgren, 1972).

Figure 1.1 actually shows two boundary curves within which all possible states are found at the actual temperature. The reason for this indefiniteness is that there is some hysteresis in the uptake and release of moisture in a porous material. A material, which comes from a wet environment, dries out following the upper curve. This process is called desorption. The lower curve, for absorption, is followed under wetting conditions. The intermediate scanning curves are followed under transition from one to the other of the boundary curves. It turns out that most states are found on such scanning curves for naturally acclimatized materials.

It is seen also from figure 1.1 that the slope of the curves becomes steeper as the relative humidity is approaching 100%. At RH–values close to this limit it is difficult to determine the corresponding moisture content unambiguously. Further, it is difficult to measure RH with accuracy at these levels. The sorption isotherms are therefore only considered valid descriptions of moisture retention up to the maximum hygroscopic moisture content which in most definitions corresponds to RH = 98%. Any moisture content lower than this is in the hygroscopic region. The reason for the steepness of the curve in the high RH region is that the large pores are being filled with water here. These pores may contain a large amount of water, but since the pore diameter here is considerable, the curvature of the menisci is relatively small and so is the depression of the vapor pressure, according to Kelvin's equation (Pedersen, 1989a). The result is a large moisture content when the relative humidity approaches 100%.

The moisture capacity is defined as the slope of the sorption isotherm. The larger

the capacity, or slope, the larger is the amount of moisture required to be absorbed or desorbed following a change of RH in the environment. The definition of moisture capacity, which is designated by the symbol ξ, is shown in figure 1.2.
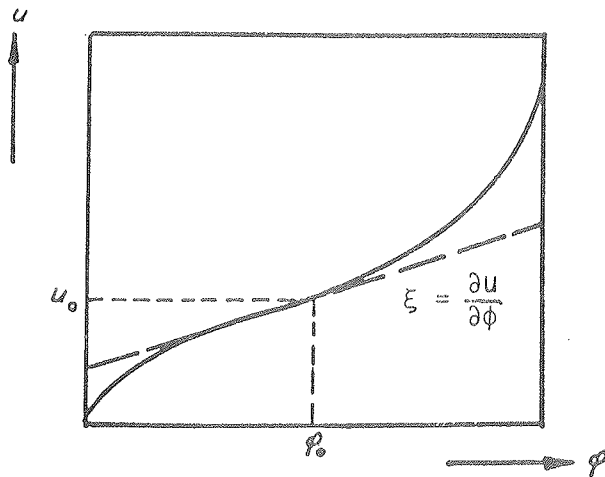

Figure 1.2   Moisture capacity is defined as the slope of the sorption curve (Lund—Hansen, 1967).

VAPOR MIGRATION:

Migration of vapor can be divided up into a convection and a diffusion process. The first one is perhaps the easiest to understand and explain. In this process, vapor is transported when air movements take place inside or through the construction. The flux of vapor equals the total flux of air multiplied by the concentration of vapor in the vapor/dry—air mixture. Though it is easy to understand, calculation of this process is quite complicated since it often involves multidimensional evaluation of air movements as a result of natural or forced convection. Convection through constructions is often caused by imperfections in air and vapor barriers that are not intended. Such imperfections are of course difficult to simulate quantitatively. Boundary conditions for convection air flow (air pressure around constructions) may also be difficult to determine. It is therefore beyond the scope of this work to treat vapor migration by convection, though this process could easily be the most important source of moisture accumulation if such air flows are present. It is often desirable to design constructions in a way that eliminates the possibilities for internal convection air flows to take place. The discussion on air flow in low slope roofs will be mentioned again later in the applications chapter.

Transfer by diffusion is the other important mechanism that accounts for how vapor moves. Diffusion can be looked upon as the statistical result of the continuous movement of molecules in the air. Any differences occurred in concentration of one type of molecules – say water vapor – in a mixture of different components will be leveled out as time goes by. This process takes place in gas mixtures as well as through porous materials – and even through apparently tight membranes as for instance a polyethylene sheet. The vapor flux through a material will be proportional to the difference in vapor pressure across it and to the water vapor permeability of the material. Further, the flux will be inversely proportional to the thickness of the material. These statements are all expressed in Fick's law of diffusion (A. Fick, 1855):

$$g_v = -\delta_P \frac{\partial p}{\partial x} \qquad\qquad (1.1.2)$$

where

g_v	=	Vapor flux	$(\frac{kg}{m^2 s})$
δ_P	=	Water vapor permeability	$(\frac{kg}{Pa \cdot m \cdot s})$
x	=	General one dimensional space coordinate	(m)

The water vapor permeability varies somewhat with temperature, so that for higher temperatures the permeability is also higher. An increase of temperature from 20°C to 40°C causes an increase of δ_P by approximately 13%. Several formulas for such corrections are found in the literature (Andersson, 1985).

What is perhaps more important is the way in which the water vapor permeability increases with moisture content. Philip & de Vries, 1957 have contributed with a plausible explanation for this. When moisture accumulates in a porous material, the narrower pores will be filled with liquid water while the wider pores remain gas filled. The higher the moisture content, the more pores will be filled with water. The water in the smaller pores tends to build bridges between the wider pores, allowing a vapor–liquid–vapor series transport to take place as illustrated in figure 1.3.

Moisture starts moving in the direction of the arrow in figure 1.3 when a vapor pressure gradient is imposed on the pore system with higher vapor pressure in the large pore on the left and lower on the right, compared with an initial state of equilibrium with equal pressures on both sides and no transport (solid lines).
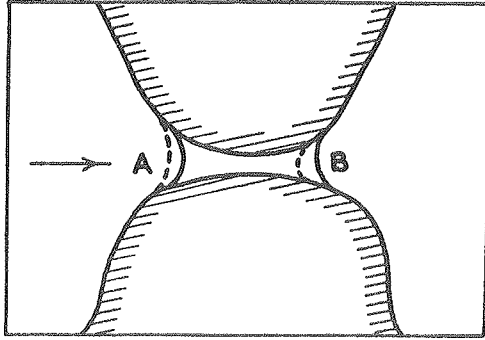
Figure 1.3   Series transport, vapor–liquid–vapor through a water filled pore
(Philip & de Vries, 1957)

Condensation of vapor at meniscus A causes its radius of curvature to increase while the radius of curvature of meniscus B decreases when moisture evaporates from it (dashed lines). The surface tension in the menisci with different curvatures causes a liquid pressure gradient in the island which transports the moisture from A to B without any large hydraulic resistance to prevent the motion. The resistance would have been larger if the moisture had to go through the narrow pore by vapor diffusion, as when the moisture content of the material is lower and the pore is dry. Similar arguments are valid if a narrow and a wide pore are coupled in parallel. The result would have been the same – increased moisture flow when more moisture is deposited in the pore system.

The way in which the temperature affects the saturation vapor pressure also affects the vapor pressures at lower RH–levels proportionally. Gradients in temperature will therefore impose gradients in vapor pressures and thereby induce fluxes of vapor. Philip & de Vries also point out that the liquid islands affect the temperature distribution. The thermal resistance is less across the water filled islands than across the large, gas filled pores. Since the overall temperature gradient is practically unaffected by the water distribution inside (at hygroscopic moisture content), there must be an increase in the temperature gradient across the remaining gas filled pore. These larger gradients in temperature will, according to Philip & de Vries, increase the passage of vapor when temperature gradients are present.

All in all, it is evident that the water vapor permeability increases with moisture content, and this has been experimentally verified a number of times, see for instance Tveit, 1966. Part of the explanation for this is, as mentioned above, a

8

transport in the liquid phase, which starts already at RH–levels around 30–40%. As seen, it is difficult to separate the liquid from the vapor transport. Applying Fick's law to describe the transfer is merely to be regarded as a convenient approximation. The series/parallel transport is usually described as if it were a pure vapor transport.

The so–called critical moisture content is reached when the moisture content is so high that the liquid islands are able to touch each other and form a continuous liquid phase between two arbitrary points of the material. At this point, the liquid moisture transfer begins, as described in the following section. As the water blocks the passage of gas molecules, the water vapor permeability decreases and becomes zero at total saturation.

There are other ways in which vapor can be driven than described by Fick's law. Knudsen diffusion (named after the Dane Martin Knudsen who published the phenomenon in 1934), also called effusion, is a phenomenon that takes place through capillaries more narrow than the mean path length of the molecules in the gas. Thermal diffusion is another, but less important, process in which the light molecules (vapor) are separated from the heavy molecules in a gas mixture when a temperature gradient is applied. Calculating both of these processes involves gradients of vapor pressures as well as of temperature, and the result is migration of vapor in the warmer direction.

Finally, a note is given on how vapor is transferred across an interface with the surrounding air. The mechanism is a convection process in which the vapor is carried away by the surrounding air. It therefore depends on the character of the air movement. The vapor flow resistance in this process is quite small compared to the internal vapor flow resistance of most materials. The transfer is described by the mass transfer coefficient:

$$g_v = \beta_P \left(p_{surface} - p_{air} \right) \qquad\qquad (1.1.3)$$

where

β_P =   Convection mass transfer coefficient $\left(\dfrac{kg}{m^2 s Pa} \right)$

The mass transfer coefficient can be calculated from the heat transfer coefficient which is mentioned later in this chapter. With good approximation it is so for

most conditions, that the heat and mass transfer coefficients will change proportionally (Lewis' law):

$$\beta_P = \frac{h_c}{R_v T \rho c_p}$$
(1.1.4)

where

h_c = Convection heat transfer coefficient $\qquad (\frac{W}{m^2 K})$

R_v = Gas constant for vapor = $461.5 \frac{J}{kgK}$

ρ = Density of air $\qquad (\frac{kg}{m^3})$

c_p = Specific heat capacity of air $\qquad (\frac{J}{kgK})$

1.1.2 RETENTION AND TRANSPORT OF LIQUID WATER

SUCTION CURVES:

When liquid water is inside a porous material it is bound in the capillaries as islands with curved menisci as boundaries. Surface tensions act on the three phase boundary at the solid/liquid/gas interface. Supposing the capillary could be regarded as a cylindrical tube, the liquid–gas surface tension has components that are perpendicular to the capillary walls as well as components that pull the liquid surface in the same direction as the cylinder axis. The whole island of water is therefore under stress tension from one meniscus to the other. The suction pressures to be found in the water can very well be of order of magnitude larger than the outside atmospheric pressure, so the resulting pressure is negative. The water is to be regarded as a liquid material under stress forces, where only the narrowness of the capillaries prevents bubble formation and boiling. The pressure is numerically larger (more negative) the smaller the capillary radius is, since the force decreases proportionally with the radius while the area the force acts on decreases proportionally with the radius squared.

It is shown thermodynamically that the hydraulic pressure can be expressed unambiguously by the relative humidity. This is expressed by the Thomson law or Kelvin equation (William Thomson (1824–1907) was ennobled Lord Kelvin):

$$\ln(\varphi) = \frac{P_h}{\rho_w R_v T} \qquad\qquad (1.1.5)$$

where

P_h	=	Hydraulic pressure = $P_{liq} - P_{atmosph}$	(Pa)
ρ_w	=	Density of water	$(\frac{kg}{m^3})$
T	=	Absolute temperature	(K)

It is seen from equation 1.1.5 that in the area close to RH = 100% where the resolution in RH is very poor, the resolution in hydraulic pressures is still kept. This means that from the maximum hygroscopic moisture content and upwards, the hydraulic pressure changes over a wide range as the large pores are being filled with water. The suction curve describes this connection between the suction pressure, P_{suc} (defined as the positive value of the hydraulic pressure) and the accumulated amount of water. Since the value of the suction pressure may vary several decades, it is customary to have the axis that represents it being in a logarithmic scale. Such curves are shown in figure 1.4. Actually, the hygroscopic region is also described quite well in such a curve, as it is seen in the region of suction pressures from 2.65 MPa and higher.
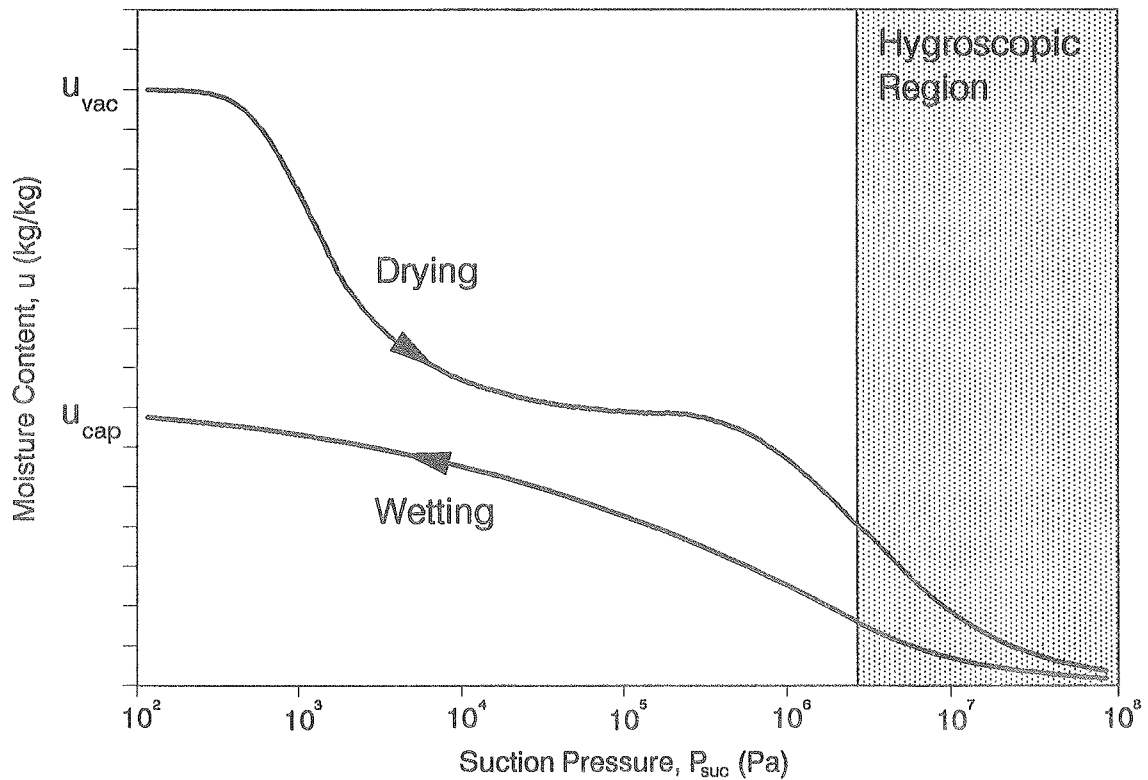

Figure 1.4   Suction curve.

To understand the behavior of the suction curve in the wet region it is necessary to study the distribution of pore sizes. Some materials tend to have collectives of pores of equal size. When they are filled (or emptied) the suction pressure is kept almost steady while, of course, the moisture content changes. The curve shown is typical for cellular concrete having two pore size collectives with radii close to 10^{-4} and 10^{-7}m.

There is also some evident effect of hysteresis in the suction curves. When, initially, all pores in the material have been completely saturated, the material follows a drying curve showing all the characteristics of the pore size distribution. The opposite way, during moistening, it will quite often turn out that the larger pores never become filled with water. This is caused by air entrapped inside the material in these pores. Such air can only escape by means of a very slow diffusion process through the water in the smaller pores which separate the large pores from the surface of the material. It is therefore questionable if, in this case, the suction curve expresses a real state of equilibrium.

The maximum moisture content during free water uptake is called the moisture content at capillary saturation, u_{cap}. When the process takes place in a vacuum chamber, it is possible to fill all the pores with water, and the moisture content at vacuum saturation, u_{vac}, is reached. The moisture content in these two cases corresponds to the starting and the ending points of the drying and the moistening curves in the suction diagram, respectively.
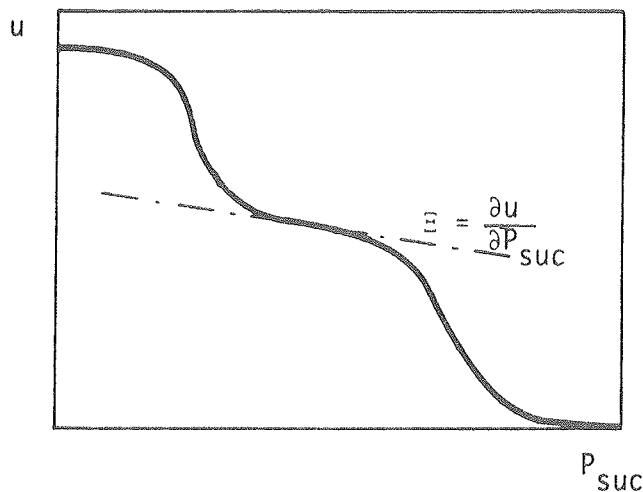

Figure 1.5   Definition of moisture capacity in the suction diagram (Sandberg, 1973).

Moisture capacities can be defined by the slope of the curves in the suction diagram in the same way as it was done previously in the sorption diagram. This is shown in figure 1.5. The figure is only schematic since the abscissa axis is logarithmic and the correct derivative will therefore not be a straight line. The moisture capacity for suction is designated by the symbol Ξ (capital ξ).

WATER MIGRATION:

Transfer of liquid moisture in porous materials is often exemplified by studying such transfer in a capillary tube. When a tube is filled with a fluid and there is a difference in fluid pressures across the length of the tube, the fluid moves towards the lower pressure under influence of the friction forces that oppose the movement. When velocities are small, the flow is laminar and the molecular layers of the fluid will flow smoothly. The only friction encountered is the friction between each fluid layer when it passes the neighboring layers that have different velocities. The amount of fluid being transferred per unit of time will under these circumstances be proportional to the pressure gradient.

The theory developed laminar transport in capillary tubes is often extended to describe the transport processes in porous materials with their complex system of cylindrical and spherical pores of different sizes. The transfer of water through sand in the bottom of a fountain was studied by H. Darcy more than hundred years ago when he published "Les fontaines publiques de la ville de Dijon" in 1856. It led to the formulation of Darcy's law which is valid when the flow is laminar, as it usually is for suction flow through building materials:

$$g_w = -K \frac{\partial P_h}{\partial x} \qquad (1.1.6)$$

where

g_w = Flux of water $\qquad (\frac{kg}{m^2 s})$

K = Hydraulic conductivity $\qquad (\frac{kg}{m \cdot s \cdot Pa})$

In this formulation of Darcy's law the gravity force has not been accounted for since for most materials it is negligible compared with the suction forces (heavily saturated, coarse pored insulation materials may be the exception). This force could be accounted for by writing $\nabla(P_h + \rho_w \cdot g \cdot z)$ (g being the acceleration of

13

gravity) in a vectorial version of equation 1.1.6.

The hydraulic conductivity of porous materials depends somewhat on the temperature since the viscosity is decreasing with increasing temperature and the conductivity is inversely proportional to the viscosity. This effect is small compared to the variation with moisture content as was the case for the water vapor permeability .

The hydraulic conductivity varies widely from the first non–zero values above the critical moisture content up to the point where the material is completely saturated. The reason for this is that the pore sizes available for transport of water become steadily larger as the moisture content increases. Since these larger pores also have much larger water transporting capabilities the influence of moisture content on the hydraulic conductivity of porous materials is considerable.

As it is seen, the description of water movement is very similar to the way vapor transfer is described. The similarity between Fick's and Darcy's laws can be extended to Fourier's law for thermal conduction and to a large number of other laws encountered in physics. These "first laws" all describe a flux as being proportional to the first derivative of a corresponding potential. A similarity was also seen in the method used to describe the amount of moisture accumulated by a material as a function of a characteristic variable (φ or P_{suc}). This variable can in both cases easily be transformed into the corresponding driving potential ($p = p_s(T) \cdot \varphi$, $P_h = -P_{suc}$).

1.2 MIGRATION OF ENTHALPY

The intention of this section is only to deal with the way in which temperature acts as a driving force for the migration of enthalpy. Presence of moisture may affect the magnitude of the transport parameters of the process studied in this section, and the question as regards how migration of enthalpy and moisture cross interfere is dealt with in the following section. The difference between "presence" and "migration" of moisture is emphasized. The migration of moisture through part of the material may significantly change its enthalpy balance, especially if the moisture changes phase during its passage. This is independent of the amount of moisture present.

1.2.1 RETENTION OF ENTHALPY

"Retention of enthalpy" in materials having heat capacities is the term deliberately used here to emphasize the similarity to the description of the moisture retention. Enthalpy is the quantity to keep track of here and the corresponding potential is temperature. The retention of enthalpy is simply described as:

$$h = h(T) \tag{1.2.1}$$

where

h	=	Mass specific enthalpy	$(\frac{J}{kg})$
T	=	Temperature	(K)

It is not common to write the enthalpy in an absolute way as here. Instead, changes of enthalpy are usually observed. By describing these changes in a differential way, the specific heat capacity is defined as the slope of the h–T curve:

$$c_P = \frac{\partial h}{\partial T} \qquad (\frac{J}{kgK}) \tag{1.2.2}$$

The heat capacity only varies insignificantly with temperature. It may be worthwhile, however, to correct for the "presence" of water:

$$c_P = c_{P,dry} + \sum_{\substack{i= \text{ice} \\ \text{water} \\ \text{vapor}}} u_i \cdot c_{P,i} \tag{1.2.3}$$

The heat capacity calculated in this way is specific with respect to the dry weight of the material.

1.2.2 TRANSPORT OF ENTHALPY

CONDUCTION:

Internally in porous materials, conduction of heat is the most important way in which enthalpy is transported, though conduction in the normal sense in a porous material comprises radiation as well as convective heat transfer on a microscopic

level. Macroscopic convection in a construction is not dealt with here. Macroscopic radiation across air spaces is discussed later.

Conduction heat transfer is described by Fourier's law (J. Fourier, 1822):

$$q = -k \frac{\partial T}{\partial x} \qquad (1.2.4)$$

where

q = Heat flux $\left(\frac{W}{m^2}\right)$

k = Thermal conductivity $\left(\frac{W}{mK}\right)$

The thermal conductivity of building materials increases with increasing temperature. This is mainly due to the nonlinear behavior of the microscopic radiation transfer that depends on the difference between temperatures raised to the 4th power. This dependence may be worthwhile considering together with the effect of "presence" of water.

The presence of moisture in porous materials increases the thermal conductivity. First of all the moisture has replaced some of the air in the pores, and water has a higher thermal conductivity than air. A further cause for an increased conductivity is that on a microscopic level a small heat pipe may be generated in which moisture is evaporated from the warmer side of a large pore. It diffuses through the pore as vapor, condenses on the colder side and is finally wicked back in the finer, surrounding pores to where the evaporation took place. This local transfer of latent heat is best described as an increase in thermal conductivity. However, the macroscopic transfer of latent heat by "migration" of vapor from one end to another of the material must not be described as an increase in thermal conductivity. Such a process would be much influenced by the nonlinear dependence of vapor pressures on temperature and is therefore not described very well by Fourier's law. The relationships often seen between moisture content and thermal conductivity are specific for the conditions under which they were measured unless efforts have been made to report only on the conduction heat transfer, keeping the effect of latent heat transfer separate. Sensible heat is the term used later for non—latent heat.

RADIATION:

A surface that is exposed to thermal radiation from the sun or from other surfaces will absorb a fraction of the radiative heat given by its absorptance, α. Supposing the irradiance from the sun is E (W/m²) after it has been corrected for diffuse and reflected contributions, for the path of the sun across the sky and for the tilt angle of the studied surface, the absorbed amount of heat will be:

$$q_r = \alpha E \qquad\qquad (1.2.5)$$

The other way round, a surface having a certain temperature will emit radiation proportionally to its temperature to the 4th power and depending on the character of the surface. The emissivity, ϵ, is the fraction of radiation the actual surface emits compared to the maximum value emitted from an ideal black body. α will equal ϵ for a material when it is exposed to radiation at the same wavelength as it is emitting. Radiation heat transfer between two bodies across from each other is described by:

$$q_r = \frac{\sigma_s(T_1^4 - T_2^4)}{\frac{1}{\epsilon_1} + \frac{1}{\epsilon_2} - 1} \qquad\qquad (1.2.6)$$

where

σ_r = Stefan–Boltzmann constant = $5.67 \cdot 10^{-8} \; \frac{W}{m^2 K^4}$

ϵ_i = Emissivity of surface "i" $\qquad\qquad$ (–)

This equation will look simpler if one of the two bodies could be considered black. If ϵ is the emissivity for the remaining grey surface, the formula will be:

$$q_r = \epsilon \sigma_r(T_1^4 - T_2^4) \simeq 4\epsilon\sigma_r T^3(T_1 - T_2) = h_r(T_1 - T_2) \qquad\qquad (1.2.7)$$

where

T = Average temperature $\qquad\qquad$ (K)

h_r = Radiation heat transfer coefficient $\qquad\qquad$ $(\frac{W}{m^2 K})$

Radiative heat exchange with the sky can be described this way, calculating an effective sky temperature assuming the sky as a black body.

CONVECTION:

The outer surfaces of a construction exchange heat with the surrounding air by convection. This is described similarly to the way convection vapor transfer was described in the first section:

$$q_c = h_c(T_{surface} - T_{air}) \tag{1.2.8}$$

The convection heat transfer coefficient, h_c, depends on the character and velocities of air flows around the construction and also on the dimension of the construction itself. In the analysis of moisture transfer a large number of uncertainties are involved. For instance, in determining the material properties, a very exact description of the temperature distribution in the construction may be considered a waste of calculation effort (unless heat flows are the major concern). An approximate formula for calculating the convection heat transfer coefficient from the surrounding air velocities is given here (Bisgaard, 1974 quoting Jürges):

$$h_c = \begin{cases} 5.82 + 3.96 \cdot v & v \leq 5 \text{ m/s} \\ 7.68 \cdot v^{0.75} & v > 5 \text{ m/s} \end{cases} \qquad \left(\frac{W}{m^2 K}\right) \tag{1.2.9}$$

At the inner side of a construction the imposed air velocities are normally negligible, and the main reason for convection heat transfer is natural convection due to differences between surface and room temperatures. If it is supposed that the other inner surfaces of the room have the same temperature as the room air, the convection and radiation heat transfer coefficients can be added and are often assigned a fixed value. In the Danish rules for design calculation of building heat losses (Dansk Ingeniørforening, 1986, DS 418), an inner surface resistance of 0.13 m²K/W is used. This corresponds to a 7.7 W/(m²K) heat transfer coefficient that probably also suits many calculations of moisture transfer.

1.3 CONTINUITY EQUATIONS

The two previous sections dealt with the transport equations for moisture and heat that can be used under steady state and quasi stationary conditions to describe the flux of water vapor, liquid water and enthalpy. Further, the sorption and suction curves together with the definition of heat capacity designated some "equations of state" that made it possible to relate the value of the driving potentials to the

18

contents of moisture and enthalpy. These are the variables kept track of in the continuity equations in this section. Keeping track of moisture and enthalpy is done for infinitesimal control volumes which are exposed to fluxes of vapor, liquid water and heat. Accounting for the ability of the control volumes to store moisture and enthalpy will allow the transient investigation of the coupled transfer phenomena.

1.3.1 CONTINUITY EQUATION FOR MOISTURE

A one dimensional infinitesimal control volume with thickness dx is surveyed (figure 1.6). Moisture enters the left side with the flux g_i and the same flux with a gain $\frac{\partial g_i}{\partial x} \cdot dx$ leaves the right side. The index, i, refers to the liquid and gaseous phases in which the water can move (the ice phase is considered immovable). Thus, the amount transported will be described by Fick's and Darcy's laws. In some cases there will be a production or a consumption of moisture internally in the volume. This must be accounted for in the continuity equation as a source term (with the proper sign).
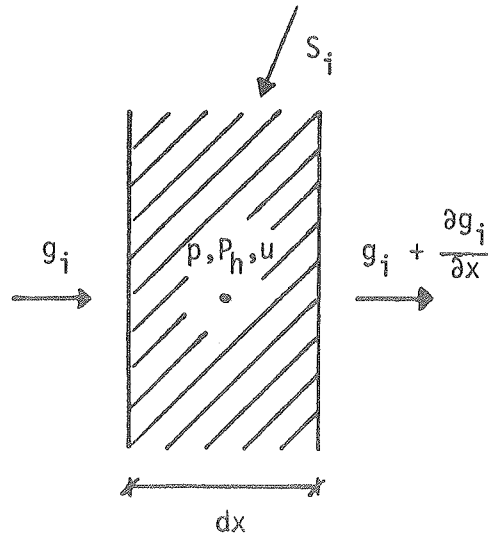
Figure 1.6   Moisture balance for a control volume.

When the change of moisture content in the control volume during a short time interval, Δt, in which the fluxes and sources can be regarded as constant (quasi stationary conditions), is known, the balance can be expressed as the amount that flows in, minus what flows out, plus the source term. If it is assumed that the dry density of the material is unchanged during the moistening process (no

swelling/shrinkage phenomena) the moisture balance may be expressed as:

$$\Delta m_i = A \, dx \, \rho_0 \, \Delta u_i = \left[A \left(g_i - (g_i + \frac{\partial g_i}{\partial x} dx) \right) + A \, dx \, S_i \right] \Delta t \qquad (1.3.1)$$

where
m_i	=	Mass of moisture in phase "i"	(kg)
A	=	Area perpendicular to flow direction	(m^2)
ρ_0	=	Dry density of the material	$(\frac{kg}{m^3})$
S_i	=	Source of moisture in phase "i"	$(\frac{kg}{m^3s})$

In wood, for instance, the swelling during moisture absorption could be so heavy that it might be worth considering. This is done by writing $\Delta(\rho_0 u_i)$ instead in the middle term of equation 1.3.1.

The volume $A \cdot dx$ can be divided out of the equation. If the time steps are made differential and swelling/shrinkage disregarded, the equation will now be:

$$\rho_0 \frac{\partial u_i}{\partial t} = -\frac{\partial g_i}{\partial x} + S_i \qquad (1.3.2)$$

The source term, S_i, may be caused by contributions that are not described by the diffusive laws giving the moisture fluxes g_i. Such a source could arise from chemical conversions of the water in the control volume. This is known, for instance, with the consumption of water in newly cast concrete during the hydration process. Besides from such sources that are specific to certain problems, there will always be source terms due to conversion of water between the different phases. In the following, these kinds of sources are considered the only ones in the continuity equation. Production of water in the phase "i" (from either of the two other phases) will be designated I_i. This being the only source changes equation 1.3.2 to:

$$\rho_0 \frac{\partial u_i}{\partial t} = -\frac{\partial g_i}{\partial x} + I_i \qquad (1.3.3)$$

where

I_i = Production of phase "i" by phase changes $(\frac{kg}{m^3s})$

When this equation is rewritten phase by phase the following equations are

20

obtained:

Vapor:

$$\frac{\partial g_v}{\partial x} \simeq I_v \qquad (1.3.4)$$

Liquid water:

$$\rho_0 \frac{\partial u_w}{\partial t} = -\frac{\partial g_w}{\partial x} + I_w \qquad (1.3.5)$$

Ice:

$$\rho_0 \frac{\partial u_{ice}}{\partial t} = I_{ice} \qquad (1.3.6)$$

The fact that the mass of vapor in a control volume is vanishing, compared with the mass of liquid water and ice, is used in formula 1.3.3. With a zero on the left side, it rewrites to become equation 1.3.4. Since ice is solid and therefore immovable, another simplification can be made by disregarding the transport term in 1.3.3 and letting equation 1.3.6 describe the amount converted into ice. No such simplifications are valid in the continuity equation for liquid water (1.3.5). Since the gain of water in one phase must come from either of the other two phases, the following equation is valid:

$$\sum_{\substack{i= \\ ice \\ water \\ vapor}} I_i = 0 \qquad (1.3.7)$$

It could be of interest to write the continuity equation for the total amount of water since this is what is measured on a balance. Defining $u = \Sigma u_i$ and $g = \Sigma g_i$ and adding the equations 1.3.4 through 1.3.6 using equation 1.3.7 now yields:

$$\rho_0 \frac{\partial u}{\partial t} = -\frac{\partial g}{\partial x} \qquad (1.3.8)$$

A common method to create "second law" types of equations is by inserting Fick's and Darcy's laws into this equation and using the retention curves to express differentials of the driving pressures by differentials of moisture content (using the moisture capacities). Such equations express the time derivative of a certain

quantity as a diffusivity multiplied by the second space derivative of the same quantity as it is known from the Fick's and Fourier's second laws. Some temperature effects can also be expressed as proportionalities with the second temperature derivative thereby defining thermal gradient coefficients. Such work has been done by a large number of researchers, A.V. Luikov being one of the most well known (Luikov, 1966). An excellent review of such methods was presented by Hartley, 1987.

Expressing the combined transfer mechanism in this way is attractive since all effects are described in one single partial differential equation, providing simple means of solution by a numerical technique, or under simplified circumstances even analytically. The major drawback is that the driving potential for the moisture transport is not the physical driving one. Moisture content does not cross material interfaces continuously and special treatment of these will therefore be needed (transferring back to pressures). Furthermore, the basic transport laws and retention descriptions have been rewritten in a way that makes it difficult to separate fluxes in vapor phase from those in liquid phase.

In this work it has been tried to stick to the physics and to the basic laws. The use of second law descriptions will not be further discussed here (referring to earlier work by the author (Pedersen, 1989a) for derivation of such equations).

1.3.2 CONTINUITY EQUATION FOR ENTHALPY

To describe the flow and accumulation of enthalpy a similar infinitesimal control volume will now be engaged to the one that was analyzed with regard to the flow of moisture. The control volume is shown in figure 1.7.

The accumulated amount of heat is equal to the amount flowing in, minus the amount flowing out, plus an amount from a source term. As before, this is studied over the time step Δt, and within a cross sectional area A, assuming the dry density to be constant:

$$A \, dx \, \rho_0 \, \Delta h = \left[A \left(q - (q + \frac{\partial q}{\partial x} dx) \right) + A \, dx \, S_q \right] \Delta t \qquad (1.3.9)$$

where

S_q = Source of enthalpy $(\frac{W}{m^2})$
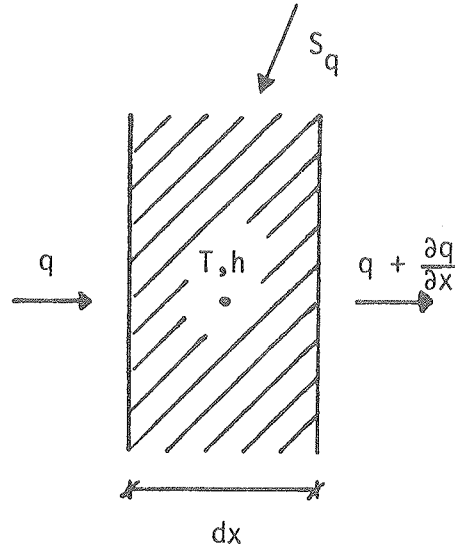
Figure 1.7   Enthalpy balance for a control volume.

Making time steps differential and dividing by the volume, A dx, yields:

$$\rho_0 \frac{\partial h}{\partial t} = -\frac{\partial q}{\partial x} + S_q \tag{1.3.10}$$

Again, the source term contains all the contributions that are not suitable for presentation by the diffusive heat flux, q. It could be heat released by chemical reactions (hydration of concrete). However, with the scope being combined heat and moisture transfer, phase conversion enthalpies, released as a cause of moisture migration, will be the primary sources.

These phase conversion enthalpies contribute with an amount of heat to the control volume that in many cases constitute the dominant effect of moisture on the thermal balance. Heat transported by convection of vapor and water coming from zones with different temperatures, will usually bring only negligible contributions, since the velocities are quite small. By production of the amount I_{ij} [kg/(m^{3}s)] of moisture in the phase "i" at the expense of phase "j", the control volume gains the following amount of heat as a source:

$$S_q = \Delta h_{ij} \cdot I_{ij} \tag{1.3.11}$$

23

where

$$\Delta h_{ice\text{-}water} \quad = 3.34 \cdot 10^5 \, \frac{J}{kg} \text{ (at } 0^oC)$$

$$\Delta h_{water\text{-}vapor} \ = 2.45 \cdot 10^6 \, \frac{J}{kg} \text{ (at } 20^oC, \text{ absorption enthalpies not included)}$$

These figures for the phase conversion enthalpies which are slightly dependent on temperature should be applied with the right sign, so that for instance evaporation within a control volume corresponds to a negative contribution of enthalpy ($\Delta h_{ij} = -\Delta h_{ji}$). Phase conversion by sublimation could also be possible with a phase conversion enthalpy equal to the sum of the two above mentioned conversion enthalpies, at the actual temperature of sublimation.

Second law types of equations can be written also for the enthalpy balance including terms of moisture and temperature contributions. However, this is not being a subject of discussion here, either.

1.4 COMBINED HEAT AND MOISTURE TRANSFER

For each of the transfer processes of moisture and heat three types of equations are available. These are the transport equations, equations of state and the continuity equations. The equation of state ties the driving potentials to the variable controlled in the continuity equation, i.e. the retention curves and the h–T curve. A transient calculation of the development of these processes may now proceed as outlined in figure 1.8.

Suppose a distribution of the driving potential (temperature or pressures) is given for the transport process to be investigated. Thus, the gradients imposed cause a transfer given by the transport equation. Supposing this transfer continues for a period of time, short enough for the driving potential not to change its value significantly (quasi stationary conditions), the continuity equation describes the changes of the quantity that is to be kept track of (enthalpy or mass of moisture). Other sources of enthalpy or moisture should be accounted for here. Finally, the equation of state is used to update the result into changes of the potential that originally drove the transport. A new distribution is then given, and the whole operation can go on again in the following time step.
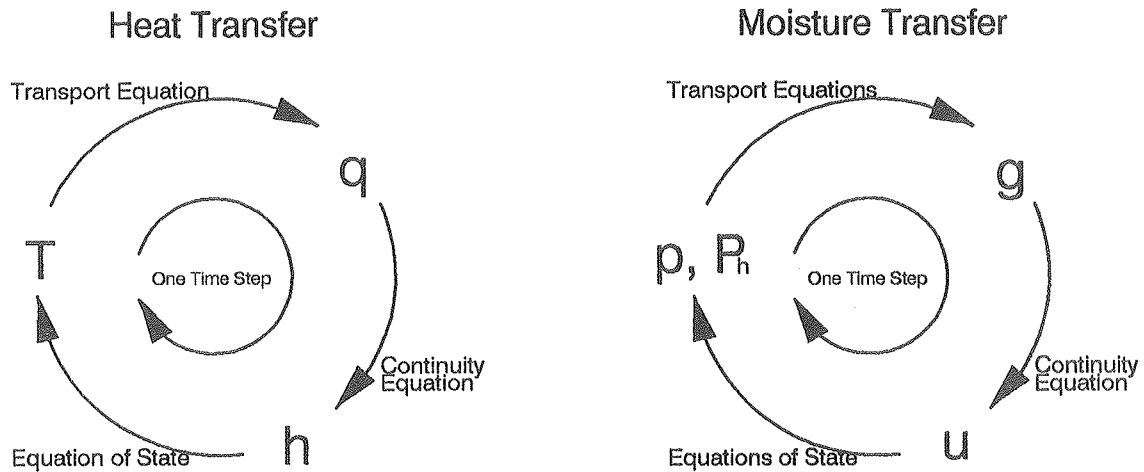
Figure 1.8   Methodology when the equations of transport, continuity and state are used successively in one time step.

This procedure leads to the way of thinking in explicit difference, numerical methods. How the equations are formulated into a well working numerical model is described in the next chapter.

The equations needed for calculation of coupled heat and moisture transfer are all basic transport equations and well known relationships between various quantities that appeal to the "stick to the physics" concept. The idea is to choose those effects that are considered important from the vast bunch of equations and relationships that are valid, while second order effects should be left out. The coupling between the transfer of moisture and heat can be grouped into effects on each of the three types of equations. Some of the more important ones are mentioned in the following list. The two effects that usually dominate where transfer of moisture and heat interfere are marked with asterisks.

TRANSPORT EQUATION:

−   Temperature affects the water vapor permeability.

$$T \uparrow \implies \delta \uparrow$$

−   Temperature affects the viscosity and thereby the hydraulic conductivity.

$$T \uparrow \implies \mu \downarrow \implies K \uparrow$$

— Temperature is directly a part of the driving potential in some of the secondary transport equations.

— Presence of water and ice increases the thermal conductivity.

$$u \uparrow \implies k \uparrow$$

CONTINUITY EQUATION:

— Temperature affects the ice formation.

$$T \downarrow \implies I_{ice} \uparrow$$

* Migration of vapor carries a considerable amount of latent heat.

— Migration of moisture also gives (small) convective transports of sensible enthalpy.

EQUATION OF STATE:

* The saturation vapor pressure is a steeply increasing function of temperature.

$$T \uparrow \implies p \uparrow$$

— The sorption curves are dependent on temperature.

$$T \uparrow \implies p|_u \uparrow$$

— Surface tension and thereby suction pressure depends on temperature.

$$T \uparrow \implies \sigma \downarrow \implies P_{suc} \downarrow$$

— Heat capacity is equal to the sum of heat capacities of all components in the system.

$$u \uparrow \implies c_P \uparrow$$

(c_P is specific with respect to the dry density)

CHAPTER 2
THE MATCH PROGRAM

This chapter describes the way the computer program MATCH is constructed. MATCH is an abbreviation for *Moisture and Temperature Calculations for Constructions of Hygroscopic Materials.* In the description of the numerical procedure details with standard explicit versus implicit difference schemes will be avoided, since this discussion is already found in the literature. Some special techniques are involved, however, in describing the combined effects of the various transport phenomena. These techniques will of course be described. A unique feature of the computer program is its ability to account for the hysteresis in the moisture retention curves. The way in which this is done will also be described.

The main features of the program are as follows:

o   A finite control volume numerical method is used.
o   Moisture as well as temperature distributions are calculated in a transient way.
o   The calculations are one–dimensional.
o   Transport of vapor as well as of liquid water is considered (liquid transport is optional).
o   Convection transfer of heat and moisture is not considered, except at the boundaries.
o   Properties of materials are variable (primarily with moisture content).
o   Environmental data may be kept constant or taken from a file of measurements or test meteorological data.
o   Hysteresis in the moisture retention curves is taken into account (optional).
o   Phase conversion enthalpies are taken into account.
o   A user friendly preprocessor is developed which provides default values for all parameters.
o   Data base with properties of materials supplied (see appendix).
o   The program is written in Turbo Pascal and runs on an IBM compatible PC.
o   Results are shown graphically as the calculation proceeds (optional).
o   The program is developed to analyze roofs, but constructions may be tilted so that the program applies to most building constructions exposed to the exterior.

2.1 MOISTURE TRANSFER

Before the procedures involved in the actual calculations of the variables are dealt with, some transfer functions will be defined. These functions are general helping tools whatever the numerical method will be. They include the required information about the transport parameters and retention curves for the materials. How these are described as analytical expressions is therefore also shown.

To establish the terminolgy: The terms "old" and "new" refer to the values of a variable at the beginning and the end of the current time step. "Explicit" refers to variables that are already available — often as "old" ones, while "implicit" refers to something determined by "new" variables, yet to be found.

2.1.1 VAPOR TRANSFER FUNCTIONS

In the following, a model consisting of three consecutive layers as shown in figure 2.1 will be studied. The three layers are treated in a general way in which they are supposed to be of different materials and thicknesses. A grid point in each control volume has a moisture content that represents the value of moisture content of the whole volume. The grid point may be displaced within the volume to any place within the two boundaries, described by the displacement factor, f. Thus, f=0 corresponds to a grid point at the outer boundary, while f=1 corresponds to an inward grid point. Further, the layers have numbers, i=1..n, starting from the outmost layer.

VAPOR MIGRATION:

In the following Fick's law is written using finite differences. The diffusive moisture flux through a layer "i" with thickness Δx_i, water vapor permeability $\delta_{p,i}$ and a difference Δp in vapor pressure across the material, is:

$$g_v = -\delta_{p,i} \frac{\Delta p}{\Delta x_i} = -\frac{\Delta p}{z_i} \qquad (2.1.1)$$

where

z_i = Diffusion resistance across layer "i" $\left(\frac{Pa \cdot m^2 \cdot s}{kg}\right)$
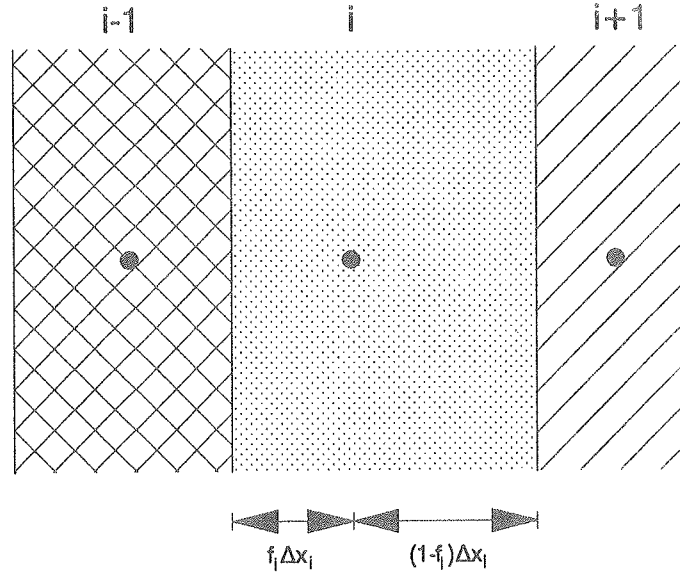
Figure 2.1   Three consecutive layers in the calculation. Each layer may be of a separate material, i.e. have separate material properties.

For diffusion to take place from grid point "i–1" to "i" in figure 2.1, the overall resistance is:

$$z_{i-1 \rightarrow i} = (1-f_{i-1}) \, z_{i-1} + zx_i + f_i \, z_i \qquad (2.1.2)$$

where

zx_i =   Extra resistance between layers "i–1" and "i" $(\frac{Pa \cdot m^2 \cdot s}{kg})$

f_i =   Displacement factors as described in fig. 2.1 $(-)$

The extra resistance could represent vapor retarders, air gaps and layers that are not contributing transiently to the development of the migration process (because of a lack of noticeable hygroscopic capacity).

Now, the transfer function is defined as:

$$hz_i = \frac{1}{z_{i-1 \rightarrow i}} \qquad (\frac{kg}{Pa \cdot m^2 \cdot s}) \qquad (2.1.3)$$

The transfer function is calculated for each time step, using the values of moisture content from the former time step to evaluate the current values of the permeabilities. No iteration is performed to determine the material properties in the middle of the actual time step. The inaccuracy of these properties is much

29

larger than the corrections an iteration would give. The computational effort would probably be better used if the size of the time steps were decreased. The vapor permeabilities are calculated from this simple function that only requires two δ_p—values as input (a "dry" and a "wet" one):

$$\varphi < 60\ \%\quad:\ \delta_p = \delta_{p,dry}$$

$$60 \leq \varphi < 98\quad:\ \delta_p = \delta_{p,dry} + \frac{\varphi - 60}{98 - \varphi}\left(\delta_{p,wet} - \delta_{p,dry}\right) \qquad \left(\frac{kg}{Pa \cdot m \cdot s}\right) \qquad (2.1.4)$$

$$\varphi \geq 98\quad:\ \delta_p = \frac{u_{vac} - u}{u_{vac} - u_{98}}\,\delta_{p,wet}$$

where

u_{98} = Maximum hygroscopic moisture content (at $\varphi=98\%$) $\left(\frac{kg}{kg}\right)$
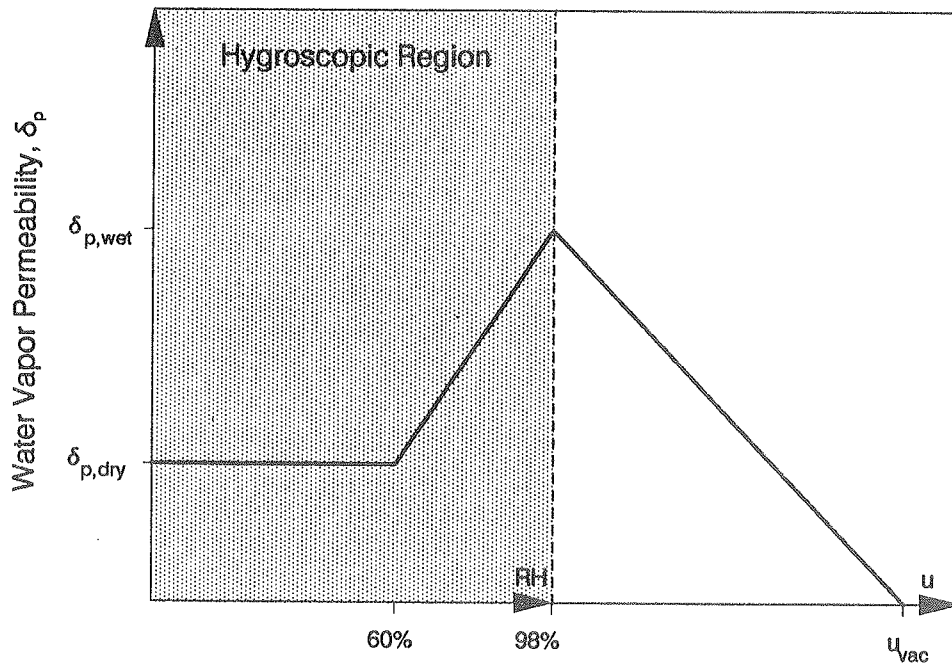
This is shown schematically in figure 2.2.

Figure 2.2   Schematic diagram showing water vapor permeability as a function of moisture content. The abscissa is linear with RH up to the end of the hygroscopic region content and with u above this limit.

Finally, the moisture flux from grid point "i−1" to "i" may be calculated as:

$$g_{v,i} = -hz_i\left(p_i - p_{i-1}\right) \qquad (2.1.5)$$

BOUNDARIES:

The extra resistance "zx" is also defined at the boundaries (with indices 1 and n+1). $z_{i-1 \to i}$ is defined the same way as above except that it does not have contributions from the nonexisting layers (0 and n+1). Here $z_{i-1 \to i}$ is the resistance between the outmost grid point and an imaginary point in the bulk of the free air.

The inner and outer boundaries are treated separately, since the inside conditions usually are relatively constant, while the outside varies somewhat with the climatic conditions. Equation 1.1.4 is used to calculate the vapor resistance at the boundaries in both cases.

$$z_{boundary} = \frac{1.6 \cdot 10^8}{h_c} \qquad\qquad (\frac{Pa \cdot m^2 \cdot s}{kg}) \qquad\qquad (2.1.6)$$

where
h_c must be in the units $[W/(m^2K)]$.

At the inside, zx_{n+1} is the resistance calculated from the convection part of the usually constant inner heat transfer coefficient. This is done by default when the preprocessor is used ($zx_{n+1} = 5.1 \cdot 10^7$ $Pa \cdot m^2 \cdot s/kg$) or another value may be chosen to account for layers at the internal boundary with some resistance — as for instance a layer of paint. zx_{n+1} is kept constant throughout the calculation.

At the outside, the resistance is calculated at each time step from the actual wind velocity and added to the zx_1–resistance. This way, zx_1 is still available to describe for instance the resistance of a roofing membrane in those cases where the membrane is not included in the transient calculation as a separate layer.

As mentioned in chapter 1, the convection boundary resistances for vapor flow are relatively small compared with the internal resistances of most materials.

CONTINUITY:

The balance equation for layer "i" in figure 2.1 is:

$$\Delta u_i = -\frac{\Delta t}{\rho_{0,i} \Delta x_i} (g_{v,i+1} - g_{v,i}) \qquad\qquad (2.1.7)$$

where

Δt = Time step (s)

This equation only accounts for the transfer of vapor. Later, when the liquid transport is added, a similar term will be appended.

USING THE "EQUATION OF STATE"

To get from new moisture content to new vapor pressure, it is necessary to use the equation of state, which in this case is the sorption isotherm. For finite differential changes this is described using the moisture capacity:

$$\Delta(\frac{p_i}{p_{s,i}}) = \frac{\Delta u_i}{\xi_i} \qquad (2.1.8)$$

where

ξ_i = Some representative value of the moisture capacity, which for small steps could be the value from the beginning of the time step.

Using this equation together with equation 2.1.7 gives the possibility of eliminating the Δu's and finding the changes of relative humidities directly from the vapor fluxes g_v:

$$\frac{\xi_i \rho_{0,i} \Delta x_i}{\Delta t} \Delta(\frac{p_i}{p_{s,i}}) = hz0_i \Delta(\frac{p_i}{p_{s,i}}) = -(g_{v,i+1} - g_{v,i}) \qquad (2.1.9)$$

This equation defines the transient transfer function, hz0, that describes the storage capability of the control volume. If it is assumed that the "new" as well as the "old" temperature distribution and thereby the saturation vapor pressures are known, it is also possible to find the new vapor pressures as the solution to this equation. The temperatures are therefore calculated before the vapor pressures (as described in section 2.2).

The sorption isotherms must preferably be given by analytical expressions that also allow the derivatives (capacities) to be found. Such an expression is found by P.F. Hansen, 1985 and used by K.K. Hansen, 1986 in a catalogue of sorption isotherms for most common building materials. The expression used requires three constants (u_h, A and n) to describe the curve:

32

$$u = u_h \left(1 - \frac{\ln \varphi}{A}\right)^{-\frac{1}{n}} \qquad\qquad (2.1.10)$$

These expressions are fitted by K.K. Hansen in the region 20% < RH < 98% which should be adequate for most applications. For some materials a curve has been fitted for absorption as well as for desorption.

The saturation vapor pressures are also calculated from an analytical expression (Danvak, 1988):

$$p_s = \exp\left(23.5771 - \frac{4042.9}{T[K] - 37.58}\right) \qquad (Pa) \qquad (2.1.11)$$

The accuracy of this expression is better than 0.15% for temperatures between 0 and 80°C. The same expression is also used below 0°C however, as the depression of the freezing point in porous materials makes it uncertain which p_s to use — the pressure over ice or the pressure over liquid water.

2.1.2 LIQUID TRANSFER FUNCTIONS

Description of the liquid transfer is now quite straightforward since all definitions are similar to those given above. However, there are some characteristics of the liquid transfer that differ from those of vapor transport, and special attention will be paid to these.

WATER MIGRATION:

The most important of these characteristics is probably the variation in orders of magnitude of the suction pressure and the hydraulic conductivity with moisture content. This means that even small gradients in moisture content correspond to steep gradients in pressures and in conductivities. Such steep gradients are not suitable for a numerical method with discrete values at the grid points since it would require a very fine mesh to give a good description of the continuity in distribution of the values. Instead of using directly the hydraulic pressure in Darcy's law (1.1.6), the natural logarithm of the suction pressure can be used:

$$g_w = -K \frac{\partial P_h}{\partial x} = K \frac{\partial P_{suc}}{\partial x} = K \cdot P_{suc} \frac{\partial(\ln P)}{\partial x} \qquad (2.1.12)$$

where
"lnP" is a short name for $\ln(P_{suc})$ used here and in the following.

lnP has a variation which is much more similar in size to the variation in u. Thus, the product, $K \cdot P_{suc}$, defines a new material parameter which also varies less than the usual hydraulic conductivity does, because K and P_{suc} have exponential variations with moisture content that go in separate directions and some of these variations are weighed out in the multiplication.

The variations in lnP and $K \cdot P_{suc}$ are comparable to the variations in u and $D_{\theta w}$ respectively, in the widely used Luikov model ($D_{\theta w}$ being the moisture diffusivity for liquid flow).

Now, the liquid resistance can be defined as above for the vapor resistance when a pressure difference is present across the layer "i":

$$g_w = K_i P_{suc,i} \frac{\Delta \ln P}{\Delta x_i} = \frac{\Delta \ln P}{z \bar{1} iq_i} \qquad (2.1.13)$$

where
$z liq_i =$ Hydraulic resistance $\left(\frac{Pa \cdot m^2 \cdot s}{kg}\right)$

If extra resistances, zxliq, are defined as above for any kind of barrier towards water flow between two neighboring grid points, the transfer function can be written as:

$$hzliq_i = \frac{1}{(1-f_{i-1})\ zliq_{i-1} + zxliq_i + f_i\ zliq_i} \qquad (2.1.14)$$

The hydraulic conductivity which is involved in finding the resistances against liquid flow is calculated in each time step as:

$u < u_{cr}:$ $K =$ negligible value $\left(\frac{kg}{Pa \cdot m \cdot s}\right)$

$u_{cr} \leq u < u_{cap}:$ $K = A_k \cdot \exp(B_k \cdot u)$ $(2.1.15)$

$u \geq u_{cap}:$ $K = A_k \cdot \exp(B_k \cdot u_{cap})$

34

where

u_{cr} = Critical moisture content $\qquad$ (--)

This, admittedly, is a rough estimate on how the hydraulic conductivities vary but probably as exact as the present knowledge on these values allows. However, such functions may of course easily be changed in the program to conform with any improved knowledge on the variation with moisture content.

The transfer of liquid from point "i−1" to "i" is now calculated as:

$$g_{w,i} = hzliq_i \left(\ln P_i - \ln P_{i-1}\right) \qquad (2.1.16)$$

BOUNDARIES:

The boundary conditions for the water are some very small suction pressures, as when the surface is exposed to a free water reservoir. For most conditions the surfaces to be calculated are dry and there is no liquid transfer across them. This is described by some very large resistances $zxliq_1$ and $zxliq_{n+1}$ that are chosen by default when the preprocessor is being used.

CONTINUITY:

The balance equation looks exactly the same as for vapor transfer (now only accounting for liquid transfer):

$$\Delta u_i = - \frac{\Delta t}{\rho_{0,i} \Delta x_i} \left(g_{w,i+1} - g_{w,i}\right) \qquad (2.1.17)$$

EQUATION OF STATE:

Finite differential changes of liquid tension are found from the differential changes of moisture content as:

$$\Delta P_{suc,i} = \frac{\Delta u_i}{\Xi_i} \qquad (2.1.18)$$

35

The capacity transfer function may now be defined the same way as for vapor transfer:

$$hzliq0_i = \frac{\Xi_i \rho_{0,i} \Delta x_i}{\Delta t} \qquad (2.1.19)$$

When analytical expressions for the suction curve are looked for another problem arises that makes the description of liquid transfer a little more tricky than for the sorption isotherms. The expression for the sorption isotherms applies to most materials since their curves quite often have the typical S–formed shape. The suction curves are much more dependent on the distribution of pore sizes over a wide range from micro to macro pores. This distribution may vary considerably from one material to another. The curvature may also change direction a number of times, making it difficult to have a simple analytical expression describing the curve. Further, the shape of the curve for wetting does not always look the same as the curve for drying and special attention must be paid to this fact also.

A suction description has been made that applies to materials with two pore size collectives of which only the one with the smaller pores is being filled during wetting. Such a description should be quite well fitting for aerated concrete but it may also be suitable to some extent for other materials. Each suction curve is made up of several pieces of curves. Figure 2.3 should give some idea on how this is done.

The wetting curve is described first since it is the simpler of the two:

98% relative humidity corresponds at 10°C to the suction pressure being $2.64 \cdot 10^6$ Pa (lnP = 14.79). Higher pressures than this are in the hygroscopic region and here the absorption isotherm is valid. The Kelvin equation 1.1.5 is used to do the transformation between relative humidity and suction pressure. For lower suction pressures than this limit (higher moisture content) another formula is being used:

$$u = u_{cap} - A_{wet} \cdot \ln P^{B_{wet}} \qquad (2.1.20)$$
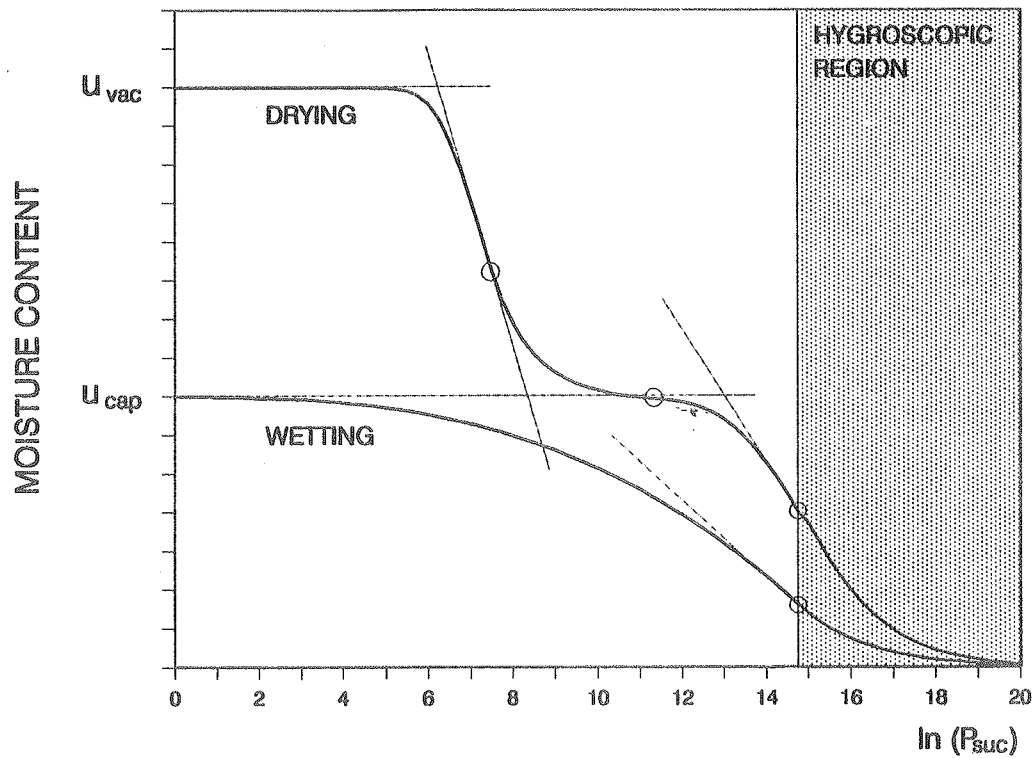
Figure 2.3   Suction curves for wetting and drying. The circles mark those places where different curve descriptions take over from each other.

This makes u equal to the value at capillary saturation for $\ln P = 0$ (which is equal to $P_{suc} = 1$ Pa $\simeq 0$ Pa). The values A_{wet} and B_{wet} are determined so that the suction curve passes smoothly (continuously and differentiably) into the curve described by the absorption isotherm at $\ln P = 14.79$. Whether B_{wet} is more or less than 1.0 determines the hollowness of the wetting curve, which will be either upwards or downwards directed (this in turn depends on the size of u_{cap} compared to the intersection with the u-axis of the linear extrapolation, $u = A_{abs} - B_{abs} \cdot \ln P$, of the absorption curve from RH=98%).

The curve for drying similarly takes the desorption isotherm and transforms the RH—values into suction pressures in the hygroscopic region. For moisture contents above this region, the curve consists of three hyperbolic functions that are joined smoothly. The first and the third of these hyperbolas are defined by some asymptotes, that guide them. The second hyperbola is constructed so that it goes smoothly from the first and into the third hyperbola.

The lines that guide the first hyperbola (closest to the u—axis) are the horizontal

37

line u = u_{vac} and the tangent at the inflection point that is involved in describing the course of the suction curve around the largest pore size collective. The lines that determine the third hyperbola are u = u_{cap} and the linear extrapolation of the desorption isotherm from the maximum hygroscopic moisture content and upwards. If the intersection between the u–axis and the linear extrapolation of the absorption isotherm is less than u_{cap}, u = A_{abs} is used as the horizontal asymptote for the third hyperbola.

The required input to describe the suction curves will be the sorption isotherms for absorption and desorption, moisture content at capillary and vacuum saturation and some estimate of the tangent at the inflection point. This tangent may be estimated from experimental determinations of the suction curve or it may be derived from a pore size analysis. Where one hyperbola takes over from another is determined by qualified guessing.

The inflection point tangent being u = $A_{ipt} - B_{ipt} \cdot lnP$, and the linear extrapolation of the desorption isotherm being u = $A_{des} - B_{des} \cdot lnP$, the mathematical expressions for the curves will be:

1st hyp. $\quad : u = A_{ipt} - [(B_{ipt} \cdot lnP)^{exp} + (A_{ipt} - u_{vac})^{exp}]^{\frac{1}{exp}}$

2nd hyp. $\quad : u = u_0 + A_{dry} (lnP - lnP_0)^{B_{dry}}$ $\hspace{2cm}$ (2.1.21)

3rd hyp. $\quad : u = A_{des} - [(B_{des} \cdot lnP)^{exp} + (A_{des} - u_{cap})^{exp}]^{\frac{1}{exp}}$

The four unknown values for the 2nd hyperbola are found so that the smoothness of the curve is maintained at the connections with the two other hyperbolas. The exponent used in the first and the third expression is chosen large enough for the curves to converge fast towards their asymptotes. In the program exp = 30 is used.

It might seem that this description concentrates more on the mathematical formulation than on optimizing real, measured data. This is true, but unfortunately, many measurements reported in literature appear to be rather uncertain and this, relatively convenient, description will probably be as good as any other (at present). Some of the best suction measurements have been reported by for instance Bomberg, 1974 and Andersson, 1985.

2.1.3 COMBINING THE VAPOR AND LIQUID TRANSFER

Most transfer of moisture is so slow a process that an explicit calculation of its progress will proceed with time steps that are acceptably large and not causing any problems with instability of the results. However, for a few materials, for example mineral wool, the hygroscopic capacity is very low and at the same time they have a large vapor permeability. In roofs, where the thermal gradients may be quite large, it is sometimes preferred to have a fine mesh of grid points, and stability may therefore be a potential problem. For this reason, the moisture transport is described in an implicit way.

Having more than one type of transport (vapor, liquid and heat) requires the simultaneous solution of three interconnected systems of equations if the solution method should be fully implicit. This is a computationally not very efficient way to manage the problem, since it would require a solution with either full Gauss–elimination or the application of an iterative method. In this work another procedure is used.

Each type of transport is treated implicitly with respect to its own driving gradients. Effects from other mechanisms are added explicitly. The stability is much improved by this and the calculation only involves solving a tridiagonal system of equations which can be done computationally quite efficiently. This method, which was inspired by the ADI–method in calculating multidimensional heat flow, could be called an Alternating Parameter Implicit method (API, adopted from Pedersen & Rasmussen, 1986) since the driving potentials alternately will occur in an explicit and in an implicit way.

VAPOR IMPLICIT, LIQUID EXPLICIT:

The purpose of this part of the calculation is to find the new vapor pressures. As indicated in the headline this is done by treating the diffusive contributions to the transport in an implicit way, which means that the vapor fluxes are calculated from new (and yet unknown) vapor pressures, while the liquid transport is described explicitly with old liquid pressures in the Darcy equation. Equation 2.1.9 is now written accounting for explicitly written liquid fluxes also:

$$hz0_i \, \Delta(\frac{p_i}{p_{s,i}}) = -\,(g_{v,i+1}^{new} - g_{v,i}^{new}) - (g_{w,i+1}^{old} - g_{w,i}^{old}) \tag{2.1.22}$$

The superscripts "new" and "old" refer to the vapor and liquid pressures respectively to be entered in Fick's and Darcy's laws. It is assumed that the saturation vapor pressures are known as new and old values (the temperature calculation comes first) and that the old liquid pressures are known from the previous time step (or from the initial conditions). Equation 2.1.22 now represents a system of equations (when written for all "i") that can be solved with respect to p^{new} by an efficient solution technique since all the elements of the coefficient matrix are in the three center diagonals. This provides the new vapor pressures.

LIQUID IMPLICIT, VAPOR EXPLICIT:

Similarly, the new suction pressures are determined by describing the liquid transfer implicitly and the vapor diffusion explicitly:

$$hzliq0_i \, \Delta P_{suc,i} = -\,(g_{w,i+1}^{new} - g_{w,i}^{new}) - (g_{v,i+1}^{old} - g_{v,i}^{old}) \tag{2.1.23}$$

With the old vapor pressures known, a new set of equations to be solved with respect to the new liquid pressures is given. If the solution to equation 2.1.22 is found first, the new vapor pressures could be used in the Fick's law part of equation 2.1.23. However, for consistency reasons this is not done.

NEW MOISTURE CONTENT:

The vapor and liquid pressures are not calculated in the same routine and therefore they may no longer be exactly compatible with each other (using the Kelvin equation). Finding the moisture content with the sorption and the suction curves respectively could also give two results that are not totally equal. Instead, the above pressures are treated as intermediate results that go into Fick's and Darcy's laws again to set up the balance equation that gives the new moisture content.

The new moisture content is calculated from the intermediate, new vapor fluxes from the vapor implicit/liquid explicit routine (2.1.22) and the intermediate, new liquid fluxes from the liquid implicit/vapor explicit routine (2.1.23):

$$u_1^{new} = u_1^{old} - \frac{\Delta t}{\rho_{0,i}\Delta x_i} [(g_{v,i+1}^{new} - g_{v,i}^{new}) + (g_{w,i+1}^{new} - g_{w,i}^{new})] \qquad (2.1.24)$$

The new moisture content may now be used to find the vapor and suction pressures from the retention curves. These pressures are the final "new" ones, that are used explicitly in the next time step.

Even if there was only one kind of transport (no liquid transport for instance) this way of proceeding would be necessary. The reason for this is that the moisture capacity is not constant. In the solution of equation 2.1.9 a straight line in the sorption diagram is followed during a time step (figure 2.4) resulting in an ending point that is somewhat off the curve on the convex side. The amount of moisture that is added to the control volume is assumed to be equal to the change in RH (given by the intermediate new vapor pressure) multiplied by the moisture capacity. Taking the new moisture content as the sorption curve value corresponding to the intermediate vapor pressure would therefore give a value that is too high (the triangle in the figure). Instead, the moisture content at the intermediate point is the one that fulfills the moisture balance, and the corrected new vapor pressure must be the sorption curve value corresponding to this moisture content (the square).
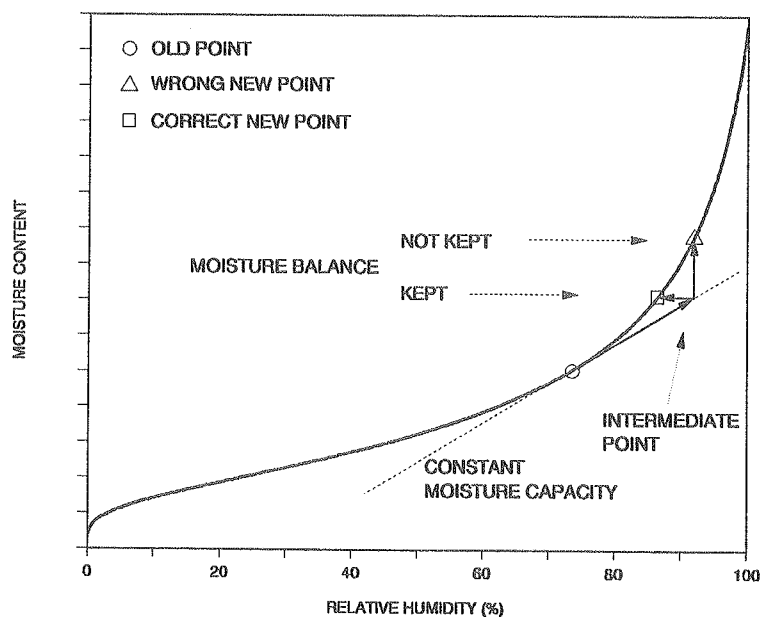

Figure 2.4   Paths in the sorption diagram during a time step.

However, since this is "cheating" with the new vapor pressure, the most correct thing to do is to perform an iteration in which the moisture capacity is fitted in each step towards a chord between the old and the new point. However, the uncertainty in material parameters means that such accuracy should not be necessary. The important thing is to keep the moisture balance.

2.1.4 CALCULATION OF HYSTERESIS

The way the calculations proceed in the MATCH program makes it easy to include hysteresis effects from the sorption and suction curves in the calculation. These effects are often mentioned when the sorption isotherms are presented and various reasons have been suggested to explain the phenomenon (Cohan, 1944; Luikov, 1966; Ahlgren, 1972; Pedersen, 1989a). However, it has never been thoroughly investigated what the practical implications of the hysteresis effects are for constructions of hygroscopic materials that have this effect.

In describing the hysteresis it is necessary to know the absorption as well as the desorption isotherms. The sorption properties of each material will therefore be described by two expressions like equation 2.1.10. How the wetting and drying suction curves are described has already been shown in section 2.1.2. The way hysteresis is accounted for will only be described for the sorption curves. Hysteresis in the suction diagram is dealt with in a similar way and will therefore not be shown.

When the moisture history of the material changes (from absorption to desorption for instance) the relation between relative humidity and moisture content is described by the scanning curves. The task here is to find a plausible way to describe such scanning curves. Experimental knowledge on these curves is not very exact but the scanning curves must be less steep than the absorption and desorption curves. Depending on the current direction of the moisture history, the scanning curves are asymptotically moving towards the curves describing either the pure desorption or the pure absorption situation.

In the program, the slope of the retention curves is the parameter that is used in the transfer functions to describe in what direction the pressure/moisture content relationship moves. An analytical expression has been derived to express the slope

42

of the scanning curve when the slopes of the absorption and desorption curves at the same relative humidity are known and the current direction of the moisture history is known. When for instance the absorption curve is left because the situation is changing towards drying, the slope of the scanning curve that is entered is set to one tenth of the slope of the absorption curve just left. As the desorption curve is approached, the slope is becoming more and more like that of desorption. This is described by:

$$u_{new} \leq u_{old} \quad : \quad \xi_{hys} = \frac{(u-u_a)^2 \cdot \xi_d + 0.1 \cdot (u-u_d)^2 \cdot \xi_a}{(u_d-u_a)^2}$$

$$u_{new} > u_{old} \quad : \quad \xi_{hys} = \frac{0.1 \cdot (u-u_a)^2 \cdot \xi_d + (u-u_d)^2 \cdot \xi_a}{(u_d-u_a)^2} \tag{2.1.25}$$

where

ξ_{hys} = Moisture capacity at hysteresis

ξ_a = Absorption moisture capacity at the current RH

ξ_d = Desorption moisture capacity at the current RH

u = Current moisture content

u_a = Absorption moisture content corresponding to current RH–value

u_d = Desorption moisture content corresponding to current RH–value
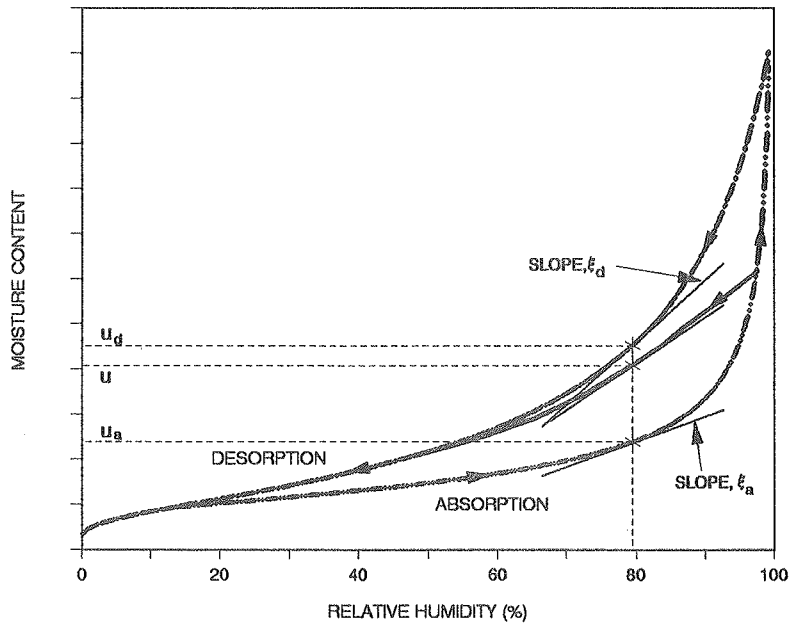
Figure 2.5   Absorption, desorption and scanning curves. The scanning curve is for the moisture history turning from absorption towards desorption.

Figure 2.5 shows these quantities. They are all derived from RH and u values from the previous time step.

With this moisture capacity in the transfer functions, the "intermediate" vapor pressures can be calculated. When the distribution of these vapor pressures is used in the transport equation (Fick's law) this gives vapor flows that result in the new moisture content. The final "new" vapor pressures are simply set equal to the "intermediate" values since there is no demand here that (φ,u) should lie on either the absorption or desorption curve (see figure 2.4). However, it is checked that (φ,u) is not outside the space between the two curves.

2.2 HEAT TRANSFER

Heat transfer is described in a similar way as the two types of moisture transport above. First, some transfer functions are defined as helping tools in the description of sensible heat transfer. These include functions that describe the boundary conditions with convection and radiation heat flows. Next, these transfer functions are used together with the influence from moisture transport to describe the changes of temperatures from one time step to another.

2.2.1 HEAT TRANSFER FUNCTIONS

To evaluate the transfer functions that describe the heat flow by conduction internally in the construction between consecutive layers, figure 2.1 is used again. The temperature in each grid point represents the temperatures of all points in the control volume it belongs to. The heat flow between the layers is described by the individual material properties of each layer, their thicknesses and the position of the nodes within the layers. The control volumes and the distribution of grid points in these are the same as in the calculation of moisture migration. Also, the time steps used in both calculations are the same.

HEAT CONDUCTION:

For heat conduction across a layer "i" with thickness Δx_i and a difference ΔT in

temperatures from one side to the other Fourier's law of heat conduction reads:

$$q = -k_i \frac{\Delta T}{\Delta x_i} = -\frac{\Delta T}{R_i} \qquad (2.2.1)$$

where

R_i = Thermal resistance $\qquad\qquad (\frac{m^2 K}{W})$

The resistance between two neighboring grid points can now be calculated as:

$$R_{i-1 \rightarrow i} = (1-f_{i-1})\, R_{i-1} + Rx_i + f_i\, R_i \qquad (2.2.2)$$

where

Rx_i = Extra thermal resistance between layers "i−1" and "i" $\quad (\frac{m^2 K}{W})$

Air gaps and layers that are not treated transiently could be represented by such an extra resistance between layers.

The conduction heat transfer function is now defined similarly to the definition of moisture transfer functions:

$$h_i = \frac{1}{R_{overall,i}} \qquad\qquad (\frac{W}{m^2 K}) \qquad (2.2.3)$$

Heat transfer functions are also updated at the beginning of each new time step using the old values of the variables to determine what the material parameters are in the current time step. In the computer program the thermal conductivity depends on the content of ice and liquid water in the material. This is done simply here by assuming all water to be frozen when temperatures are below 0^oC. The influence of temperature on the thermal conductivity is described by a linear relation as with the moisture influence:

$t < 0\ ^oC$: $k = k_{dry} + f_{k,ice} \cdot u + f_{k,t} \cdot T\ [^oC]$

$t \geq 0\ ^oC$: $k = k_{dry} + f_{k,w} \cdot u + f_{k,t} \cdot T\ [^oC] \qquad (2.2.4)$

where

$f_{k,ice}$ &

$f_{k,w}$ =   Water/ice content correction coefficients $(\frac{W}{m \cdot K})$

$f_{k,t}$ =   Temperature coefficient $(\frac{W}{m \cdot K \cdot ^0C})$

The correction factor for water/ice should only consider the effect of increased heat conductivity that is due to additional conduction in the water or ice and to the microscopic evaporation/condensation phenomena across the large pores. Macroscopic transfer of latent heat across the material is accounted for separately (as described later).

After the heat transfer function has been calculated as described above it can be used to calculate the heat flux by conduction from grid point "i–1" to "i" as:

$$q = - h_i (T_i - T_{i-1}) \tag{2.2.5}$$

BOUNDARIES:

Boundary conditions are not as simple for heat transfer as they were for moisture transfer since convection as well as radiation heat transfer between several objects has to be accounted for. In the following the boundary conditions will be discussed for radiation and for convection. Other phenomena at the boundaries are also mentioned that deal with different sorts of precipitation.

RADIATION:

Solar radiation is calculated for a tilted surface according to geometric formulas from Duffie & Beckman, 1980. The calculation accounts for direct, diffuse and reflected radiation. The passage of the sun across the sky is calculated from latitude, time of year and day and the declination of the sun. Required input is the global and diffuse radiation on a horizontal surface as hourly values, surface tilt angle and azimuth, reflectance of the ground and the latitude of the location. Finally the calculated irradiance, E [W/m²], is multiplied by the absorptance of the surface to yield the solar gain for the outmost layer (equation 1.2.5). The calculation does not account for shadows from surrounding objects or for the effect of snow on the surface characteristics of the surrounding ground and the construction itself.

46

The radiation exchange with the sky is calculated according to equation 1.2.7. Based on the assumption that the sky may be treated as a black body, its temperature is calculated approximately according to the following formula from Duffie & Beckman, 1980. The assumption that the dewpoint temperature has some correlation with the density of moisture (and other particles) in the atmosphere is used to account to some extent for the effect of clouds to increase the effective sky temperature:

$$T_{sky} = T_{out} \left(\frac{0.8 + T_{dew}}{250}\right)^{0.25} \tag{2.2.6}$$

All temperatures are given in Kelvin units in 2.2.6. The outdoor ambient temperature as well as the dew point temperature is read from the weather file.

A tilted surface sees more of the surrounding ground and vegetation than does a horizontal surface. As a first approximation they are treated as black bodies having the same temperature as the ambient air. The effective temperature with which the surface exchanges long wave radiation is then calculated as:

$$T_{rad} = \frac{1+\cos(\theta)}{2} T_{sky} + \frac{1-\cos(\theta)}{2} T_{out} \tag{2.2.7}$$

where
θ =   Surface tilt angle $(^0)$

This is the temperature that is being used for radiation heat exchange with the outer surface. In order to make the problem linear the radiation heat transfer coefficient is calculated in each time step as shown in equation 1.2.7:

$$h_r = \epsilon \, \sigma_r \frac{(T_1 + T_{rad})^3}{2} \tag{2.2.8}$$

where
T_1 =   Temperature of outmost layer (layer 1)   (K)

CONVECTION:

Convection heat transfer from the outer surface is described as in equation 1.2.8

using the convection heat transfer coefficient from equation 1.2.9. Wind velocities are read from the weather file as hour by hour values, and the transfer coefficient is updated each time. An extra surface resistance, Rx_1, may be added to the convection resistance, $1/h_c$. Rx_1 will probably be zero for all practical cases since the first grid point will be placed as far to the outside as possible in order to provide a good description of the rapidly changing conditions here.

Convection heat transfer from the inner surface is joined with the radiation heat transfer (it is assumed that the inner surfaces have room temperature). This is described by assigning Rx_{n+1} to the inverse of the sum of the radiation and convection heat transfer coefficient. The value 0.13 m2K/W is chosen by default when the preprocessor is used to create an input file. This value is kept constant during the calculation.

MEASURED SURFACE TEMPERATURES:

When the surface temperatures are measured in an experiment they are read by the program into the variables that contain the indoor and outdoor ambient temperatures. The radiation parameters are all fixed at the value zero, while the outside convection heat transfer coefficient is made artificially large. These precautions provide an outer surface temperature equal to the one measured.

The inner thermal resistance Rx_{n+1} must be fixed at an artificially small value to have the inner surface temperature equal the one measured or it could be kept at some reasonable value if the indoor room temperature is the one measured. This has to be done manually.

RAIN:

The impact of rain on the thermal equilibrium of roofs is of great importance. However, it is rather uncertain how rain stays on roofs. Some of it runs off, some stays as ponded water in small areas of the roof if it does not have a sufficient slope, and finally some evaporates over a period of time after the rainfall. Rain and other precipitation are therefore not considered in this work but the uncertainties involved in the description of other parameters should be viewed in

this perspective.

SNOW:

The effect of snow on the construction is not accounted for. A possible layer of snow provides some extra insulation on the outside of a horizontal construction, thus keeping its surface temperature higher during severe frost. At the same time it blocks the incidence of solar radiation and thereby prevents high peaks in daytime surface temperature. All in all, the impact of snow on the long time moisture distribution is limited (Sandberg, 1973).

SURFACE CONDENSATION:

In the night, when external surfaces may cool down below the dewpoint of the air, a layer of dew may form. The heat of condensation is released at the surface during this process. The reverse process takes place in the daytime when the surface warms up and the dew evaporates.

The computer program accounts for this phenomenon as it is easily described by the surface resistances for heat and vapor transfer. No accounting has been done, however, for the possibility that some of the condensed water may run off the surface if this is not horizontal.

CONTINUITY AND THE EQUATION OF STATE:

When thermal calculations are performed the enthalpy (compared to some reference level) is normally not computed. Instead the differential changes are converted directly to differential changes in temperature. The continuity equation for layer "i" for finite changes under quasi stationary conditions will therefore be (with the assumption that there are no source terms from the effects of moisture migration):

$$\frac{\rho_{0,i} \, c_{p,i} \Delta x_i}{\Delta t} \, \Delta T_i = - (q_{i+1} - q_i) \qquad\qquad (2.2.9)$$

The transfer function, h0, which describes the accumulation of enthalpy is implied herein since it is defined as:

$$h0_i = \frac{\rho_{0,i}\, c_{p,i}\, \Delta x_i}{\Delta t} \qquad (2.2.10)$$

The specific heat capacity c_p is calculated in each time step according to equation 1.2.3 consisting of the dry c_p–value plus the contributions $u_w \cdot c_{p,w}$ and $u_{ice} \cdot c_{p,ice}$ from the moisture as water and ice (since the content of vapor is insignificant).

2.2.2 COMBINING MOISTURE WITH HEAT TRANSFER

In permeable materials or at low moisture content the most important impact of moisture on heat transfer, as mentioned in section 1.4, is the release or uptake of latent heat by phase conversions. As described in chapter 1, these conversions give reason to sources of enthalpy within a control volume. However, the ice–water conversion is not being treated the same way as the water–vapor conversion.

The heat of ice formation is included in the heat capacity instead of being treated as a source. This is done by assuming the ice formation to take place over a range of temperatures from $-\Delta T_{ice}$ to 0^0C. In this region, the c_p–value is increased by the amount:

$$\Delta c_p = \frac{u \cdot \Delta h_{ice,w}}{\Delta T_{ice}} \qquad (2.2.11)$$

This is in accordance with the depression of the freezing point that takes place in porous materials because the ice is formed in the larger pores already at temperatures close to 0^0C and later in the smaller pores at lower temperatures. To treat the freezing point depression in the linear way shown above can be regarded as a first approximation.

Treating phase changes by increasing the heat capacity is also advantageous since it improves the stability of a numerical method whereas conversions that are treated as sources of heat within a control volume tend to decrease stability. However, heat of evaporation/condensation can not be treated the same way since this process takes place at all temperatures depending on the level of vapor pressures.

50

When the heat of evaporation or condensation is included in the continuity equation as a source, the equation will be:

$$h0_i \, \Delta T_i = - (q_{i+1} - q_i) - \Delta h_{w,v}(g_{v,i+1} - g_{v,i}) \qquad (2.2.12)$$

It is assumed that the difference between the amount of vapor that enters and leaves the control volume is condensed, i.e. there is no significant change of vapor content within the volume (since its amount is close to zero).

The temperatures are calculated first in each time step since they are used to determine the new saturation vapor pressures needed in the calculation of vapor transport. Thus, the fluxes of vapor used in equation 2.2.12 are those found from the vapor pressures of the previous time step. No attempts are made to perform an iteration in each time step or to solve the equations of moisture as well as heat simultaneously in an implicit method. This will require an excessive amount of computational effort and the accuracy gained is not justified by the somewhat uncertain material properties.

In some calculations of constructions with for instance mineral wool, which have a high thermal resistance and a high moisture permeability, the amount of latent heat can be as large or even larger than the heat conducted through the material. Since the latent heat is calculated explicitly this can give stability problems if the time steps are not adjusted accordingly. In the program a stability check is built in that reduces the time steps when changes in temperatures of interior points exceed the changes at the surfaces or exceed some reasonable number.

Convection heat transfer with the moving moisture in a construction is not accounted for since the amounts are very small compared with other heat transfers. However, when a dry control volume at a certain temperature is filled with liquid moisture at the same temperature no heat has been transferred. But since the heat capacity has increased according to equation 1.2.3, so has the amount of enthalpy within the control volume (if the temperature is higher than the reference for calculating enthalpy). This is an effect that has to be accounted for when the thermal balance of a construction is calculated.

CHAPTER 3
APPLICATIONS

The purpose of this chapter is to show some examples of interest for either the researcher or for the designer of building constructions where the developed model may be useful. Whenever possible, these examples have been supplemented with results of experiments that either have been carried out as part of the work in this project or have been described in the literature. Such experimental results have not been produced in such a way that — in the strict sense — they may serve as a validation of the model. Instead, they are used to indicate the ability of the model to simulate the experimental results — given the right material parameters. Once an agreement between model and experiments has been established, the experimental results may be extrapolated to other situations, using the model. The model has also proven to be a good tool in designing some of the experiments shown and in better understanding the results measured (Childs, Courville, Pedersen & Petrie, 1990).

The first section shows some examples of constructions calculated with and without hysteresis in the moisture retention curves being accounted for. The second section shows a simulation of experimental results for aerated concrete accomplished at the Thermal Insulation Laboratory in the beginning of the seventies. The experiment shown involves liquid as well as vapor transport and is therefore very suitable for comparison with the model since transport in the liquid phase is quite unimportant in the rest of the applications shown in this chapter. The third section describes typical design of low slope roofs and their problems. A new vapor retarder for such roofs is described, and results of some calculations on various constructions are shown. The fourth section deals with the transfer of latent heat caused by evaporation of liquid moisture from a warm area, migration as vapor and condensation at a cold spot. In some cases this becomes a very significant form of heat transfer — quite often the most important way in which moisture affects the thermal balance of a construction.

3.1 CALCULATIONS WITH HYSTERESIS

The presence of hysteresis in the retention curves has been known quite long and has often been reported as part of experimental results. Nevertheless, the practical implication of the hysteresis has not been subject to much research. In the first subsection, an example will be shown where the effect of the hysteresis has been artificially enhanced with the purpose of showing the shape of the simulated scanning curves. Next, a calculation for a real roof construction exposed to the Danish climate follows. Though accounting for hysteresis has been done in the sorption as well as in the suction diagram only the sorption scanning curves will be shown. This section should first of all be of interest for the researcher who develops models for moisture transport, while the importance for the construction designer is limited.

3.1.1 SPECIMEN WITH EMPHASIZED HYSTERESIS

A calculation has been performed on a piece of aerated concrete. The specimen, which is 3.5 cm thick, is equally divided into 7 layers and exposed at the bottom surface to a constant climate at 25°C. The top surface is exposed to a climate that gives surface temperatures varying between 0°C and 30°C in a sinusoidal way with time. The period of the sine function is 6 days. Both surfaces are sealed in order to be vapor tight and the starting moisture content corresponds to 56% RH at desorption.

Figure 3.1 shows the path in the sorption diagram followed by the (φ,u)–data of the top layer as time goes by . Top temperatures start falling from 15°C and therefore the upper layers tend to become more wet. The absorption curve is approached during this process with the first scanning curve. Within the first 3–4 days (the first piece of curve) the (φ,u)–data come quite close to the absorption curve. Then, a period with higher top surface temperatures follows and the (φ,u)–data now follow another scanning curve, rapidly moving away from the absorption curve and approaching the desorption curve more and more closely as time goes by. Finally, two more reversals are shown.

The example is somewhat hypothetical since most constructions are exposed to a climate that varies in diurnal cycles (except in the laboratory). However, the

example serves to show that the scanning curves followed have a plausible looking shape.
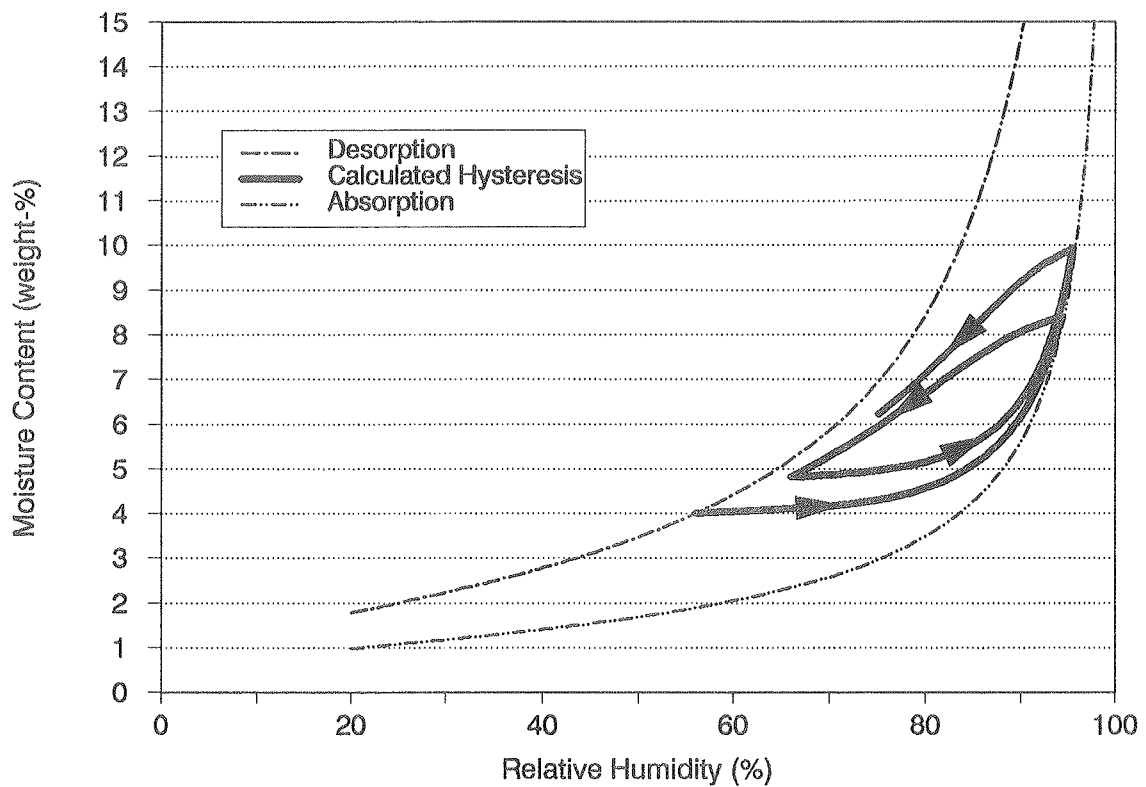
Figure 3.1   Scanning curves followed in the sorption diagram during extended periods of drying and wetting.

3.1.2 NATURALLY EXPOSED CONSTRUCTION

To the knowledge of the author only one earlier calculation has been reported in literature that accounted for the effect of hysteresis. Sandberg, 1973, calculated the drying of an aerated concrete roof using piecewise linear descriptions of absorption, desorption and scanning curves. Not surprisingly, since the whole construction was drying most of the time, it was found that the results of the calculation that accounted for hysteresis were close to those from a calculation that only used the desorption curve.

To determine whether hysteresis is important under periodic stationary conditions for real constructions exposed to a varying climate, a flat roof construction as shown in figure 3.2 was calculated. Its vapor retarder is of a new kind called the Hygro Diode, which is mentioned in section 3.3.2. The moisture content that is

critical for such a construction will often be that in the plywood deck (as mentioned in section 3.3). The moisture content here is therefore shown in the following figures. The outdoor climate is defined by the Danish Test Reference Year (TRY), while the indoor climate is kept at 21°C with a constant 3 g/m³ higher moisture content indoors than outdoors (dwelling conditions).
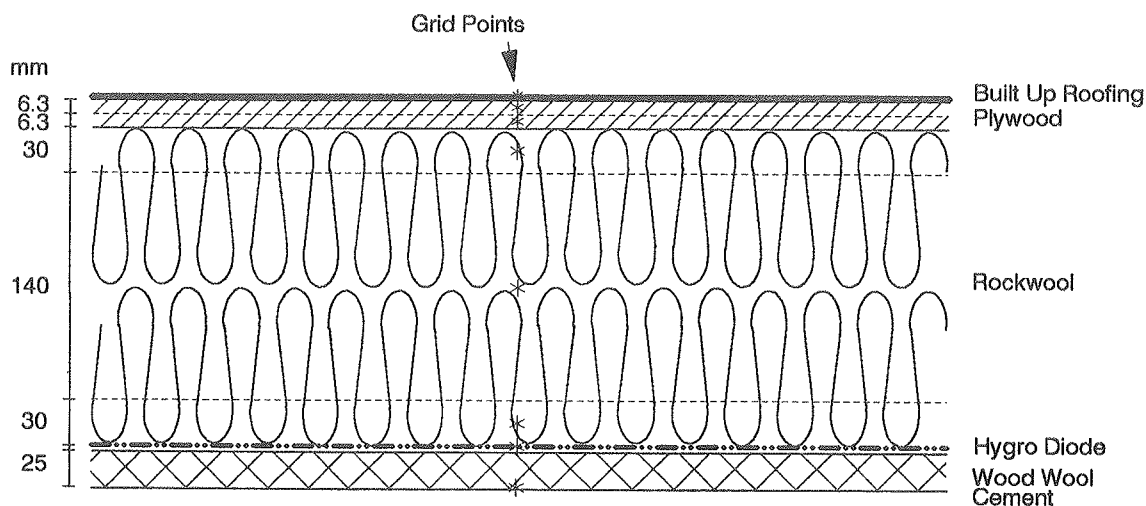
Figure 3.2   Flat roof construction in the calculation of hysteresis. Grid points are shown with markers.

The calculation is performed four times. The first calculation uses the absorption isotherm for the materials, the second uses the desorption isotherm, the third uses an average sorption curve while, finally, the fourth calculation assumes hysteresis to take place according to the model described in section 2.1.4. Results are shown in figure 3.3 as daily average moisture content as a function of time. Four years have been calculated but only the last is shown, as the first years are used for establishing initial periodic stationary equilibrium.

Not surprisingly, the results from the calculation that uses the absorption curve give the lowest moisture content, the calculations with desorption give the highest while the two other calculations give results laying in between. In this example, the results from the calculation with hysteresis follow the results of using the average curve quite closely. The results with hysteresis are slightly higher all the time. In a calculation for aerated concrete shown by Pedersen, 1989b the calculation with hysteresis gave results a little below the results obtained from the use of the average sorption curve. In any case, there is no reason why the results from accounting for hysteresis should be any more accurate than those of calculations using the average curve — considering the uncertainty such calculations

56
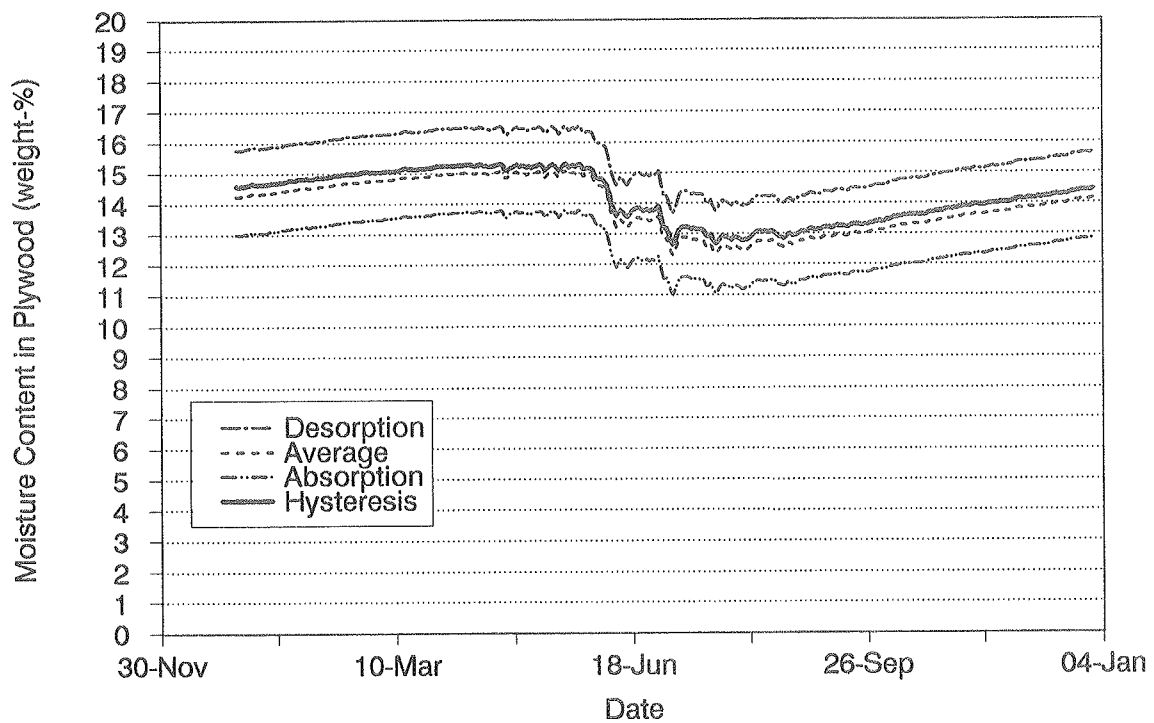
Figure 3.3   Moisture content in plywood deck as a function of time for calculations with absorption, desorption and average sorption curves and with hysteresis.

are performed with and the uncertainty in determining sorption parameters.

Why is it that the results with hysteresis do not come close to the absorption results during winter or to the desorption results in the summer? Figure 3.4 follows the path of the (φ,u)–data during some summer days that have been calculated with hysteresis. Though the wood is drying out somewhat from the first to the last day, there are shorter periods in the nights where it actually absorbs moisture. As the calculations of hysteresis are performed, a wetting scanning curve moves rapidly away (with a low moisture capacity) from the desorption curve, if the (φ,u)–data point is close to that curve. In the daytime, a drying scanning curve will have almost the same, larger moisture capacity as the nearby desorption curve and will therefore only approach this curve slowly. The result is that even small diurnal variations in the moisture history will bring the (φ,u)–data points close to the middle between the absorption and desorption curves. Only for extreme conditions of long periods of constant drying or wetting will the scanning curve coincide with either the desorption or the absorption curve, as shown in
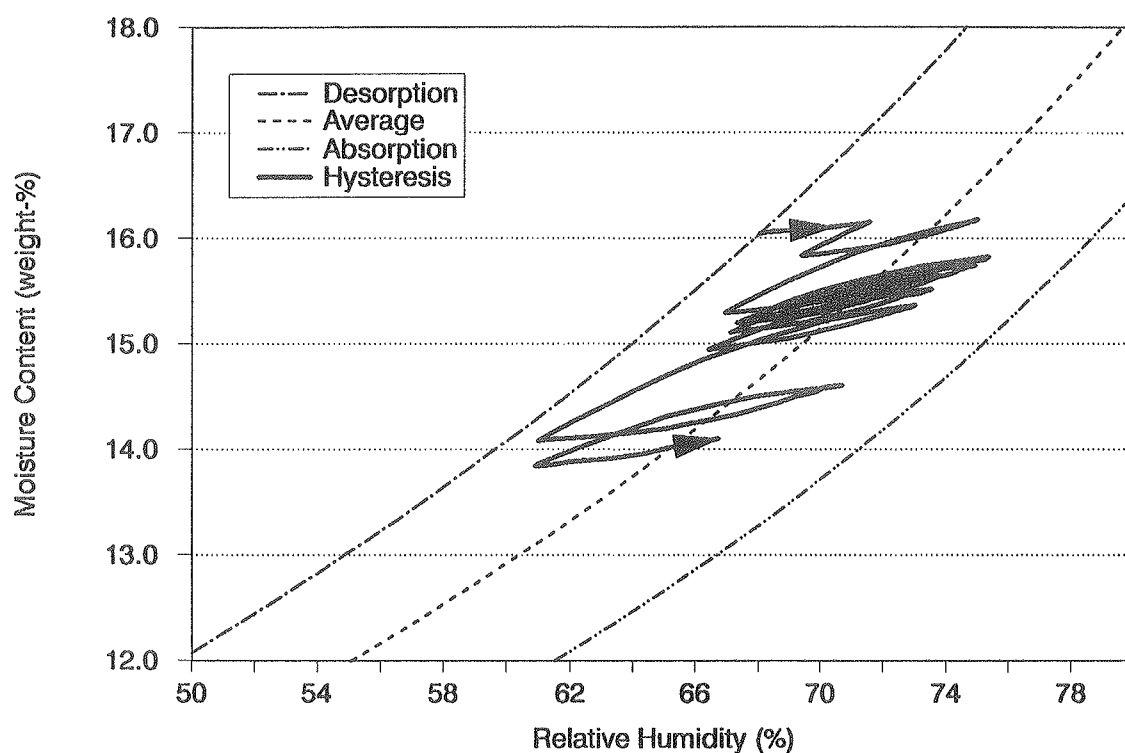
Figure 3.4   Path in the sorption diagram of the (φ,u)–data during a few
summer days (June 1 – June 9).

section 3.1.1.

For practical calculations the middle curve between absorption and desorption will give sufficiently accurate results, considering the ever remaining uncertainty in material properties.

3.2 SIMULATION OF DRYING EXPERIMENT

Most of the applications shown in chapter 3 deal with simulations with MATCH on constructions where the liquid transport is negligible. In order to validate the ability of MATCH to take also the liquid transport into account, predicted results of a drying experiment are compared with some older experimental results performed at the Thermal Insulation Laboratory of the Technical University of Denmark.

The experiments were performed on aerated concrete, initially saturated with water by use of vacuum. A gamma ray equipment was used in the experiments, carried out by Nielsen (1974) to determine the profiles of moisture content within the material. A cross section of one of the specimens is shown in figure 3.5. The specimen consisted of a 121 mm wide and 50 mm high cylinder of aerated concrete. The side and one of the ends of the specimen were sealed with layers of acryl and aluminum foil — being totally moisture tight. This setup was located in a room where the temperature was kept almost constantly at 23°C, with the dewpoint varying between 7°C and 13°C (the actual variation with time was reported by Nielsen and taken into account in this work). A fan kept the air velocity over the specimens at 1.5 m/s. Apart from the cooling that took place when the moisture evaporated from the surface of the specimen, the experiment was almost isothermal.

Figure 3.5   Specimen of aerated concrete used in drying experiment by Nielsen, 1974.

The initial drying rate for the specimen investigated (no. 197 in Nielsen's notation)

was almost constantly around $8.1 \cdot 10^{-5}$ kg/m²·s. This corresponds to the so-called first phase in a drying experiment (Krischer, 1978), when the capillary action inside the material transports the moisture to the surface at least as fast as the moisture is evaporated from the surface. Thus the drying rate is determined by the convective mass transfer coefficient. To ease the ca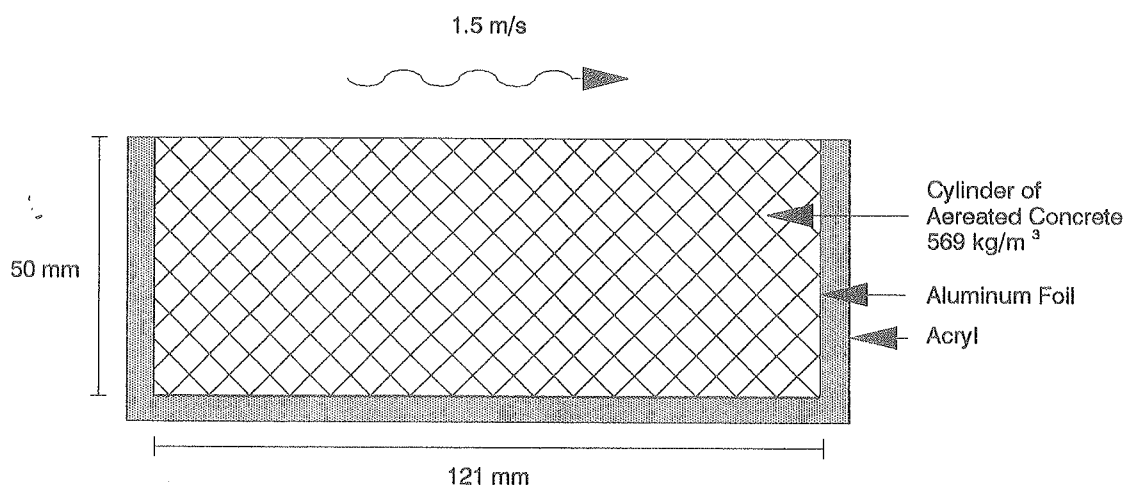lculation, it was assumed that the surface temperature was identical to the room temperature. This was insured in the calculations by having a large heat transfer coefficient at the surfaces. Under these conditions, an apparent mass transfer coefficient may be determined from the drying rate measured and from the difference in vapor pressures between the air (the dewpoint was measured) and the surface (saturation at the surface temperature). Alternatively, the actual surface temperatures would have to be calculated from temperatures that were measured in interior points and in the air.

At least the initial drying rate will be simulated correctly by assuming isothermal conditions. The assumed temperatures will be too high, but this should not be important in the first period when the internal moisture transport takes place in the liquid phase, since small changes of temperature do not affect the liquid transport much. Later, when the drying takes place by vapor diffusion, the drying rates are so small that the cooling by evaporation of water is limited. The mass transfer coefficient is not important in determining the drying rate accurately when the material is in the hygroscopic region, because the internal vapor resistance is much larger, i.e. the surface resistance corresponds to the resistance of approximately 0.5 mm aerated concrete. Thus, this simplified method of assigning values to the apparent convective mass transfer coefficient and the surface temperature should be allowable.

Moisture diffusivity as a function of moisture content was reported by Nielsen for the actual specimen (figure 3.6). This is, however, not the material parameter needed for MATCH. The moisture diffusivity is an effective quantity that includes information about the transport and the moisture retention properties of the material in one figure – common for both the hygroscopic and the over-hygroscopic region. The correlation between hydraulic conductivity, moisture capacity in the suction diagram and the liquid part of the moisture diffusivity is given by Pedersen, 1989a. The suction curve was determined according to the analytical expressions described in section 2.1.2 with the help of the pore size distribution given by Nielsen and using the values: $u_{vac} = 1.37$ kg/kg (78 vol-%) and $u_{cap} = 0.59$ kg/kg (34 vol-%). Thus, the hydraulic conductivity

Diffusion coefficient D_θ for cellular concrete determined by:
1. drying experiments (decreasing moisture content)
2. a stationary moisture flux (decreasing moisture content) } KOOI
3. a stationary moisture flux (increasing moisture content)
4. drying experiments (decreasing moisture content)
5. a stationary moisture flux (decreasing moisture content) } KRISCHER
6. theoretical curve for contribution of vapour transport ($D_{\theta v}$)
━━━ drying experiments by A.F. Nielsen, 1974

Figure 3.6   Moisture diffusivity for aerated concrete as determined by Kooi
              and Krischer and determined for the actual specimen by Nielsen.

was calculated in several intervals from:

$$K = D_\theta \cdot \rho_0 \cdot \Xi$$ (3.2.1)

Where

D_θ = Moisture diffusivity (m^2/s)

The water vapor permeability used was defined according to equation 2.1.4 by
$\delta_{dry} = 30 \cdot 10^{-12}\,kg/(Pa \cdot m \cdot s)$ and $\delta_{wet} = 60 \cdot 10^{-12}\,kg/(Pa \cdot m \cdot s)$. Finally, the
critical moisture content for the material was 0.314 kg/kg (18 vol-%).

Nielsen measured the moisture content in nine points in the material, each 5 mm
apart with the first point 5 mm from the open surface. To calculate moisture
content at the same points in which they were measured, a grid for the numerical
solution was chosen with 21 control volumes of which the central 19 were 2.5 mm
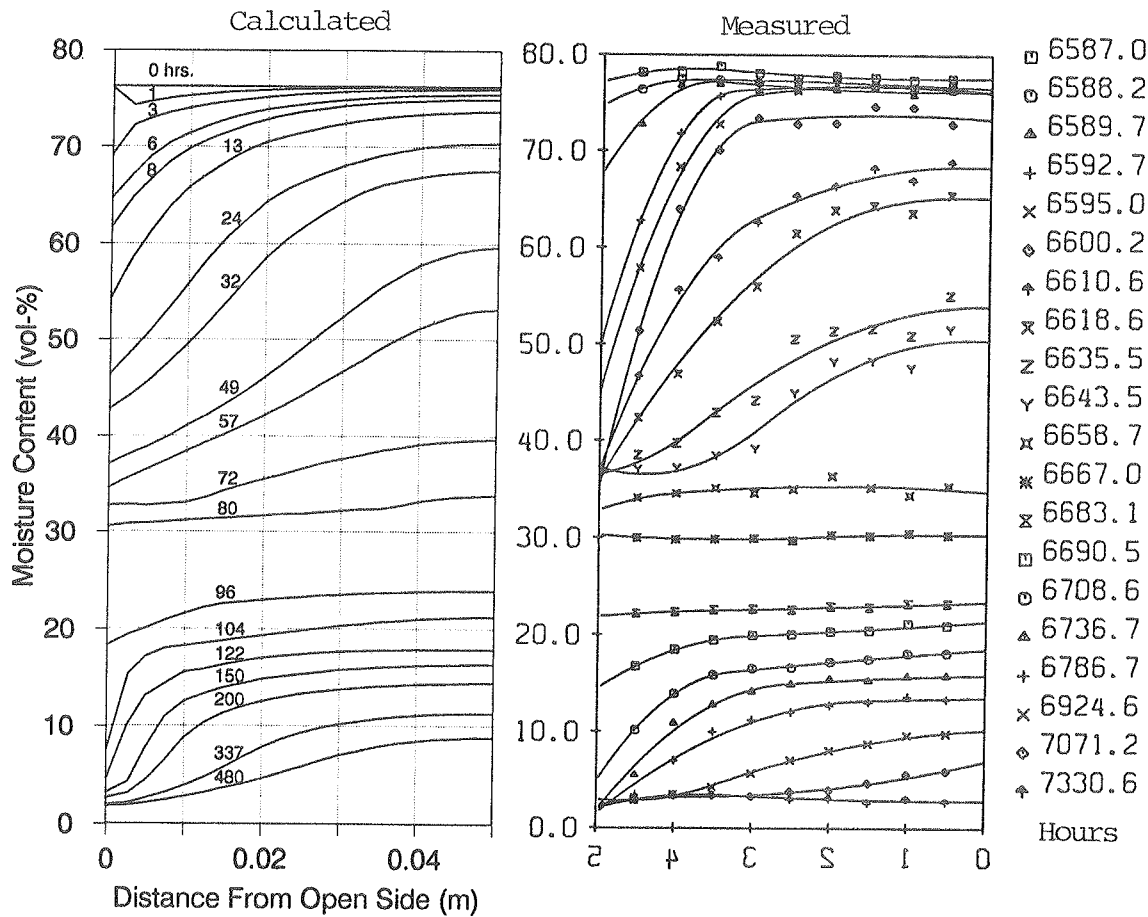
Figure 3.7   Calculated and measured distribution of moisture content (vol–%) at different times.

wide and the two next to the boundaries only 1.25 mm.

Calculated and measured results are compared in figure 3.7 and 3.8. Figure 3.7 shows the distribution of moisture within the specimen at certain times. The times at which the calculated results are shown correspond (usually within an hour) to those for the measured results, except for the last set of measured results which was not calculated. The agreement is quite satisfactory. The calculation does, however, deviate in the following ways: (1) The first hour the calculated moisture distribution has the wrong slope close to the open surface. There is apparently some slight instability in the beginning. (2) The moisture content measured for the surface tends to gather around 40% for the first approximately 60 hours. This is not seen as clearly with the calculated results. (3) Conversely, the calculated slope of moisture content next to the surface is larger than the measured slope for moisture contents less than 20%. (4) The drying rate is a little less in the

62

calculated results than in the measured results.

The general shape of the curves may be explained as follows:

— Initially, all the internal moisture transport is in the liquid phase. The moisture capacity is not very high when moisture content is close to vacuum saturation and all of the material therefore dries out quite easily — this is why the moisture distributions in the first few cases in figure 3.7 are almost horizontal lines.

— As soon as the moisture content has decreased a little the moisture capacity increases to a large value (compare with the slope of the drying curve at suction pressures around 1000 Pa in figure 1.4, which could have been for aerated concrete). In this region large gradients in moisture content do not correspond to very large gradients in liquid pressure. The moisture content in the deeper layers will therefore not change much before the moisture content close to the surface has become appreciably lower, i.e. large moisture content gradients are seen when the moisture content itself is between 40 and 70 vol–%.

— Around the moisture content for capillary saturation the moisture capacity becomes small again. Small moisture content gradients will now correspond to large pressure gradients that give the sufficient transport — even though the hydraulic conductivity is declining. All points of the material therefore have almost the same moisture content for a period shortly before 100 hours.

— Later, the liquid transport vanishes and at approximately the same time the hygroscopic region is entered. This gives vapor pressure gradients that lead to the rest of the transport. The shape of the moisture distribution curves may be explained by similar arguments as before for the moisture capacity — now in the sorption diagram.

In terms of moisture diffusivity (figure 3.6), the same trends could have been explained by a high moisture diffusivity close to vacuum saturation, a small diffusivity between 40 and 70 vol–%, an increase to a local maximum around the value for capillary saturation and a decline in the liquid part of the moisture diffusivity when the moisture content decreases further. The vapor part of the moisture diffusivity often has a shape like a narrow bell with a local maximum in the middle of the hygroscopic region. This maximum is a result of the low slope of the sorption isotherm at RH–levels between 20 and 80%.

Figure 3.8 shows the development of the moisture content with time for the points in which it was measured. The measured and calculated results agree quite well in

this diagram also. The largest discrepancy occurs after 100 hours when the critical moisture content is passed. The problem is the numerical description when the hydraulic conductivity, within a very short range of moisture content, is reduced to a negligible number. When this happens, the surface layer feels less moisture coming from the inside and therefore it becomes hygroscopically dry very fast. Thus, for the layers next to the surface layer to dry out, moisture has to diffuse through the surface layer, while at the same time liquid moisture keeps coming from the deeper layers. This causes the deflections seen and is also the reason why the surface layer dried out very fast in the calculated curves of figure 3.7 for moisture contents less than the critical.
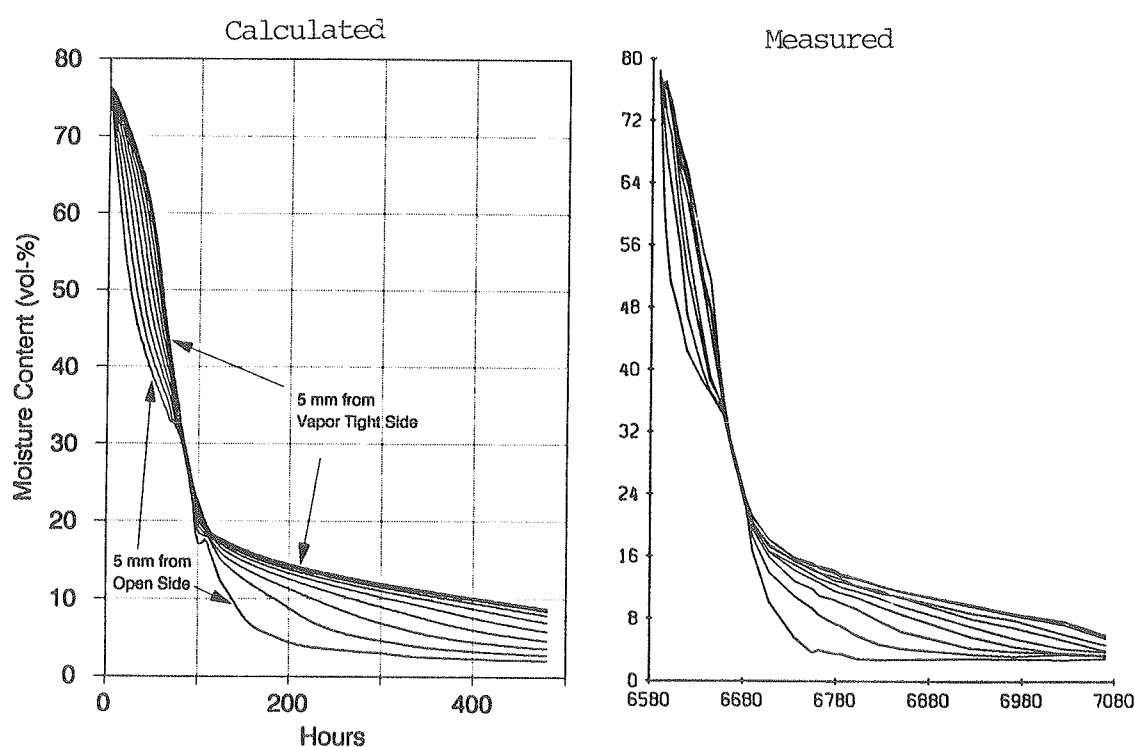
Figure 3.8   Calculated and measured changes of moisture content with time for the points measured.

The other small discrepancies mentioned before may not be easily explained. It should be noted though, that Nielsen, in determining the moisture diffusivity, artificially generated some extra curves like those from figure 3.7 in between measurements. This was done by parabolic fitting, with time as the independent variable, of the measured results in each point (his figure 5.19). These curves look somewhat more like those shown in figure 3.7 for the calculation in the region before 60 hours, where the surface moisture content does not immediately drop to

64

40%.

It appears from working with the computer program on this example that there are a number of material, convectional and grid generational parameters that can be varied, and quite many of them may change the calculated results significantly. Thus, to some extent, it is possible by qualified guessing to achieve the desired results by iteratively varying the right parameters. The material parameters were chosen here quite neutrally by using the data given by Nielsen or by making sensible judgments of how to assign certain values to the parameters (the convective mass transfer coefficient for instance). But also by working on the numerical grid is it possible to alter the results obtained significantly. However, most of the results from varying some of the parameters in this example affected either the time scale of the processes or gave some odd numerical deflections. The general shape of the curves was always the same, which must mean that the model handles the physical description of the problem correctly.

It has often been said among moisture researchers that it is easier to produce the numerical models for combined heat and moisture transport than it is to determine the material properties required by such models. This conclusion may also be a true one for the calculation of this example, though some of the material data were quite well defined this time. But to obtain further agreement between measurement and calculation it is probably also necessary to give a more accurate description of the convective heat and mass exchanges at the surface and to devise a numerical grid that handles the area next to the surface better.

3.3 MOISTURE PROBLEMS IN LOW SLOPE ROOFS

Unfortunately, low slope roofs have had a bad history in Denmark in the last decades with an appreciable number of cases with failure due to moisture intrusion. The most important impact of the moisture is the deterioration by corrosion, rot decay and physical disintegration of the construction materials that calls for repair if the failures have been discovered in time or for total replacement of the roof if the process has been going on for too long. Secondary problems are the decreased thermal performance of the roof when it is wet and the discomfort or damage that arises from possible dripping from the ceiling. The northern, coastal climate in Denmark with moderately cold and humid winters is not the only climate in which moisture problems occur in low slope roofs. In the United States it is realized that many roofs do not last for much more than 10 years before they need repair or replacement. Such short lifetime cycles must be regarded as a loss of construction materials — especially when many roofs do not perform very well before they are replaced.

The first subsection, 3.3.1, is a survey of typical low slope roof types and their characteristic moisture related problems. The second subsection describes a new type of vapor retarder developed around five years ago, which has the ability to dry out wet roofs and at the same time prevents further accumulation of moisture in the roof cavity. The last subsection shows applications of the MATCH program in the analysis of various types of roofs under conditions where convection flow has been eliminated.

3.3.1 LOW SLOPE ROOF SYSTEMS

There are three main types of low slope roof systems as shown in figure 3.9. Variations of these types may be seen as new roofs and as re–roof constructions where extra insulation has been added — usually on top of the existing roof. Such variations, called hybrid roofs, will not be dealt with here as their performance may be derived from the description of the three main types.

66

A: Cold Deck Roof

Membrane
Deck
Air Space

Insulation

Vapor Retarder
Ceiling

B: Warm Deck Roof

Membrane

Insulation

Vapor Retarder

Deck

C: Inverted Roof

Ballast

Insulation

Membrane
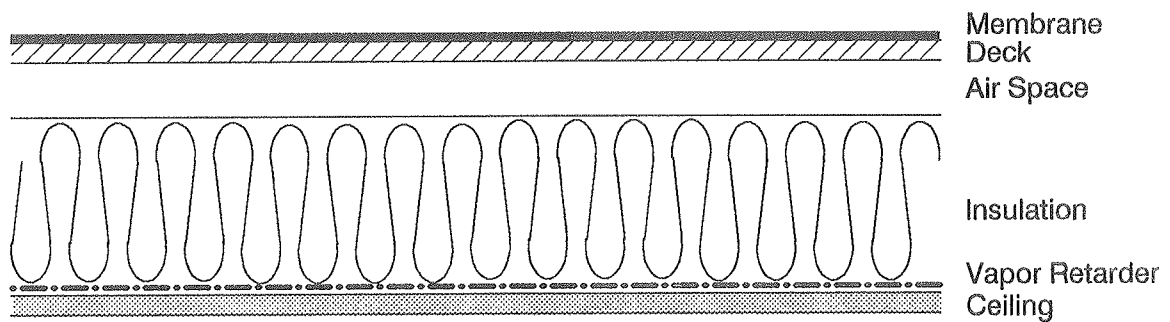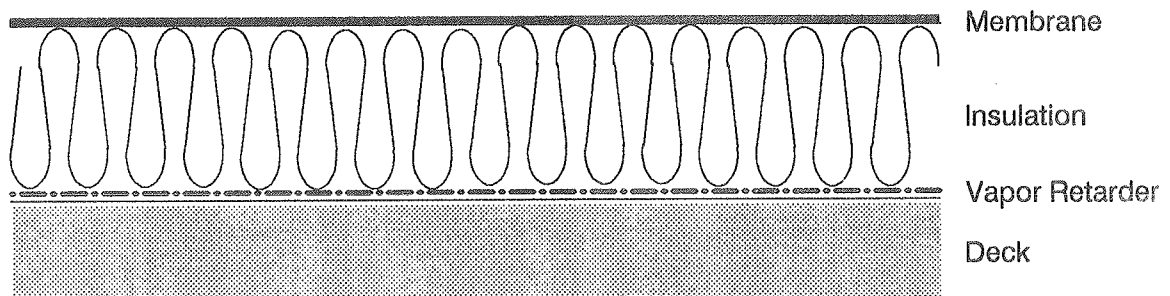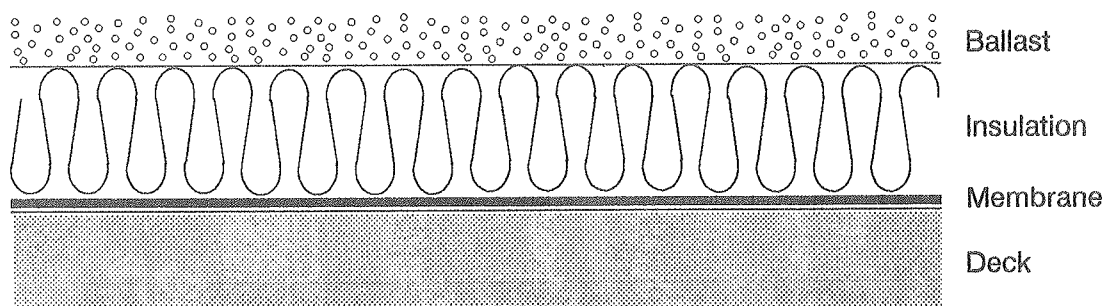
Deck

Figure 3.9   Three main types of low slope roof systems.

COLD DECK ROOFS:

The cold deck roof (drawing A) is one in which the structural deck is placed on the outside of the insulation, the cold side. The deck is either of wood and supported by wooden beams or it is a steel deck in a steel structure. On top of the wooden deck is the weather protecting membrane of for instance modified bitumen or built up of bituminous roofing felt. Between the deck and the insulation there is an air space, no less than 4–5 cm if it is ventilated. The Danish Building Code, BR 82 (Byggestyrelsen, 1982) requires that roof constructions are designed in a way to eliminate the possibility of harmful condensation on surfaces inside the construction, for instance by providing ventilation of the air space by air gaps at the perimeter of the roof and/or by vents distributed over the roof surface. The total cross sectional area of these openings should be 1/500 or more of the roof area. The validity of this precaution will be discussed later. The insulation will often be a low density mineral wool (10–30 kg/m³). The underside of the beams is clad with a ceiling material – for instance gypsum, wood, wood wool cement or there is a suspended ceiling. At least in northern climates a vapor retarder should be added on the warm side of the construction, i.e. between the ceiling and the insulation, and the retarder should be sealed properly around edges and at overlaps.

In one version of the cold deck roof the ventilated air space is omitted or, at least, there is no ventilation with outdoor air (the void becomes necessary if, for mechanical reasons, the construction height must be above the desired insulation thickness). The unvented roof may also fulfill the requirement of the Danish Building Code, as will be shown later. The definition of a cold deck roof has often been that it was ventilated, and the unvented roof has sometimes been called a compact roof. In the rest of the text the specification of a cold deck roof will refer to the location of the deck relative to the insulation and it will be specified separately if it is ventilated.

WARM DECK ROOFS:

The warm deck roof (drawing B) is one in which the structural deck is located on the warm, interior side of the insulation. The deck may consist of concrete, aerated concrete, steel or wood. Above the deck is the vapor retarder. It serves to

68

prevent moisture intrusion from the room, but also to prevent construction moisture from the deck from migrating upwards into the roof cavity. Above the vapor retarder comes the insulation, and finally a membrane. Most types of insulation may be used here. The requirement is that it can withstand the load from traffic on top of the roof. This is ensured by various insulations (extruded and expanded polystyrene, polyisocyanurate, polyurethane and mineral wool with vertical fiber orientation). Mineral wool should be of high density (80 kg/m^3 or more) and have a plate of wood fibers or compressed mineral wool on top to distribute the load. Fire preventing requirements may also prohibit the use of inflammable materials next to the surface. The membrane may be of modified bitumen, a built up of roofing felt or a single ply rubber or plastic membrane. It may be attached by fasteners that penetrate the insulation, adhered to the insulation or held in place by a ballast of gravel or pavers. The membrane may be provided with a small number of pressure release vents to prevent a build up of high pressures within the roof cavity in warm weather, though the necessity of taking this precaution may be doubtful.

INVERTED ROOFS:

The inverted roof (drawing C) is a version of the warm deck roof where the weatherproofing membrane is moved down below the insulation. At this location it is less exposed to variations of temperature, UV–radiation or mechanical stress and should therefore last longer. The insulation is exposed instead, so now *it* must be able to sustain the outdoor climate. On top of the insulation is a ballast of gravel or pavers that keep the insulation from blowing off.

MOISTURE SOURCES:

The moisture enters a roof in three ways. Here they are listed according to relative importance: (1) By leaks in the weatherproofing membrane. (2) By convection of indoor air into the colder roof cavity where condensation may take place. (3) By diffusion. Further, there may be considerable amounts of moisture left from the construction phase – either because the construction materials have not been dried out or because precautions against penetration of rain have not been sufficiently careful before the final sealing of the roof.

LEAKS IN THE MEMBRANE:

Leaks in the weatherproofing membrane ought to be simple to take care of, but in practice it is not enough to specify that the work should be carefully done. Of course errors like puncturing a membrane with a shovel during construction are trivial, but errors may also occur in the design of the roof. Here a few such errors will be mentioned:

- Bad selection of interacting materials around flashings and at penetrations may cause differential movements due to different temperature coefficients for expansion. This may cause wear that eventually results in failure of the membrane.

- The same is the result if the membrane is not flexible (like non–modified bitumen products) and adhered to a support that changes dimension with temperature and moisture content – as polystyrene does.

- The roof should be designed with a slope of at least 1:40 towards a drain to avoid the possibility of ponding water that may cause damage during freezing/thaw passages. Sometimes the drain is the highest point of the roof because it is located at the same place as the support of the roof and the rest of the roof will therefore stay more or less sagging.

- The addition of a PVC single ply membrane on top of a built up roof in a re–roof job causes migration of the plasticizer out of the PVC and as a result it becomes less flexible.

CONVECTIVE AIR FLOW:

Convective air flows are caused by pressure differences that arise from the stack effect (warm indoor air being lighter than cold outdoor air), from wind pressures and from mechanical ventilation. The air pressure difference from the stack effect of a 2.3 m high room is calculated when the temperature is 20°C indoors and 0°C outdoors:

$$\frac{\partial \rho}{\partial T} = -\frac{P}{R_a \cdot T^2} = -\frac{101\,300 \text{ Pa}}{287.1 \frac{J}{kgK} \cdot (283 \text{ K})^2} = -0.00441 \frac{kg}{m^3 K} \qquad (3.3.1)$$

$$\Delta P = -\Delta\rho \cdot g \cdot h = -9.81 \frac{m}{s^2} \cdot (-0.00441 \frac{kg}{m^3 \cdot K}) \cdot h \cdot \Delta T =$$

$$0.043 \frac{Pa}{m \cdot K} \cdot h \cdot \Delta T = 0.043 \frac{Pa}{m \cdot K} \cdot 2.3 \text{ m} \cdot 20 \text{ K} = \underline{2.0 \text{ Pa}} \qquad (3.3.2)$$

where

ρ	=	Density of air	$(\frac{kg}{m^3})$
R_a	=	Gas constant for air	$(\frac{J}{kg \cdot K})$
P	=	Atmospheric pressure	(Pa)
g	=	Acceleration of gravity	$(\frac{m}{s^2})$
h	=	Room height	(m)

Equation 3.3.1 is calculated from the equation of state for ideal gases at the average temperature 10°C. "Δ" means "indoor minus outdoor" so that the pressure is constantly higher indoors when it is cold outside. Thus, there is a constant potential for convection of indoor air out through the construction.

Suppose there is a 1 mm by 1 m crack in the vapor retarder under these pressure conditions. The air flow through the crack will be $1.13 \cdot 10^{-3}$ m³/s (Tagpapbranchens Oplysningsråd, 1985), and if the indoor relative humidity is 50% (8.6 gram vapor per cubic meter of air) 35 g moisture will penetrate through the opening per hour — some of which will condense at the top of the roof which is close to 0°C (saturation vapor concentration is 4.8 g/m³). In comparison, the diffusion through an intact 0.05 mm polyethylene vapor retarder (z = 100 GPa·s·m²/kg) will only give a moisture transport around 0.02 g/m²h. The condensate from the air flow through the crack is therefore, in magnitude, the same as that which diffuses through approximately 1000 m² of vapor retarder. This illustrates the importance of convection.

The pressure field around buildings when the wind blows is characterized by high air pressures on the windward side and low pressures above the roof and on the lee side, compared with the pressure inside the building. An investigation by Nicolajsen, 1983 of low slope roofs showed that even when a cold deck roof is ventilated from one roof edge to the other, without vents on the roof surface, the pressures within the cavity, on average, are less than inside the building. The purpose of such roofs being vented is, allegedly, to have the dry outside air absorb whatever moisture migrates to the top of the roof. However, once the air space is vented, it is at a lower air pressure than indoors, and convection into the construction takes place at a steady rate no matter how efficient the ventilation is. The effect of the ventilation is often that more moisture is driven up in the cavity by convection than is removed. Only when the roof slope is increased to 1 in 12 or

more does the stack effect within the roof cavity help making the ventilation efficient enough to remove the moisture (Tobiasson, 1988). Danish investigations of several commercial and residential roof constructions concluded that neither ventilation of cold deck roofs nor pressure equalization of warm deck roofs proved effective in solving moisture problems. Sometimes these precautions even made the problems worse (Korsgaard et al., 1984). A similar conclusion was drawn by Tobiasson, 1983. In these reports it was shown that mechanical ventilation of the roof cavity with outdoor air provided the needed drying effect.

So far the discussion has not been dealing with the effect on convection of a possible vapor retarder. If the vapor retarder is attached perfectly tight at all edges, and seams are tightened properly, there should be no convection problems at all. It turns out, however, that in practice the vapor retarder is almost never perfectly air tight. As it is located at the warm side of the roof, penetrations for electrical equipment and other utilities are hard to avoid and these are not always tightened as they should be. Canadian building researchers often talk about an air–vapor retarder instead of only a vapor retarder to emphasize the importance of stopping the intrusion of humid indoor air. Sometimes a relatively air tight but diffusion open material like plates of gypsum or plywood may be preferable, when the cracks are tight, to having a perforated vapor tight membrane.

DIFFUSION:

As illustrated by the calculation example above, vapor transport by diffusion contributes to a much lesser degree to the moisture equilibrium of the roof than that which may be transported by convection or, of course, by direct intrusion of liquid water. Diffusion therefore is only worth considering once all other transport mechanisms have been eliminated.

When it comes to diffusion, it will take quite some time for large amounts of moisture to migrate into an initially dry roof or reversely to dry out an initially wet roof if a vapor retarder is present. It is important, though, to notice that even if there is no potential for convection the vapor retarder must be kept tight along its perimeter and at penetrations. Small holes will significantly reduce the overall vapor resistance of the retarder. Such holes will also serve as a path for any accumulated summer condensate to drip into the room — thereby causing a drying

72

of the roof, in an undesirable way.

If the roof membrane is practically diffusion tight (for example a built up of bituminous felt), all the vapor transfer is between the room and the roof cavity. In most climates, moisture will diffuse into the roof in winter and out in the summer. In order to evaluate, in a simple way, what way the moisture content goes for a whole year, one may look at the sum of the vapor pressure differences across the vapor retarder for each hour of the year. By using the Danish Test Reference Year (TRY) these "Pascal–hours" were calculated with MATCH for a warm deck roof with a black surface ($\alpha = \epsilon = 0.9$) insulated with 15 cm mineral wool and supported by 25 mm wood wool cement. 1 kg moisture was added to the cavity per square meter roof. Thus, there would always be condensation at the coldest spot in the cavity. The results of the calculations are shown in table 3.1 and 3.2 for different indoor vapor concentrations. The sums are made separately for pressure gradients up and down. In the first table it is assumed that the indoor moisture concentration is a constant value higher than the outdoor value (higher air exchanges in the summer period are not considered), and the relative humidity is constant in the second table. Indoor temperature is 21°C throughout the year.

$c_{in}-c_{out}$	1	2	3	4	5	g/m^3
Upward	435	967	1571	2210	2886	kPa·h
Downward	4300	3643	3058	2508	1995	kPa·h

Table 3.1   Sum of vapor pressure differences between the indoor air and a moist low slope roof cavity at different higher moisture concentrations, c, indoors than outdoors. The roof surface is dark and the indoor temperature is 21°C.

RH	40	50	60	%
Upward	1078	2099	3264	kPa·h
Downward	5648	4489	3474	kPa·h

Table 3.2   Sum of vapor pressure differences between the indoor air and a moist low slope roof cavity at different indoor relative humidities. The roof surface is dark and the indoor temperature is 21°C.

It is seen from these tables that the indoor relative humidity must be 60% or less if it is constant over the year, or the moisture concentration must not be more than 4 g/m³ higher indoors than outdoors if long term moisture accumulation is to be avoided. If the roof surface is not dark, or if the saturation pressures do not occur within the structure because it is dry or because there is a hygroscopic layer in the cavity, the balance between upward and downward gradients may be changed so that moisture accumulation will take place even if the tables do not say so.

Roofs with single ply membranes have a vapor resistance towards the exterior that may be the same as for the vapor retarder or less. The permeabilities of some membranes (at least EPDM – "Ethylene Propylene Diene Monomere") have been reported to increase significantly with increasing temperature (Dupuis, 1985). It has been a concern in hot, humid climates that the moisture may have easy access to the interior of the roof when it diffuses through the membrane under these conditions. However, in most climates it would be regarded as an advantage to have this low vapor resistance at the exterior because it allows the amount of moisture diffused through the vapor retarder to diffuse further out to the exterior before it causes damage. A transient calculation with MATCH of a roof with an EPDM membrane is be shown in section 3.3.3.

IMPLICATIONS ON COLD DECK ROOFS:

As described above, ventilation of cold deck roofs may do more harm than good unless it is insured that the ventilation is highly effective in all parts of the roof, preferably as over–pressure maintained by mechanical ventilation. If the ventilation is omitted the moisture equilibrium – in the ideal case with no imperfections of the roof and its membrane in particular – will depend on a fine balance between the amount diffused into the roof in the winter, and out of the roof in the summer. A high moisture content within the roof, for example from the construction phase, will have little chance of escaping before causing damage. If the underlying room has a high relative humidity this may lead to a long term moisture accumulation in the roof, because more moisture will enter than leave the cavity in the annual cycles. A new kind of vapor retarder, the Hygro Diode Membrane, will be described in the next section. This vapor retarder should be able to dry out reasonable amounts of moisture thereby increasing the permissible range of indoor humidities.

74

IMPLICATIONS ON WARM DECK ROOFS:

Most of that which has been described for a cold deck roof also applies to a warm deck roof. If a roof is supplied with openings for pressure equalization, convection of air from the underlying room may still be possible through inevitable leaks. Such leaks may themselves serve as holes for pressure equalization towards the underlying room. Thus, it may be better to make the roof membrane perfectly air tight, without breather vents, to insure that no convection takes place. Any air/vapor at high pressure inside the cavity will probably always find a way to escape.

With decks of concrete or similar materials, construction moisture may migrate from the deck into the insulation if there is no vapor retarder in between. It is therefore necessary in all climates to use a vapor retarder over such decks.

IMPLICATIONS ON INVERTED ROOFS:

The inverted roof does not show the problems with entrapped moisture that were seen with the other types of roof. The problem with inverted roofs is to keep the insulation sufficiently dry to insure its insulation value is not decreased too much. First of all, this is insured by using materials that do not absorb moisture. Open cell foam insulation such as expanded polystyrene (bead board) is therefore not usable. Instead extruded polystyrene, with closed cells, or mineral wool, with a draining capability may be used. For these materials, a 10–20% decrease in R–value should be expected compared with their dry R–value (Statens Byggeforskningsinstitut, 1984). Research by Christensen et al., 1986 showed that also polyisocyanurate may be used as insulation in inverted roofs, while Tobiasson, 1987 found that urethane was not usable since it absorbed as much moisture as the expanded polystyrene did.

Tobiasson mentioned the following precautions against the accumulation of moisture in the insulation boards: (1) The membrane and the top of the deck must have a slope to be able to drain whatever moisture penetrates through the joints between the insulations boards and (2) gravel is better than pavers as ballast because it provides a better ventilation of the insulation with outdoor air.

An important drawback of the inverted roof is the difficult detection and repair of possible leaks in the membrane due to its inaccessible location between the other materials.

3.3.2 THE HYGRO DIODE MEMBRANE

The Hygro Diode Membrane (or just the Hygro Diode) was developed at the Technical University of Denmark in the latter half of the eighties (Korsgaard, 1985). It is a new type of vapor retarder with capabilities (1) to act as a regular vapor retarder by preventing moisture intrusion by diffusion and (2) to dry out excessive moisture from the roof cavity. The advantage, when this vapor retarder is used in a non–vented cold deck roof or warm deck roof, is that the moisture can escape even if it is located between two vapor tight materials. The design of the Hygro Diode will be described in this section and results from laboratory tests of its drying capabilities will be shown together with results from field tests. MATCH predictions will supplement both of these experimental results.

DESIGN OF THE HYGRO DIODE:

The Hygro Diode consists of 0.5 mm of synthetic felt made of a mixture of modified polypropylene and cellulose fibers. On each side of the felt, stripes of polyethylene (the material used for regular vapor retarders) are placed so that the stripes on one side overlap the space between the stripes on the other side (figure 3.10). In the version of the Hygro Diode commercially available, each stripe of polyethylene is 18 cm wide and the space between stripes is 6 cm. This leaves 6 cm where the polyethylene of a top stripe overlaps the polyethylene of a bottom stripe.
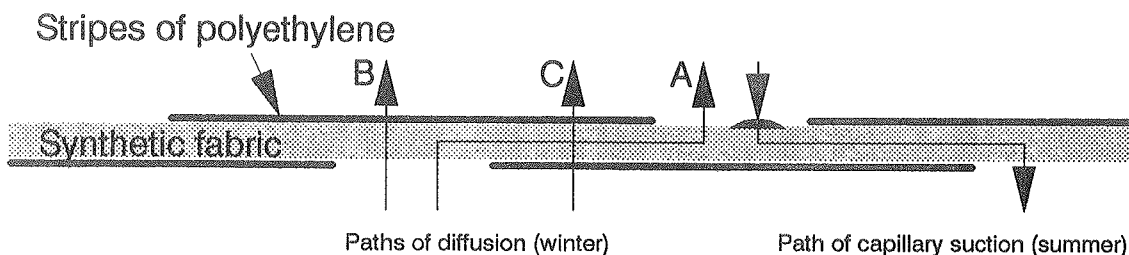

Figure 3.10   Cross section of the Hygro Diode. The arrows show the major paths for diffusion through the membrane.

Although vapor diffusion through a plain sheet of felt is practically unhindered, the design of the Hygro Diode gives a high resistance against vapor flow. The major ways in which vapor may diffuse from the room below, through the membrane and into the roof cavity above are also shown in figure 3.10. The moisture may either zigzag its way by entering the felt where it is uncovered at the underside, diffuse through the narrow path between the polyethylene stripes and exit from the uncovered part of the felt at the top (path A), or it may diffuse through the felt and through either one or two layers of polyethylene in a direction which is perpendicular to the membrane (paths B and C). The overall vapor resistance of the membrane is 75–100 GPa·m^2·s/kg. For comparison: the resistance of a plain sheet of polyethylene (0.1 mm) is around 250 GPa·m^2·s/kg, i.e. approximately three times larger. The diffusion of moisture into the roof is therefore three times faster with a Hygro Diode than with polyethylene.

The increased rate of infiltration of moisture in the winter is still quite small and should not become fatal for the roof as it has a good possibility of drying out in the summer. The condensed moisture will, by the end of the winter, be located in a thin layer under the membrane or be absorbed by the cold deck (as described in section 3.3.3). When the roof surface is exposed to solar radiation and the air temperature gets higher in the spring/early summer it is not unusual for the surface temperature to increase well above that of the interior parts of the roof for some hours in the daytime. The coldest part of the roof cavity will therefore be the vapor retarder, and the moisture will evaporate from its initial location at the top, diffuse through the insulation, and condense on the vapor retarder. The driving vapor pressure for this process will be large compared with the pressure that drove the moisture up in the winter because the saturation vapor pressure increases dramatically at these high temperature levels (surface temperatures up to 60–80°C). With a regular vapor retarder, this condensed moisture will stay on the polyethylene. With the Hygro Diode, the condensate is absorbed by the felt and by wicking action distributed over the full area of the felt. Thus, the part of the felt that was exposed at the underside of the membrane also becomes wet, and from here the moisture may migrate through the ceiling into the underlying room — or it may be absorbed intermediately by the ceiling/warm deck.

With the Hygro Diode, the moisture from inside the roof is escaping evenly distributed over the roof area. It enters the room harmlessly as vapor. This is advantageous compared to the situation of a perforated polyethylene foil where any

possible escaping moisture comes dripping at a few locations. It is important to realize that the Hygro Diode, though wet when active, stays dry most of the time, especially after it has been removing excessive moisture from the construction period. Decay of the membrane and the interior parts of the construction should therefore not take place unless the moisture keeps coming through an imperfect weatherproofing.

Experiments were conducted in the laboratory to determine the rate at which moisture could escape a roof cavity through the Hygro Diode. The setup (figure 3.11) looked like a warm deck roof where the roofing membrane was replaced by a heating plate and with a wet sheet of blotting paper added between the heating plate and the insulation. The insulation was 60 mm rock wool and the ceiling 25 mm wood wool cement. The heating plate was warmed up to 50°C and the setup, which could be removed from the wood wool concrete deck, was weighed regularly. The drying rate found in a series of such experiments was around 13 $g/m^2 \cdot h$. This gives a rough estimate of an apparent wet "diffusion" resistance for the Hygro Diode around 2 $GPa \cdot m^2 \cdot s/kg$ when the resistance of the other materials has been subtracted. The time needed to remove 1 kg/m^2 moisture from the roof would therefore be 75 hours, corresponding to approximately 10 sunny days.

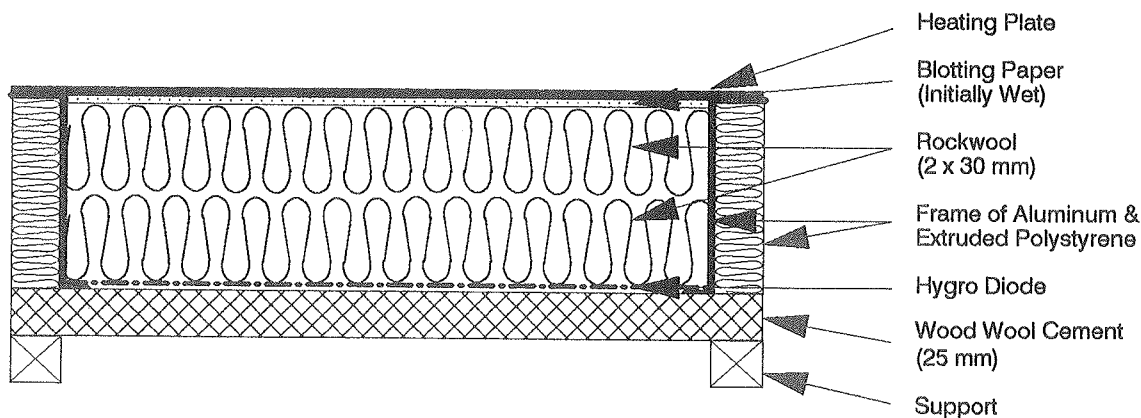Figure 3.11   Experimental setup for determination of drying rates of the Hygro Diode.

The Hygro Diode is not a diode in the usual sense as its design is not dependent on which side is up and which is down. The reason why it works as a diode is that, at its location on the warm side of the insulation, it has a large vapor resistance when the vapor drive is up while it is low when the drive is downwards.

78

The conditions of a good drying effect of the Hygro Diode are the following:

— Excessive moisture intrusion from convection and leaks must be avoided.

— Shade, light color of the membrane, ballast on the membrane and a northerly tilt of the roof are all factors that will reduce the peak temperatures of the roof surface and consequently decrease the effectiveness of the Hygro Diode. Combinations of these limiting factors should be avoided.

— The insulation should be permeable. A drying effect has been found with expanded polystyrene as insulation, but only at approximately half the rate of a construction with mineral wool.

— The ceiling or warm deck must not be totally impermeable.

SIMULATING THE HYGRO DIODE WITH MATCH:

Since MATCH is a one-dimensional model it is not possible, in a detailed way, to treat the two-dimensional flow of vapor and liquid through the fabric of the Hygro Diode. Instead, in the calculations shown later, the Hygro Diode is treated as a layer calculated transiently using its dry vapor permeability up to the maximum hygroscopic moisture content (at RH=98%). If the relative humidity is above this limit, the permeability is changed immediately into a wet value which is considerably larger than the dry value. Therefore, the vapor permeability for the Hygro Diode does not vary with moisture content according to figure 2.2. The moisture content that determines whether or not the Hygro Diode is dry is that of the previous time step. In order to simulate in the best way the changes of moisture content of the Hygro Diode that will initiate the change from dry to wet permeability, the node that represents the whole membrane should be located where the condensate is formed, i.e. on the upper surface of the Diode (displacement factor, $f = 0$, as defined in figure 2.1).

DRYING EXPERIMENT IN A "LARGE SCALE CLIMATE SIMULATOR":

Laboratory tests with the Hygro Diode were performed in the Large Scale Climate Simulator facility of the Roof Research Center at Oak Ridge National Laboratory, Tennessee, USA in the fall of 1989. The unique feature of this apparatus is the ability, in an indoor facility, to control the climate above and below roof specimens

up to 3.9 by 3.9 m. The apparatus consists of two climate chambers on top of each other where, in the upper chamber, temperatures may be varied between −40 and 66°C and in the lower chamber between 7 and 66°C. The roof specimen is the separation between the two chambers. Also the humidity may be controlled, and infrared lamps in the upper chamber may raise the roof surface temperature above that of the air. A small computer network controls the two environments according to a programmed scheme and takes care of the data acquisition.

The frame in which the specimens were located was subdivided so that it could accommodate nine 1.2 by 1.2 m test panels at the same time. Four of these panels contained cold deck roof constructions like those shown in figure 3.9A (without the air space). The deck consisted of 12.7 mm plywood, the insulation of 114 mm fiberglass and the ceiling of 12 mm gypsum. Between the ceiling and the insulation there was either a polyethylene vapor retarder, polyethylene with deliberately punched holes (5.5 mm circular holes for every 275 by 275 mm), a Hygro Diode or no vapor retarder at all. Four other panels contained warm deck roof constructions (figure 3.9B) with 51 mm of expanded polystyrene insulation above 110 mm of lightweight concrete and with the same configuration of vapor retarders. A cross section of one of the cold deck roof test panels is shown in figure 3.12 with the location of the thermal probes marked.
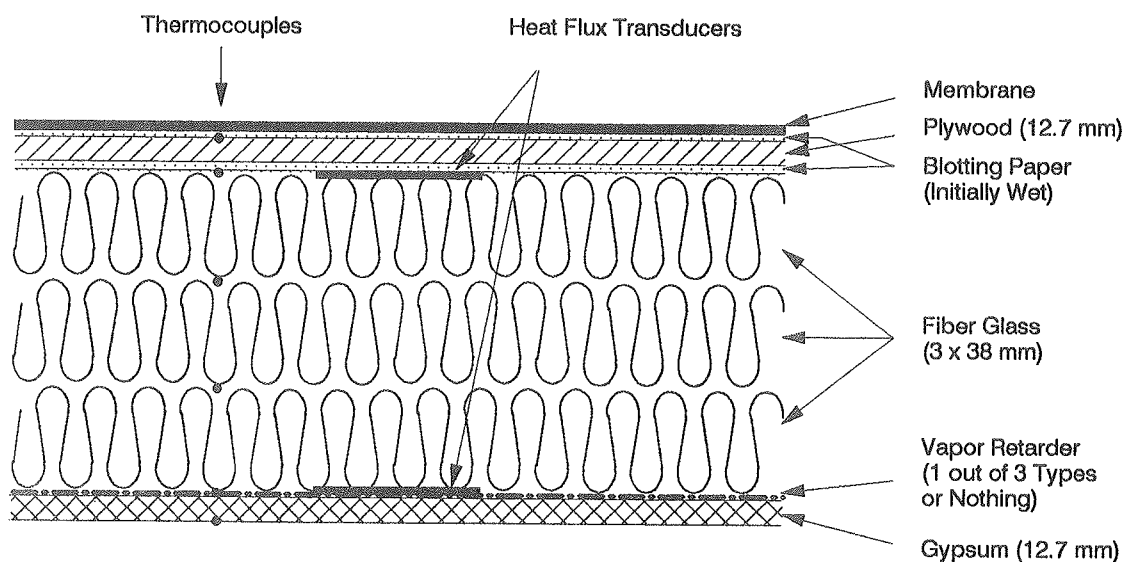
Figure 3.12   Experimental setup for tests with cold and warm deck roof specimens in the Large Scale Climate Simulator (cold deck roof shown).

Since diffusion into a roof cavity is a slow process it would require much machine time in the apparatus to get a noticeable effect of the upwards diffusion. Under ideal conditions (no unplanned punctures) this process may also be sufficiently determined from cup measurements with the vapor retarders alone. Therefore, it was decided to add 1 kg/m^2 water at the plywood deck and run the apparatus to simulate summer conditions during which the panels would dry out at different rates. Apart from different moisture probes that qualitatively gave the changes of moisture levels at various locations within the panels, specimens were taken out regularly and weighed to measure the overall change of moisture contents quantitatively.
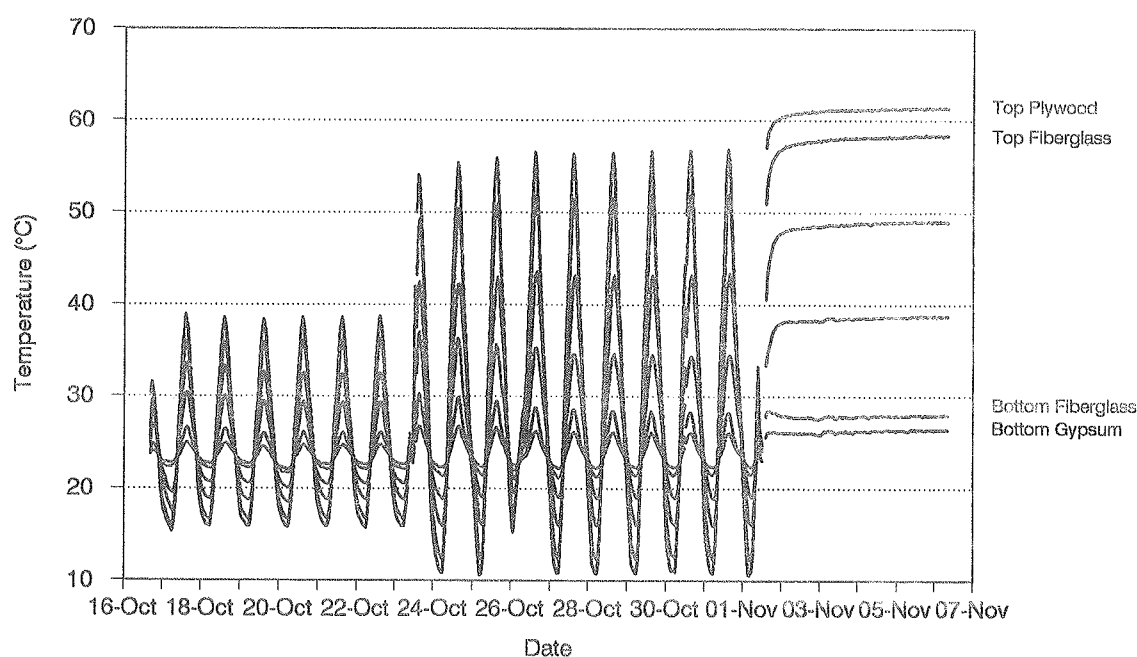
Figure 3.13   Temperatures measured in a cold deck roof panel during the three runs of the test in the Large Scale Climate Simulator.

The temperature applied was constantly 23.9°C in the chamber below the roof specimens. Above the roofs, the temperature was varied in three different runs. The first run lasted for 7 days and the temperature was varied in diurnal cycles between 15.6 and 43.3°C (corresponding to a moderately gray summer day). The second run lasted for 9 days and the temperatures varied between 10.0 and 65.6°C (a clear summer day). Finally, the third run was conducted with a constant temperature of 65.6°C above the roofs for 5 days. The shape of the varying temperature profile was taken from a clear day in the Danish test reference year, TRY, and stretched to the desired amplitudes. The temperatures measured through one of the cold deck roof panels are shown in figure 3.13. The top curve is

for the temperature between the membrane and the plywood and the remaining curves are for each intersection between materials (and between the three insulation boards) down to the temperature at the underside of the gypsum.

Results of the weighings are shown in figure 3.14 for the four cold deck panels and in figure 3.15 for the warm deck. The possibility that the curves may go down below the abscissa arises from the drying of the hygroscopic moisture that was bound in the panels before the deliberate addition of water, as the panels were assembled in the laboratory of room dried materials (around 60% RH).
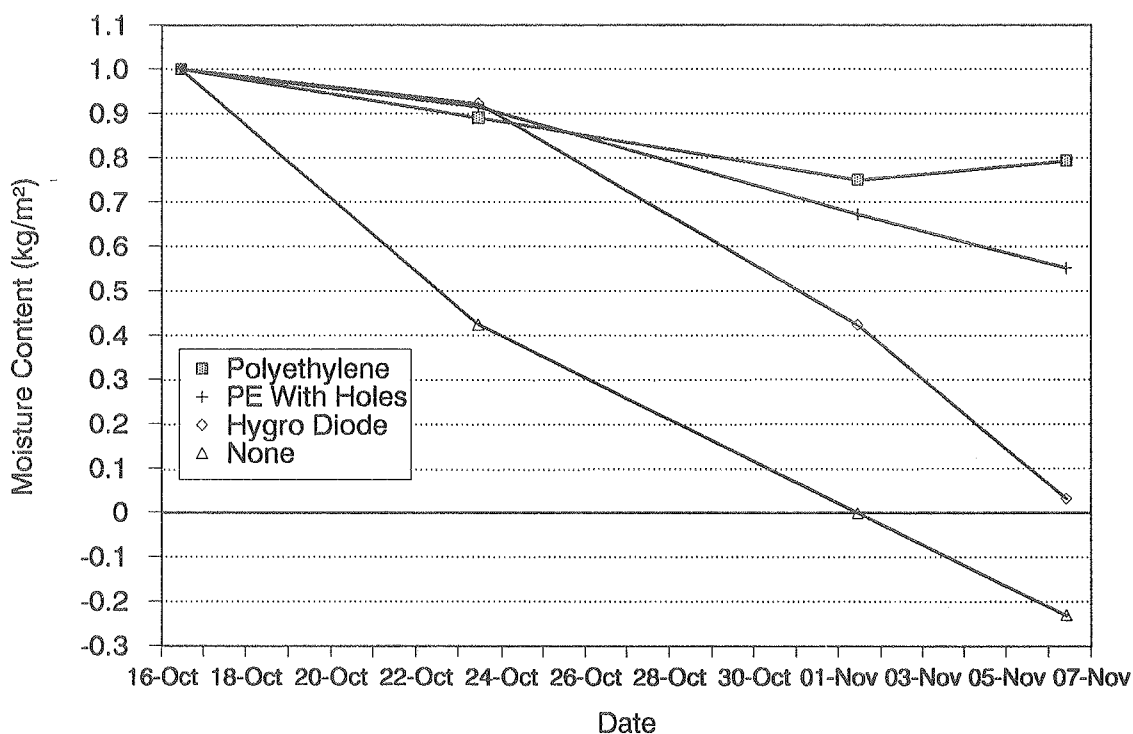
Figure 3.14   Gravimetrically determined drying rates of the cold deck roof panels with different vapor retarders.

Initial qualified guessing of the vapor resistances of the membranes serves as input to calculations where the downwards Pa·h (between the plywood and the underlying chamber) are determined over all three runs for each of the cold deck roof panels. The Pascal–hours together with the measured decrease of moisture content in this period provide information for the calculation of effective vapor resistances of the constructions. For the construction with no vapor retarder, this vapor resistance is 2.5 GPa·m²·s/kg. If this value is subtracted from the overall resistances in the other three panels, the resistances for the ideal polyethylene, the

polyethylene with holes and the Hygro Diode, are 20, 8.0 and 2.3 GPa·m²·s/kg respectively.

The vapor resistance for the polyethylene is at least a factor of 5 too low. Since there were no visible imperfections in the vapor retarder it was suspected that not all the moisture within the panel was registered by the weighing of the specimens. The moisture added in the beginning of the three runs was determined accurately as it was weighed in a jar before being poured into the roof cavity. By the later openings of the panels the moisture may have been unevenly distributed so that the specimens were not representative of the whole panel. Condensed water on the interior surfaces may also have been difficult to pick up and include correctly in the weighing. By the end of the experiment it was easier to wick up all the condensed moisture with paper tissue and that may be why the moisture content apparently increased here for the panel with polyethylene. A small amount may also have migrated into the sides of the panel that consisted of extruded polystyrene with a liquid applied sealant. Similar errors were suspected to have occurred in the other panels – at least as long as they contained condensed water.
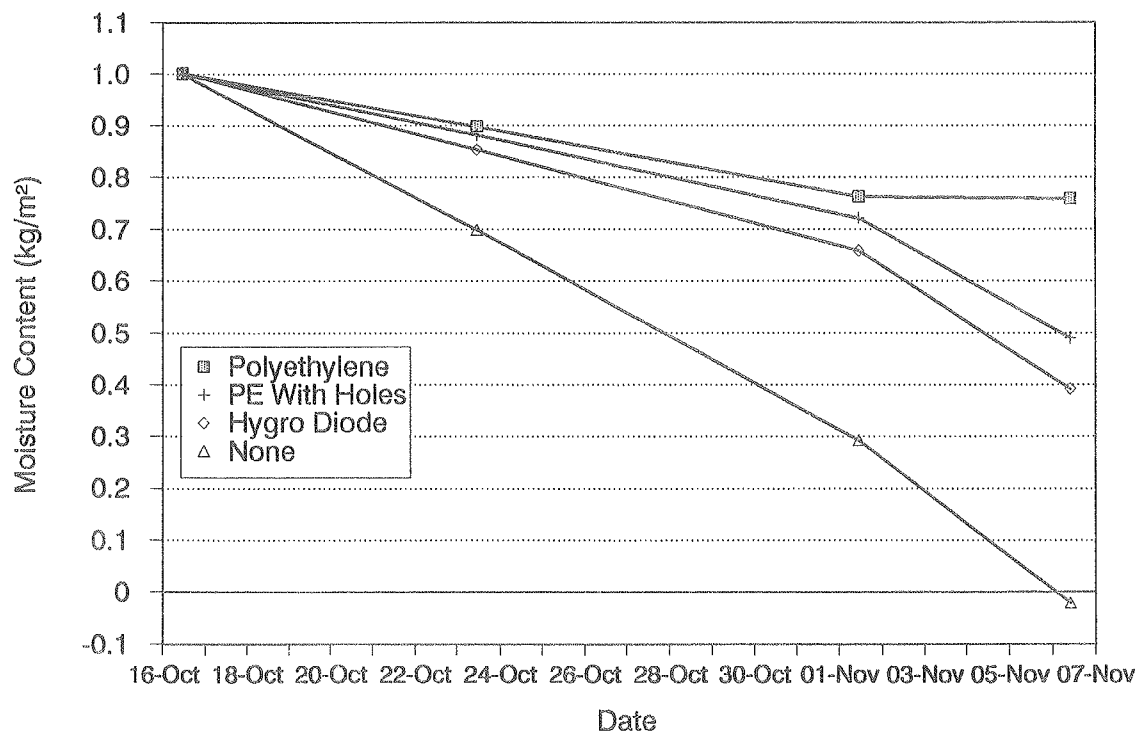
Figure 3.15   Gravimetrically determined drying rates of the warm deck roof panels with different vapor retarders.

The 2.3 GPa·m²·s/kg were used as an effective wet "vapor" resistance of the Hygro Diode in a simulation with MATCH of the drying over three runs with the measured temperatures at the top and the bottom of the panel as boundary conditions and the weighed moisture content in the beginning as the initial condition. The result of the simulation is shown in figure 3.16 together with the measured values.
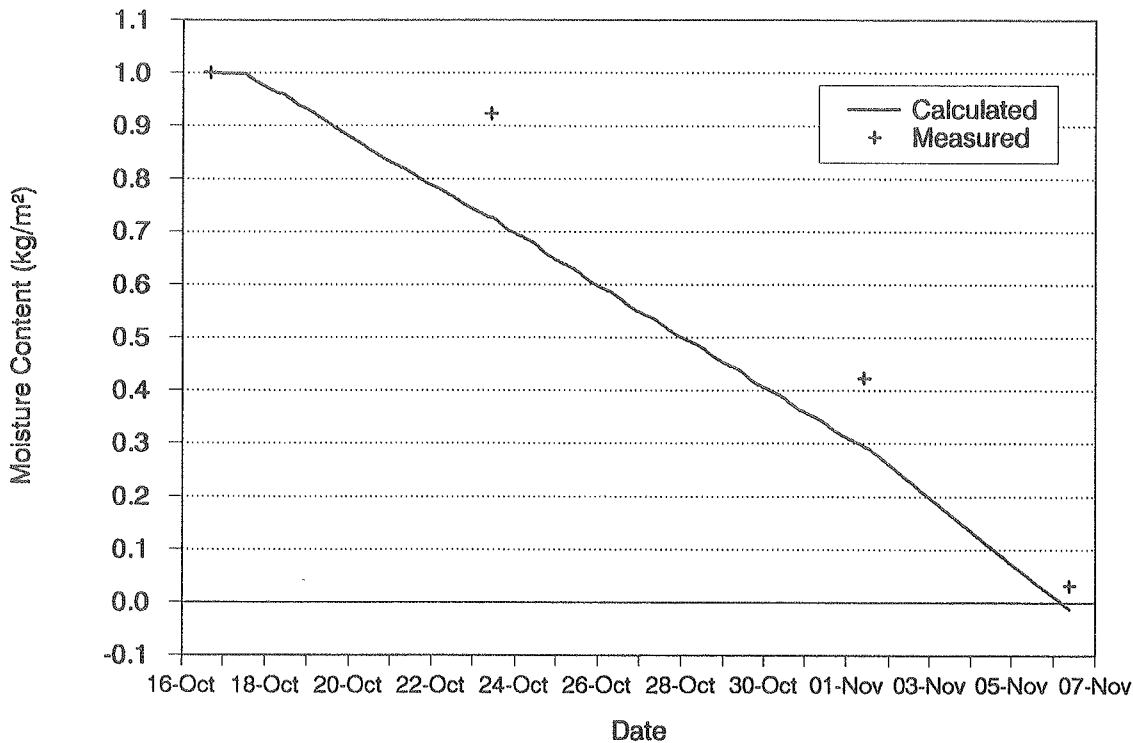
Figure 3.16   Measured and Calculated drying rates for the cold deck roof panel with the Hygro Diode vapor retarder.

It is seen that the calculated drying takes place at an almost linear rate. This is probably because there was much moisture available for drying in the beginning, when the temperature gradients were relatively small and cyclic, while there was less moisture available by the end, when the gradients were larger and constant. The measurements, on the other hand, showed almost no initial drying (no drying at all when compared to the polyethylene panels). It may be that it is necessary for some amount of moisture to be accumulated on the Hygro Diode before drying begins to take place. It is also possible that the effective "vapor" resistance used for the wet Hygro Diode may have been different when the gradients in the construction were constant as opposed to being cyclic. The constant thermal gradient may provide better conditions for sideways migration to the felt of the moisture condensed on the plastic stripes and thereby a better drying effect.

84

The way the drying rate was determined in the experiment was too uncertain to draw any conclusion about the effectiveness of the Hygro Diode under small, cyclic gradients and about the way to simulate the Hygro Diode with the computer program. Further experiments must provide a way of weighing sealed vertical units of the roof, small enough for weighing on an accurate balance, but including all the roof components from top to bottom. Some sort of weighing is still considered the only way to determine changes in moisture content quantitatively.

The inaccuracy of the weighings from the warm deck roof was the same as it was for the cold deck roof. If figures 3.14 and 3.15 are compared it is seen, however, that the drying rates of the warm deck roof with expanded polystyrene was approximately half that of the cold deck roof with fiberglass. In the warm deck, the total construction was probably not being dried out as seen from the figure, but instead the moisture that left the roof cavity was accumulated in the lightweight concrete for a while.

DRYING EXPERIMENT IN THE FIELD:

A small test building was constructed in the field at the Technical University of Denmark. The building consisted of two rooms – one of which was held at typical dwelling conditions for moisture and temperature (20⁰C and 3 g/m³ more moisture in the indoor than the outdoor air in most of the year) while the other was held constantly at 20⁰C and 60% RH. Eight rectangular holes, each 35 by 40 cm, were located above each room in the low slope roofing cassettes that covered the whole building. Different types of roof specimens were located in these holes as shown in the cross section in figure 3.17. The specimens were placed in an envelope of heavy polyethylene to make the assembly vapor tight on the top and to the sides. The insulation thickness was in all cases 150 mm. The metal plate on top of the specimens (outside the PE–envelope) served the purpose of supporting the load from traffic on top of the black built up roofing. The Hygro Diode was in most cases the material used for vapor retarder and it was attached to the PE–envelope with some durable and water resistant tape.

The insulation in the panels consisted of either mineral wool or expanded polystyrene. Most of the specimens were of the warm deck roof type with a variety of deck materials: Wood, wood wool cement, concrete, and perforated, corrugated

steel. One specimen over the humid room was a cold deck roof with a plywood sheet as the deck. Results of measurements will be shown from this panel, which was insulated with rock wool and had wood wool cement as ceiling, and from a similar warm deck construction (without the plywood) from over the room that was kept at dwelling conditions.
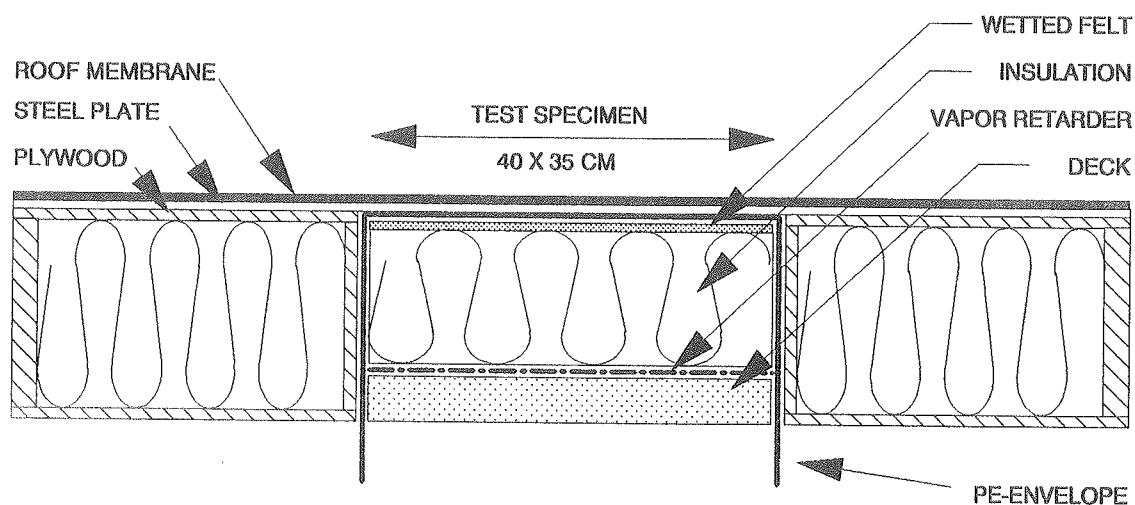
Figure 3.17   Experimental setup for the field test with the Hygro Diode.

The roof specimens were assembled from laboratory dry materials by the end of the winter 1987/88. In the beginning of May 1988 moisture was added by inserting a piece of saturated synthetic felt between the top of the insulation and the PE–envelope and by immersing the plywood deck from the cold deck roof in a water bath for a short time. The gain of moisture of the roof specimens was in both cases around 500 g/m². This corresponds, for the plywood, to an increase of moisture content from 14.5 weight–% to 23.6% – i.e. to a situation with critical moisture content. The PE–envelopes with the roof specimens were pulled down monthly and weighed with and without the underlying ceiling or deck.

By the end of the experiment all interior materials were oven–dried and weighed and thereby it was possible to calculate the absolute moisture content within the roof cavities throughout the whole experiment. The measured moisture content is shown with symbols in figure 3.18 for the two summers and one winter until the fall of 1989. The upper curve with symbols is from the cold deck roof over the humid room. The moisture content was generally higher here because the roof cavity included the plywood layer which held a lot of hygroscopic moisture. The added moisture was driven out of both roof specimens already within the first summer. The moisture content of the plywood was down at 11.6% by the middle

86

of August and the moisture content of the warm deck roof was down at hygroscopic levels (close to nothing) by this time. There was some increase of moisture content during the winter but this moisture was able to dry out the following summer.
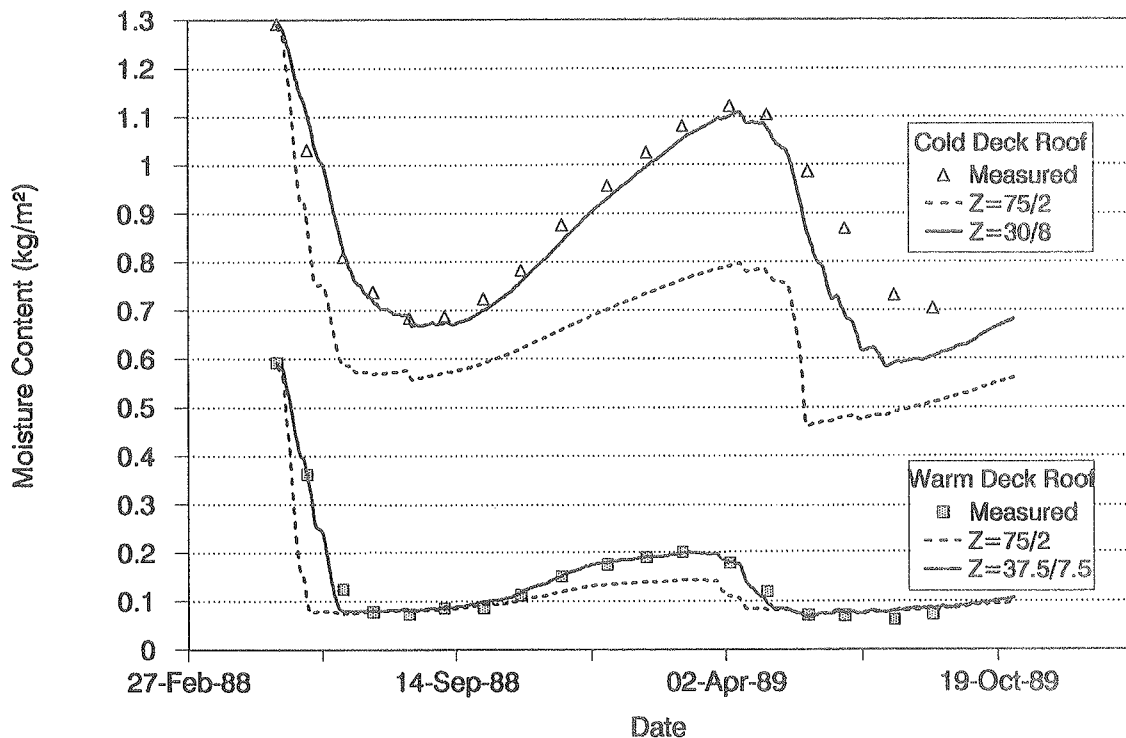
Figure 3.18   Measured and calculated moisture content in a cold and a warm deck roof specimen from the field test. The calculation was performed with ideal as well as fitted vapor resistances (dry/wet [GPa·m²·s/kg]) for the Hygro Diode.

Included in the same graph are results from calculations with MATCH using the actual, measured temperatures at the top and the bottom of the roof specimens and the humidity of the air as boundary conditions and the added amount of moisture as initial condition. One set of calculations (with dashed lines) used the separately determined vapor resistances 75 and 2 GPa·m²·s/kg in the situation where the Hygro Diode was either dry or wet. It is seen from the graph that this gives predictions of the moisture content that are too optimistic. The drying rate in the summer is too fast while the moisture uptake in the winter is too slow. A limited number of calculations gave an acceptable agreement between prediction and measurements when the vapor resistances of the Hygro Diode (dry/wet) were set to 30/8 GPa·m²·s/kg for the cold deck roof and 37.5/7.5 GPa·m²·s/kg for the warm, as shown by the solid lines. These ratios between wet and dry resistances are considerably less favorable than anticipated, but both roofs still dried out as they should and did not reach critical moisture content in the winter (maximum 19.6%

moisture in the plywood in March).

It appears that there may have been some leak around the Hygro Diode because of imperfections in the sealing of both roof specimens. This would at least account for the unpredicted high gain of moisture in the winter. The slow drying of the specimens in the summer that could be simulated with a higher apparent "vapor" resistance may, as mentioned for the experiment in the climate simulator, be caused by different conditions of drying under steady and time varying driving gradients of the vapor pressure. It should be mentioned that the version of the Hygro Diode used here was an early one where the synthetic fabric consisted purely of polypropylene. This material sometimes showed the undesirable effect of becoming hydrophobic after being moist a few times, thereby losing its ability to transport the moisture by wicking action. This hypothesis is supported by the discrepancy between measurements and predictions for the cold deck roof in the second summer. While the drying was predicted at a correct rate the first summer, the measured rate was less than that predicted the second summer. The same effect is hardly noticeable for the warm deck roof where only little moisture has to be dried out the second summer.

CONCLUSIONS ON THE HYGRO DIODE:

While there is some uncertainty in assigning correct permeabilities for the Hygro Diode for simulations under dynamic conditions with the computer program MATCH it seems that measurements prove its ability to dry out constructions with reasonable amounts of moisture (up to 1 kg/m^2) within a summer period. Even conditions where the ratio between dry and wet permeability was considerably less favorable than anticipated did not spoil the ability of the Hygro Diode to let more moisture out of the roof cavity in the summer than what enters in the winter.

Should the same conclusions be valid in practical roofing, as in the scientific experiments, it seems that the Hygro Diode has the capability wanted for — keeping dry roofs dry and even being able to dry out initially wet constructions. The requirements are that venting of the roof cavity is eliminated, that the roof surface is unshaded and that the insulation and ceiling materials used are relatively permeable to vapor diffusion.

3.3.3 MOISTURE CALCULATIONS OF ROOF SYSTEMS

This section deals with calculations to investigate two different solutions for moisture problems in low slope roofs. The purpose is to illustrate the ability of the MATCH computer program to analyze various problems and compare different solutions with each other.

The first problem is a comparison between the moisture content in an initially wet roof with a cold deck, using either a regular sheet of polyethylene as vapor retarder, the Hygro Diode described previously or no vapor retarder at all.

The second problem investigates the impact of using a somewhat permeable roofing membrane, namely EPDM, in various climates. Its permeability has been proven to increase with temperature, and it has caused some concern that moisture may accumulate in the roof when such membranes are used in hot, humid climates. In other climates it has been argued that such membranes would help in drying out excessive moisture.

HYGRO DIODE OR POLYETHYLENE?

A series of calculations was performed on a cold, unventilated roof exposed to climate conditions given by the Danish Test Reference Year, TRY, for five consecutive years. The indoor climate was defined by a constant temperature of 21^0C and a constant 3 g/m^3 higher moisture concentration indoors than outdoors. The roof consisted, listed from the outside, of: An unprotected built up roofing (5000 $GPa \cdot m^2 \cdot s/kg$), 12.6 mm plywood, 150 mm rock wool, a vapor retarder and a ceiling of 25 mm wood wool concrete. The vapor retarder was either 0.1 mm polyethylene (250 $GPa \cdot m^2 \cdot s/kg$), a Hygro Diode (75/5 $GPa \cdot m^2 \cdot s/kg$) or, for comparison, there was no vapor retarder. Initially, all the materials contained hygroscopic moisture corresponding to 80% RH at desorption except for the wood which started from 25 weight–% – a little less than fiber saturation. Other material parameters are taken from the MATCH materials library printed in the appendix.

Figure 3.19 shows the development of the moisture content in the plywood in the three cases. First of all the calculation with no vapor retarder clearly shows the

necessity for one. The moisture content varies between 14 and 50%. The critical level for initiating rot decay in wood is considered to be around 20% (sometimes the limit is fixed at 15% if the wood has been attacked previously) when, at the same time, the temperature is above 5°C. Obviously, the wood in the construction without vapor retarder is subject to potential damage as its moisture content is above these limits most of the year and also in periods where the temperature may be sufficiently high.
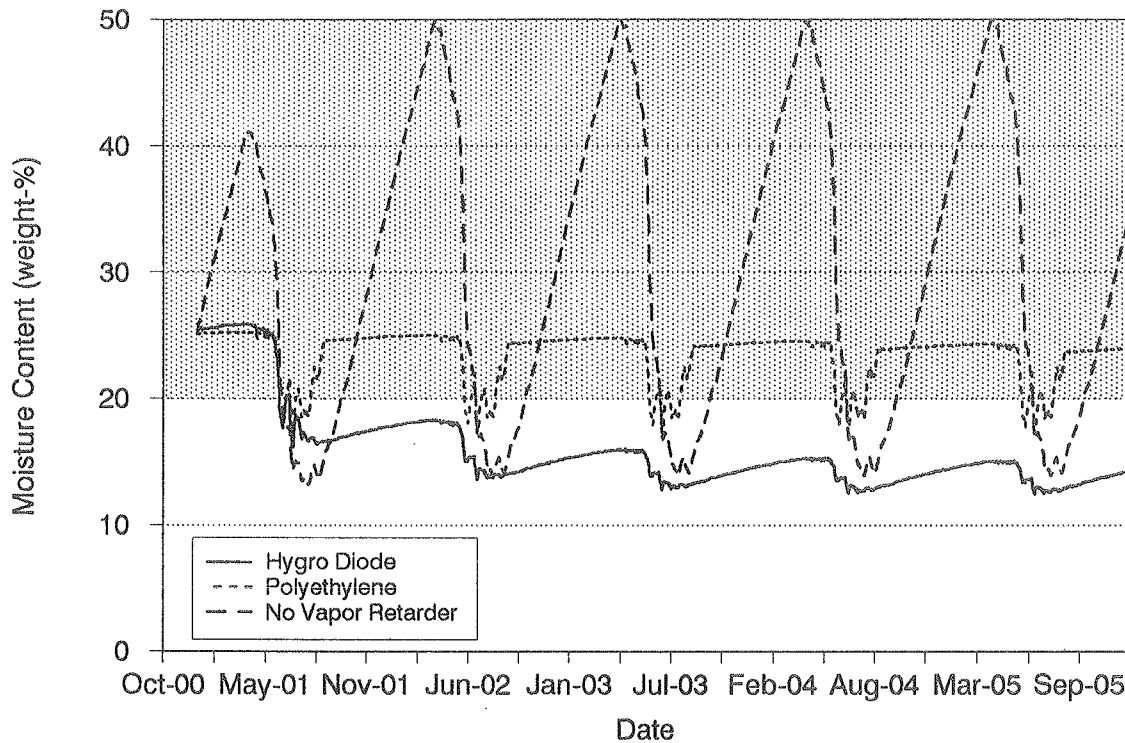
Figure 3.19   Moisture content in the plywood deck of a cold deck roof with Hygro Diode, polyethylene or no vapor retarder. Calculated for five consecutive TRY—years.

The construction with a polyethylene vapor retarder dries out insignificantly from year to year. The drying is far from sufficient to protect the wood from decay. More moisture seems to dry out of the wood every summer but, unfortunately, this moisture comes back in the fall.

With the Hygro Diode, the moisture content is down at safe levels already after the first summer's drying. Despite the small increase over the winter, dangerous moisture content is never reached again. The wood dries out a little more in the following years and ends up with a moisture content between 12 and 16%.

Figure 3.20 shows results from an analysis of the location of the moisture in the first year for the construction with polyethylene. The moisture content in the construction, present as condensed water on the vapor retarder and as absorbed moisture in the insulation and in the plywood, was plotted with stacked graphs. The amount condensed on the vapor retarder was actually calculated as if it were absorbed in the lowest, thin layer of insulation, but would probably be found in a real construction as condensate in the interface between the vapor retarder and the insulation.
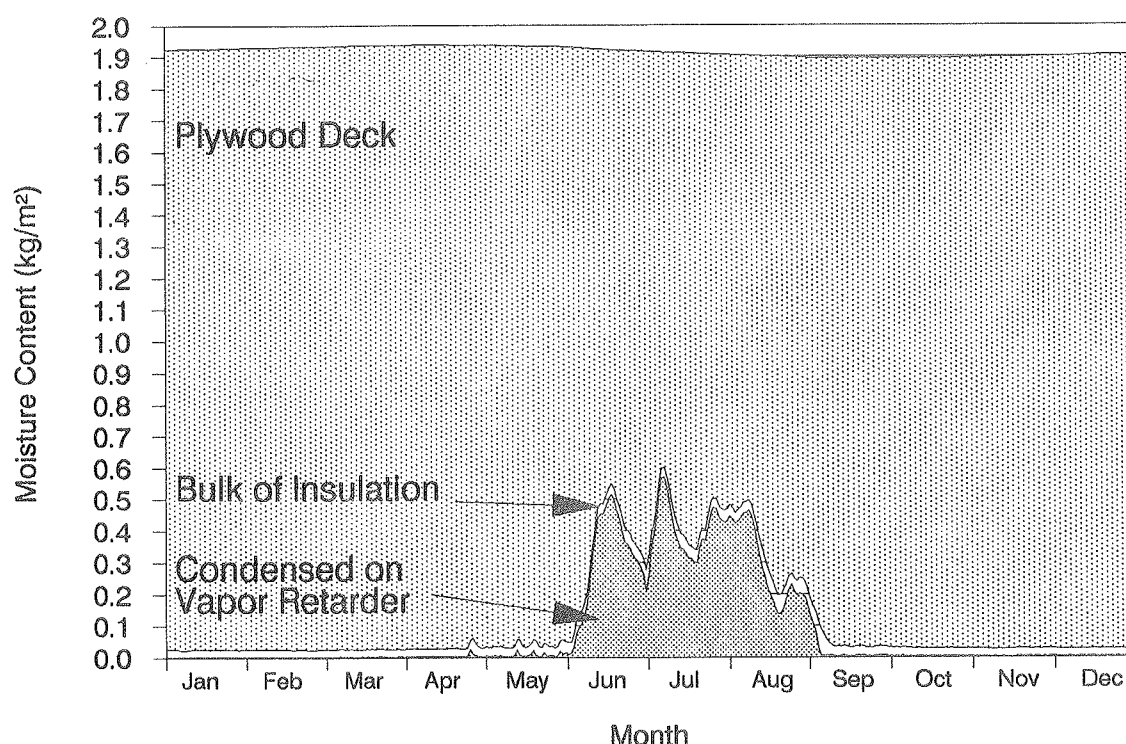
Figure 3.20 Distribution, over the first year, of the moisture within the roof cavity for the construction with polyethylene vapor retarder.

It is seen from the top curve that the total moisture content in the construction is almost constant over the year. The amount that, according to the previous graph, dried out of the plywood does not leave the construction totally but accumulates on the vapor retarder instead. In the fall, this moisture migrates back to the wood and the situation becomes the same as it was before the summer period. Though the dewpoint will fall in internal points of the insulation at times when the gradients are changing there does not seem to be any significant accumulation of moisture internally in the insulation. Most of the moisture that condenses in the insulation will be re-evaporated, transported further on and end up next to the first impermeable layer it meets. This has been experimentally verified for

91

fiberglass with a gamma–ray equipment by Kumaran, 1988.

The same information was plotted in figure 3.21 for the construction with a Hygro Diode vapor retarder. Again, a little moisture condenses on the vapor retarder, but this time the amount is less and it stays for a shorter time. While the condensate is formed on the Hygro Diode, the plywood dries out, and this moisture does not come back in the fall because it has passed the Hygro Diode, and is thereby out of the roof cavity. This is seen from the drop of the top curve which represents the total moisture content. Neither in this calculation does the insulation accumulate any moisture.
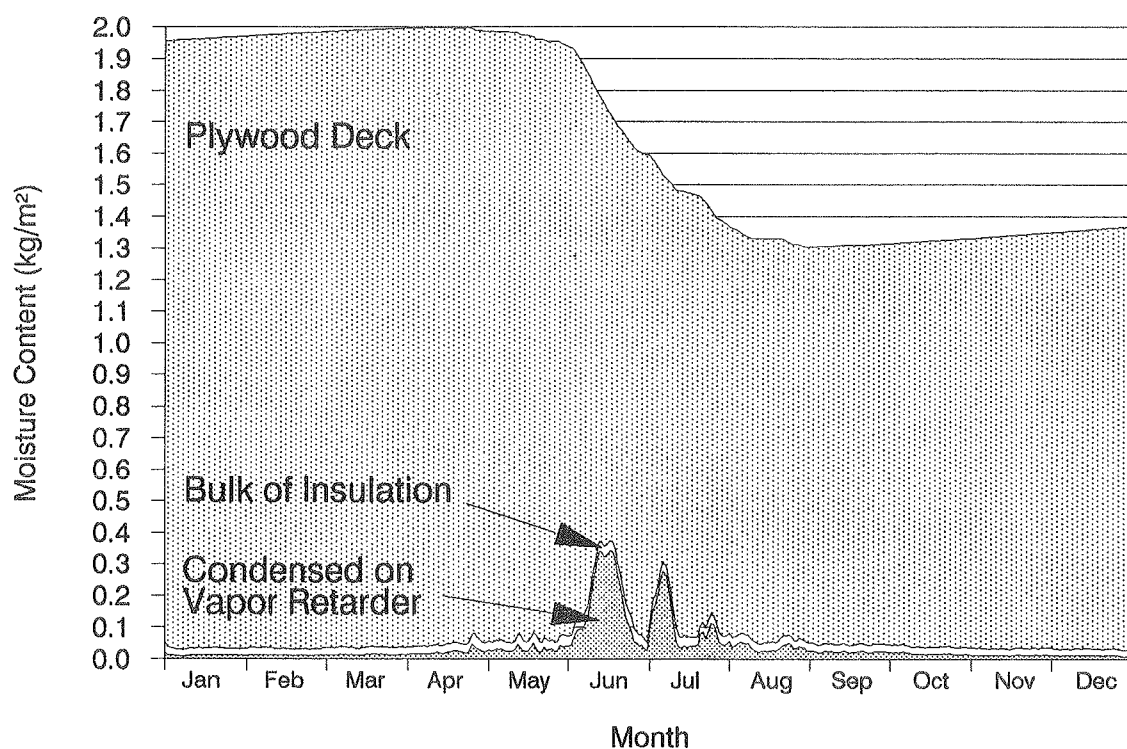
Figure 3.21   Distribution, over the first year, of the moisture within the roof cavity for the construction with the Hygro Diode vapor retarder.

Both graphs illustrate the large amount of moisture accumulated by the wood. Even the noticeable condensate on the polyethylene in the summer appears insignificant compared to the amount left in the plywood. It is not possible at usual hygroscopic levels to dry out wood totally because much of the moisture does not escape unless the vapor pressures are very low. The demand is just to get the moisture content down at reasonable levels − in this case below 1.5 kg/m² in the plywood (at density 600 kg/m³).

Certain criteria are known for a number of materials as to when deterioration will

be initiated. These criteria may for instance be combinations of temperature and moisture content. The well recognized limits for wood (T>5°C and u>20%) may be plotted together with simulation results for these two parameters. This was done in figure 3.22 for the average daily values of temperature and moisture content in the plywood deck of the construction without vapor retarder. It is seen that the moisture content is highest in the middle of the spring and is still dangerously high in the first summer months when the temperatures are sufficiently high to initiate damage. Not until the middle of the summer is the wood dried out enough to enter the safe area. But again in the middle of the fall there is a period, though not as severe, where the wood has become more moist and where at the same time the temperature is too high. Daily fluctuations will be much larger but are probably not important for determining whether or not the limit for initiating rot decay has been passed. The constructions with vapor retarders would not present themselves differently in such a diagram as the changes in moisture content is much less. Diagrams of this type, generated by a computer program as part of the post–processing, may be valuable when determining whether or not a construction is "healthy".
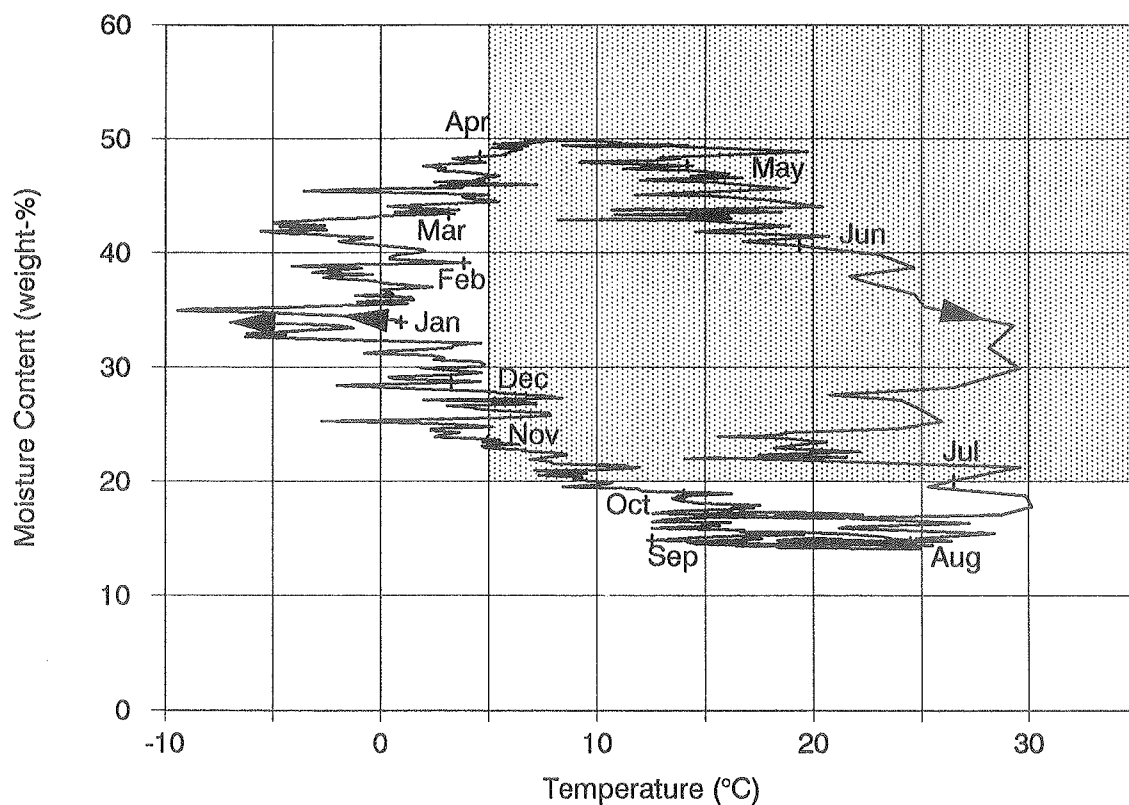
Figure 3.22   Criterion–plot of when the daily averages of (T,u) for the plywood of the construction with no vapor retarder enters a dangerous area (with shaded background). The symbols show the beginning of the indicated months.

DIFFUSION THROUGH EPDM–MEMBRANES:

It has been a concern in some climates, where the warm period is also humid, that moisture would diffuse through an EPDM–membrane and into a colder roof cavity without having a chance of escaping in colder and drier periods. The reason is that the permeability of such a membrane increases significantly with temperature. Thus, the effect of an EPDM–membrane almost becomes that of an inverse Hygro Diode – transporting large amounts of moisture when the gradients drive it into the cavity and being practically vapor tight the rest of the time. In colder climates, where the outdoor dewpoint never exceeds the indoor temperature, there is no potential for inwards transport. Instead, the membrane may be able to dry out some moisture from the cavity because its permeability is approximately the same as that of a polyethylene vapor retarder. Thus, the EPDM lets the moisture that diffuses from inside the house further out to the outdoor air.

Few data are available on the permeability of EPDM–membranes at different temperatures. Dupuis 1985, however, has reported such data for four different kinds of EPDM–membranes at three different temperatures. An average has been taken over the four types at each temperature with the following result:

$$T = 4.4^{o}C \qquad z = 627 \text{ GPa·m}^2\text{·s/kg}$$
$$T = 32.2 \qquad z = 427$$
$$T = 70.0 \qquad z = 37.5$$

It has been assumed that this average material can be represented by a thickness of 1.5 mm, whereby its water vapor permeability may be calculated. The variation of the permeability with temperature is assumed to follow an expression from ASHRAE, 1989. With this expression applied separately to the regions above and below 32.2^{o}C the result is:

$$T \leq 32.2^{o}C: \qquad \delta = 1.63 \cdot 10^{-13} \cdot \exp(-\frac{1172}{T[K]}) \qquad (\frac{kg}{Pa\cdot m\cdot s})$$

$$\text{(3.3.3)}$$

$$T > 32.2^{o}C: \qquad \delta = 1.38 \cdot 10^{-5} \cdot \exp(-\frac{6745}{T[K]})$$

The same construction has been analyzed using weather data from both the Danish Test Reference Year and the Test Meteorological Year (TMY) for Miami. Of course, constructions are usually not the same in these two different climates. A

construction is chosen which is not very well insulated for Danish Conditions but is probably too well insulated compared with the standard in Miami. However, the insulation thickness is not assumed to be very important for this calculation. Vapor retarders are probably not commonly used in Miami, either, but one is included here nevertheless -- otherwise the vapor migrating through the EPDM would be transported directly into the room without causing condensation. Having a vapor retarder may also resemble the situation when the deck has a high vapor resistance.

The construction consists of, from the outside: 1.5 mm black, unprotected EPDM-membrane, 100 mm mineral wool (120 kg/m^3), polyethylene vapor retarder (250 GPa·m^2·s/kg) and 25 mm wood wool concrete. All materials have an initial moisture content that corresponds to hygroscopic moisture at 80% RH, except for the insulation where another 0.5 kg has been added per square meter roof. This moisture has been added to see the effect of constantly having condensation at the coldest spot inside the roof, i.e. the potential for inward transport through the membrane is minimum. The indoor conditions are 21^{0}C and 3 g/m^3 more moisture indoors than outdoors in Denmark while they are 21^{0}C at a moisture gain of 1.5 g/m^3 in Miami. This will often bring the indoor air close to or at saturation in Miami, so a maximum RH-level at 60% has been added as a criterion.

The variation over the year of the outdoor dewpoint is shown in figure 3.23. It is seen that the dewpoint never exceeds the indoor temperature in Denmark, meaning that if there is any condensed moisture inside the roof cavity, the vapor pressures here are higher than in the outdoor air and the result is an outward vapor transport through the membrane. In Miami, the dewpoint of the outdoor air may be higher than the indoor temperature if the building is air-conditioned. This is why the indoor temperature is chosen as low as 21^{0}C -- otherwise the potential for inward transport through the EPDM would be less. In the coastal climate of Miami the nearby ocean sets the upper limit for the dewpoint. Warm, continental climates may have higher dewpoints. Such climates may therefore be simulated with a more reasonable indoor temperature.

Some moisture will also migrate into the room through the vapor retarder. As a reference case, a similar roof has therefore been calculated with a built up roofing (5000 GPa·m^2·s/kg). As it is seen, the two calculations for Miami do not seem to become critical. Even after the added moisture has been dried out there is no
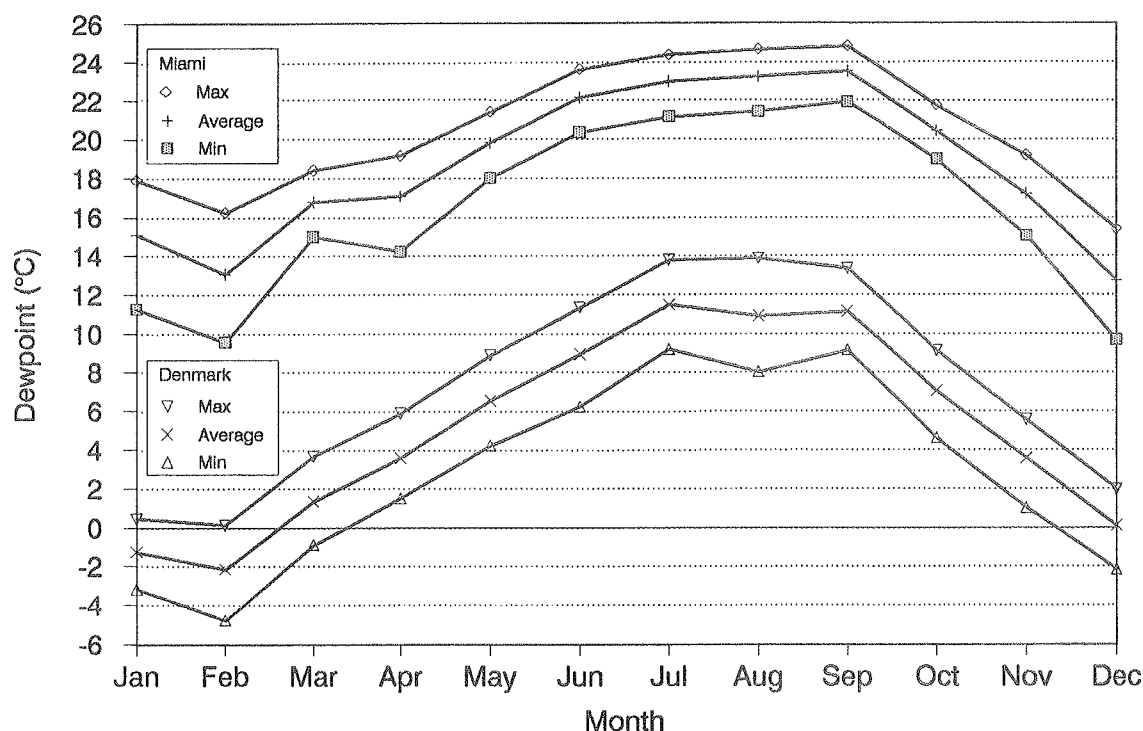
Figure 3.23   Variation of dewpoints in Miami and in Denmark. The curves
show monthly averages and monthly averages of daily maximum
and minimum values.

appreciable accumulation in the roof during summer. There are two reasons for this. One is that there will always be condensation some place inside the cavity even with only "hygroscopic" moisture left. The vapor pressure inside all of the cavity with the permeable insulation is therefore equal to the saturation pressure at the coldest spot. This spot will, on a summer day, be warmer than the indoor air. Another reason is that some moisture migrates into the building because the vapor resistance of the polyethylene is of a finite value. Therefore, in an additional calculation the insulation was replaced by expanded polystyrene starting at a moisture content equal to 50% RH and having a vapor resistance of 5000 $GPa \cdot m^2 \cdot s/kg$ towards the interior (an asphalt membrane or a "perfect" steel deck). The smaller permeability and higher moisture capacity of the polystyrene will prevent the vapor pressure close to saturation at the bottom of the insulation from being prevailing at the top. These conditions should increase the inward gradients of vapor pressure across the roofing membrane and thereby involve a larger risk that some moisture would accumulate.

Results are shown in figure 3.24. All the constructions with initially wet mineral

96

wool dry out — in Miami as well as in Denmark. The roof with a built up membrane (BUR) dries 19 g/m² the first year (through the vapor retarder) in Denmark while the same roof with EPDM—membrane dries 67 g/m². Thus, 48 g/m² dries out through the EPDM — an amount too small to count on to dry out a severely moist roof. It would take too many years. In Miami, the drying (through the vapor retarder) of the roof with a built up system is 152 g/m² the first year, while it dries 209 g/m² when it has EPDM on the top. Even here, there is some extra drying through the membrane (57 g/m²), which is a little more than in Denmark. At the end of the summer, when the dewpoint of the outdoor air is highest, the slope of the curve for the EPDM roof is around the same as for the BUR roof, but the roof with EPDM never dries out slower than the roof with BUR. After the constructions dry out in Miami, at least part of the insulation holds only hygroscopic moisture and the vapor pressures inside the cavity may become smaller. Still, no significant build up of moisture content is seen over the summer period.
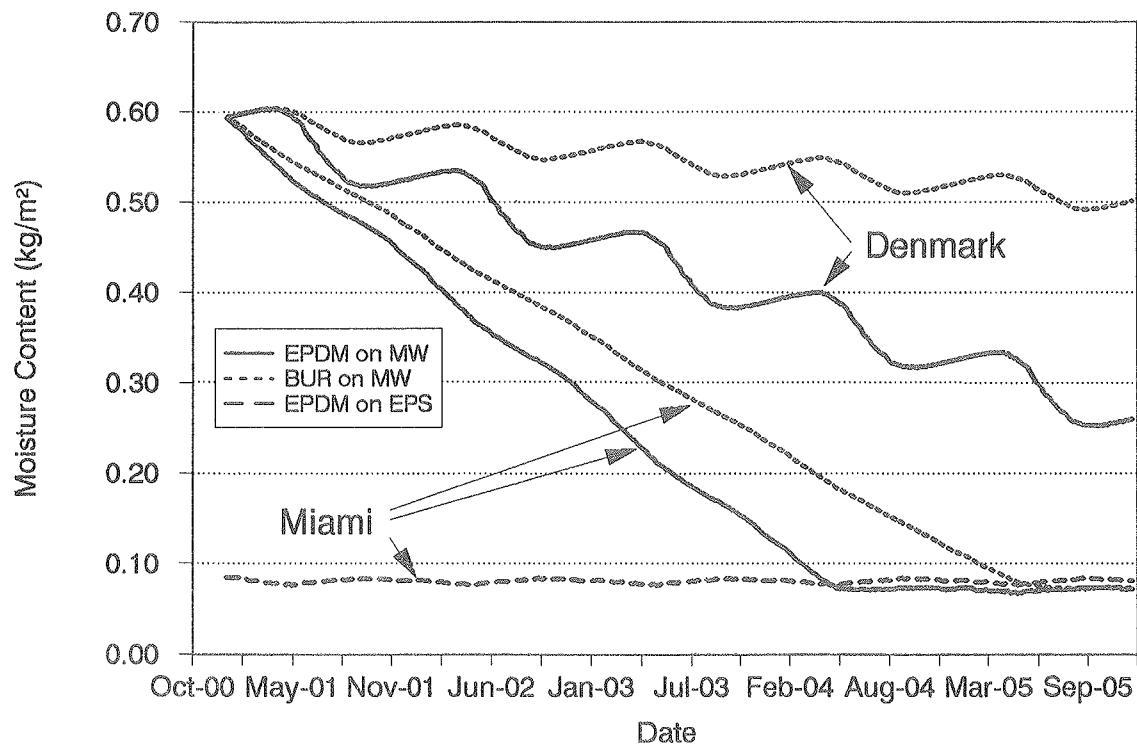
Figure 3.24   Variation of moisture content over five years of initially wet roofs with mineral wool insulation (MW), using either EPDM or built up roofing (BUR) as membrane. The calculations are shown for Miami as well as for Denmark. Also shown are results from an initially dry roof in Miami with expanded polystyrene as insulation (EPS) and an EPDM membrane.

The initially dry construction with expanded polystyrene (EPS) does not absorb moisture, either. The small amount that enters the roof in the summer leaves it in the winter. In the first year, the result is an insignificant drying of 4 g/m². In this roof, where the vapor retarder is very tight, the absorption through the membrane in summer is in balance with the drying in winter. When the roof surface heats up in summer and the membrane becomes permeable, also the top layer of the insulation becomes warm and with its hygroscopic moisture content the vapor pressures here are not too much lower than in the outdoor air. This is why the summer accumulation does not become critically large.

It should be noted that the calculations have not accounted for the accumulation of precipitation as ponded water on the roof membrane as it is hardly possible to determine for how long periods such water will be present. Ponded water will keep the vapor pressure on the outside of the membrane at the saturation vapor pressure of the surface temperature of the roof, thus increasing the inwards vapor pressure gradients as long as the water is present. The results shown should be evaluated in this perspective.

If possible effects of ponded water are disregarded, it appears that the outdoor climate must be more hot and humid than in Miami in order for damaging accumulation of moisture that has penetrated an EPDM membrane to occur. In such climates, the necessity is probably less for a vapor retarder to avoid accumulation of indoor humidity in the winter. If the vapor retarder is not there, or if it is made of a material with a permeability corresponding to a thin layer of polyethylene or less, all the moisture that possibly enters through the EPDM should be able to migrate further into the room. Damage from moisture intrusion through the membrane should therefore always be avoidable. In most climates, the membrane will even give a small drying effect of possible moisture, initially present in the roof cavity.

3.4 IMPACT OF LATENT HEAT ON THERMAL BALANCE

It has always been known that moist constructions are not as good thermal insulators as they would be if they were dry. This has usually been compensated for by increasing the thermal conductivity measured in the laboratory by a certain factor to get a practical thermal conductivity which better describes the lower thermal resistance encountered in real constructions where some moisture may be present. It is not until recent years that experimental research has concentrated on giving a physically more correct description of the moisture impact on the thermal balance than that which is given by correction factors for the thermal conductivity. Computer programs that simultaneously describe the migration of heat and moisture can easily cope with a more complex description and thereby take advantage of the information gained from recent experiments.

The first subsection is a short summary of some of the important research done in the field of studying moisture influence on thermal performance within the last 10–15 years – mostly from steady state experiments. The second subsection describes two transient experiments where the impact of the latent heat transfer on the thermal balance was studied in constructions with a small moisture content. These results have been simulated with MATCH with good agreement. The third subsection extrapolates the knowledge gained, to analyzing the impact on a low slope roof system subjected to two different types of climate.

3.4.1 LITERATURE SURVEY ON LATENT HEAT TRANSFER

As stated in chapter 1, moisture affects the thermal balance by its presence in the pore system as well as when it moves in either its liquid or gaseous state. Sandberg, 1986 looks upon heat transfer in a porous medium as being caused by three different processes:

I   Heat flow described by temperature gradients in the absence of moisture flow.
       This is caused by heat conduction in the solid material, in the air and in <u>still</u> moisture (vapor, liquid and ice) in the pores, by radiation in the pores, by local convection in the pores (macroscopic convection not considered) and, finally, by local evaporation and condensation in the single pores.
       Thermal conductivity caused by type I heat transfer may be somewhat

higher for a moist material than for a dry. It is well described by for instance letting the thermal conductivity increase linearly with moisture content.

II   Convective heat transfer with the moisture flow.

The vapor and liquid moisture carries sensible enthalpy when it comes from either a warmer or colder region of the material.

Moisture transfer is usually such a slow process that this form of heat transfer becomes negligible compared to the conducted heat.

III   Heat transfer due to phase changes (macroscopic latent heat transfer).

When liquid moisture evaporates from one area of the material, migrates as vapor and finally condenses in another area, it involves a large amount of heat, even if the moisture transfer is limited, because the specific enthalpy of vaporization/condensation is a high figure.

The process becomes important compared with the conducted heat in permeable materials with a good insulation value (mineral wool for instance) even if there is only a little moisture present.

This section deals with what can be done to give a better description of heat transfer by process III than by including it in process I. Simply increasing the thermal conductivity with the moisture content gives a poor description because (1) the vapor transfer is not described linearly by temperature gradients, (2) the latent heat transfer process takes place as soon as liquid moisture is present and does not depend much on how much extra moisture there is and (3) the process is rather described by the distribution than by the content of moisture.

Langlais et al., 1983 compared experimentally determined curves for how the thermal conductivity of mineral wool (glass and rock) increased with moisture content. These curves were independently produced by Joy and Jespersen in the fifties (Figure 3.25). The curves did not agree very well though produced for materials that were basically identical. Both researchers used specimens where the moisture distribution was uniform. Joy measured the thermal conductivity in a transient method that only lasted for 15 minutes at an average temperature of 24ºC and found the largest moisture influence on thermal conductivity, i.e. 3 times higher thermal conductivities than the dry values with a moisture content at 2 vol–%. Jespersen, who measured under "steady heat flow" conditions around 10ºC with small temperature gradients, obtained another significant impact of moisture on the thermal conductivity, but only approximately a doubling of the

100

thermal conductivity at 2 vol-% moisture. Langlais et al. in their own experiments were not even able to increase the thermal conductivity by 50% with 10 vol-% moisture when they allowed the moisture to redistribute (accumulating at the cold plate) in a steady state measurement. Their "steady state" must therefore be different from the one obtained in Jespersen's experiments.
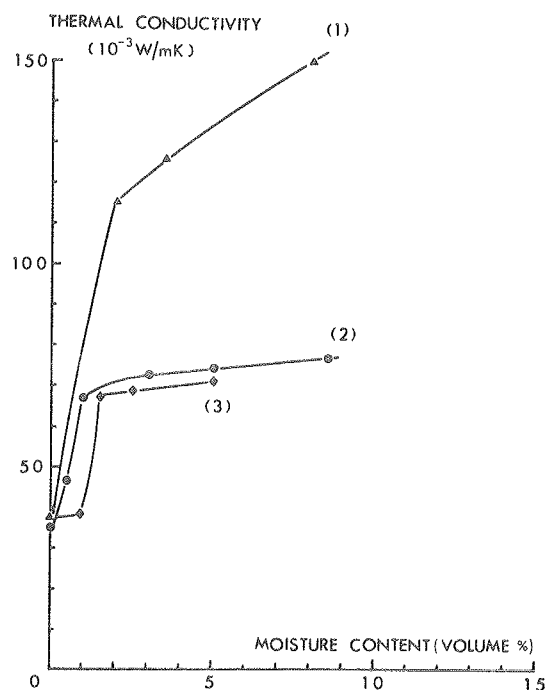
Figure 3.25   Thermal conductivity versus moisture content for mineral wool.
(1) Joy, fiber glass (92 kg/m³, 24°C), (2) Jespersen, rock wool (78 kg/m³, 10°C) and (3) Jespersen, fiber glass (62 kg/m³, 10°C). (From Langlais et al., 1983).

Langlais et al. were able, in other of their own experiments and by theoretical considerations, to reproduce the results obtained by Jespersen. The theoretical results were obtained by considering the phase changes of the vapor as long as it was migrating, thereby calculating an apparent thermal conductivity. Such a thermal conductivity, which is only valid for the initial, even distribution of moisture, changes not only with moisture content but also with mean temperature and temperature difference. The results obtained are therefore much dependent on the experimental conditions. They also become difficult to apply to conditions in the field, where circumstances of course are much more varying than in the laboratory.

Hedlin, 1983 in a transient experiment plotted 24 hour averages of heat flux as a function of corresponding averages of temperature difference measured in the field

on flat roofs with different moisture content (figure 3.26). Two puzzling results were obtained from his experiments. One was that the heat flux curve consistently crossed the abscissa at a temperature difference a few degrees higher than zero. Secondly, the resulting $Q-\Delta T$ curve, though smoothly developing over a large ΔT-interval suddenly jumped to another level from where another smoothly developing curve was followed. This jump occurred for 24 hour data lying in either the spring or in the fall.
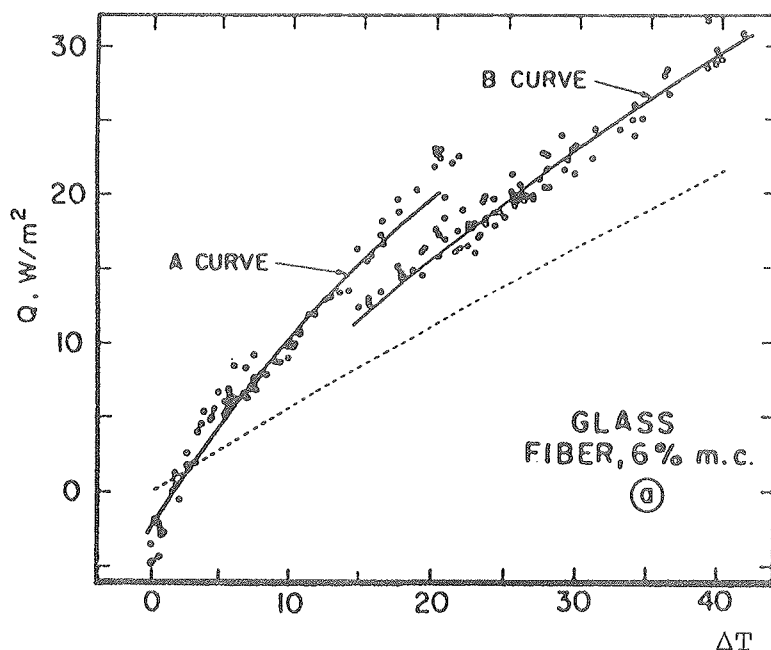
Figure 3.26   Daily averages of heat flows plotted as a function of daily averages of temperature difference from a Canadian field test on a flat roof with fiber glass insulation. (From Hedlin, 1983).

Hedlin gives the explanation himself in the same and in later papers (1987 and 1988a). On days where the mean temperature difference was close to zero, the temperature of the roof surface was as much above the indoor temperature as it was below. But the vapor pressure, being a non–linear function of temperature, on average has more downwards than upwards directed gradients, and therefore the vapor transfer and the latent heat transfer adds up to a larger value down than up. The jump from one type of $Q-\Delta T$ relation to another comes when, in the daytime, the temperature of the roof surface begins to exceed the indoor temperature. The moisture that was immovably deposited at the top of the roof in the winter now begins to move and therefore the latent heat effect begins to show itself together with the heat conduction.

Thomas et al. 1983 also waited until steady state was reached ("up to several weeks") when they determined thermal conductivities of wet fiber glass. They compared their results with calculations of the thermal conductivity from analytical models where the material contained dry insulation and moisture in either a series or a parallel connection. The results measured were somewhere in between the results of the two theoretical calculations, though closest to the one assuming a series connection. This may be explained by the location of the moisture in a thin layer next to the cold plate after steady state has been reached. The result of this work is an ability to estimate the influence of moisture on type I heat transfer. With this "effective" thermal conductivity and by accounting for the supplementary latent heat flux Thomas et al. were able, with a mathematical model, to reproduce the temperature profile at different times in an initially uniformly wetted specimen when it was subjected to a temperature gradient in an apparatus for determining thermal conductivities. They also, theoretically and experimentally, found a considerable decrease with time in the "apparent" thermal conductivity (including sensible as well as latent heat transfer) from the time when the test was initiated until steady state was reached.

These results agree with the general shape of heat fluxes plotted against time found by Kumaran, 1987 in several tests in a heat flow meter apparatus with fiber glass insulation initially wetted on the warm side. The general shape of these curves is shown in figure 3.27. A typical curve consists of three regions after the short initial deflections (A–B). First comes a period (B–C) with a constant and high heat flux, Q_1 (quasi stationary conditions). During this period the sensible heat flow as well as the vapor flow, and thereby the flow of latent heat, is constant. The period lasts as long as the warm side is saturated. Then comes a period (C–D) where the moisture is released at hygroscopic vapor pressures from the warm side, and therefore the flows of vapor and latent heat are steadily decreasing. This period does not last long for fiber glass while it is dominating over the period (B–C) for hygroscopic insulation materials like spray–cellulose. Finally, when the warm side of the insulation is dry (or rather has a vapor pressure that corresponds to saturation at the cold plate) the real steady state is reached (D–E) where the heat flow is clearly smaller and constant, Q_2. Provided there is no heat pipe effect because of liquid back–suction (for instance because of gravity) this final heat flux corresponds to the one caused by type I heat flow.

Sandberg, 1986 compared the magnitude of heat flow of type III (latent heat) for a
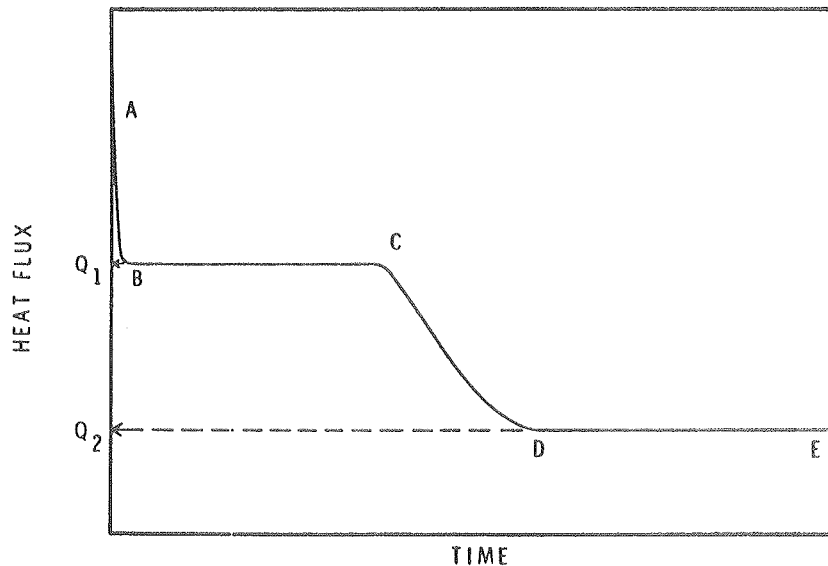
Figure 3.27   Typical development of the heat flux as a function of time measured in a heat flow meter apparatus for porous insulation, initially wetted on the warm side. (From Kumaran, 1988).

saturated material to the magnitude of heat flow of type I (sensible heat). The calculations, that assumed 10°C as an average temperature, used a 3% increase due to latent heat transport as a definition of when this effect has to be considered. The result was that latent heat transfer is important for materials like mineral wool, wood wool cement and perhaps for aerated concrete and polystyrene. Ordinary concrete, brick and wood were mentioned as materials where the latent heat flow would always be less than the limit. It may be added that a similar calculation at a higher temperature would have increased the importance of the latent heat (because of the nonlinear variation of the saturation vapor pressure with temperature). Thus, latent heat should also be considered in aerated concrete and polystyrene according to Sandberg's definition.

Sandberg, in the same report, performed a transient calculation, like those shown in the next two subsections, for a construction with permeable insulation between two impermeable membranes. The construction contained 6% moisture by volume. When the temperature on one side cycled between −10 and 30°C while 20°C was held on the other side, he found total heat flows that were considerably higher than those caused by the sensible heat. He also noticed an earlier occurrence of the peak of the heat flow and concluded that the effect of latent heat was the same as a decrease in thermal capacity.

104

These examples from literature serve to show the impossibility, for moist permeable materials, of looking upon heat flow as an unequivocal function of temperature difference. Thus, in order to get more accurate predictions of thermal performance of such materials, the definition of R–values and thermal conductivities should be supplemented with a more detailed description of moisture migration.

3.4.2 TRANSIENT EXPERIMENTS WITH LATENT HEAT TRANSFER

This subsection describes two transient experiments performed with latent heat transfer – one in the field and one in the laboratory. The field test was conducted on roof specimens in an outdoor test facility at the Saskatoon department of the Institute for Research in Construction, National Research Council of Canada. The test in the laboratory was the same test as that mentioned in section 3.3.2 about the Hygro Diode, performed as part of this work in a "Large Scale Climate Simulator" at Oak Ridge National Laboratory in Tennessee, USA.

FIELD TEST:

Hedlin, 1988b reports on a test with a flat roof insulated with 61 mm of high density fiber glass. The fiber glass contains between 0 and 1% moisture by volume, i.e. from dry insulation to insulation having somewhat more than the maximum hygroscopic moisture content. This moisture content is lower than most levels where the moisture impact on thermal performance has been studied, and the impact of moisture on sensible heat flow should be quite small.

The experimental setup is shown in figure 3.28. Heat flux is measured at the bottom of a cylinder of insulation. This cylinder is encapsulated in a wrap of polyethylene so the added moisture on the top of the insulation is kept within the area of measurement. Temperatures are measured at the top and at the bottom of the insulation. The roof surface was either black or covered with gravel in order to obtain different levels of peak temperatures.

As the experiment was conducted in the summer, the moisture added evaporated from the top of the roof in the daytime, diffused through the insulation and
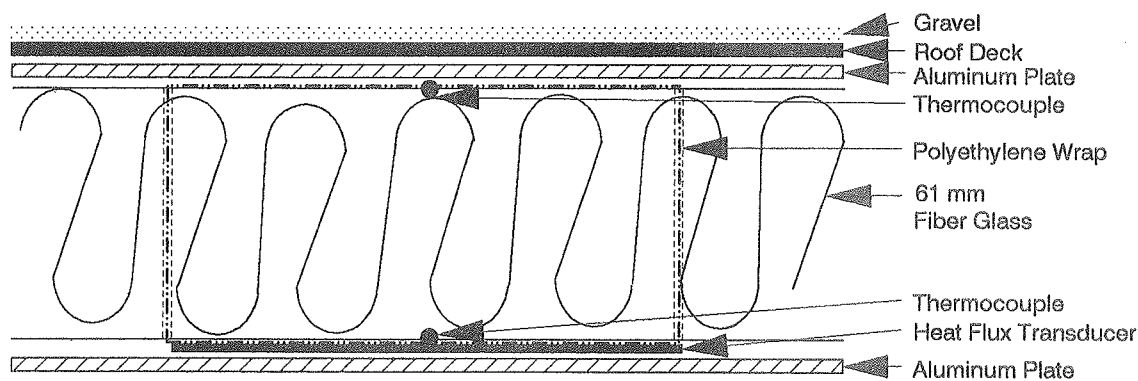
Figure 3.28   Experimental setup in a field test of latent heat transfer.

condensed at the bottom where the heat flux transducer was located. In the night, this moisture was re–evaporated and migrated to the top. The result is some sort of a heat pipe effect. At this moisture content there is no liquid transport to insure a continuous evaporation/condensation process – like in a real heat pipe – but the diurnal variations allow the same amounts of moisture to migrate back and forth over the 24 hours of a day. A simple calculation shows that already around 0.25% moisture by volume (corresponding to less than a quarter of a millimeter of condensate) the amount of moisture is sufficient for the source required at the warm side not to become depleted in one typical summer day.

Hedlin's measurements of temperature and the applied initial conditions were used as input for simulations with MATCH. The same temperature conditions were also applied to a calculation of a similar but dry roof. The calculated heat fluxes at the bottom are shown in figure 3.29 for a construction with 0.25 vol–% moisture together with the results of Hedlin's measurements. As it is seen, the agreement is quite good considering that some of the material parameters for the fiber glass had to be estimated. It is also seen how the addition of moisture severely affects the resulting heat flows – they are approximately doubled.

The total periods of the data available from the measurements performed at different moisture content varied between 3 and 14 days. For each set of data the sum was calculated separately for all inwards and outwards heat flows in Wh/m^2 (Pedersen, 1989b). The resulting deviation between measurement and calculation varied between 2 and 16%, i.e. the agreement was satisfactory.

106
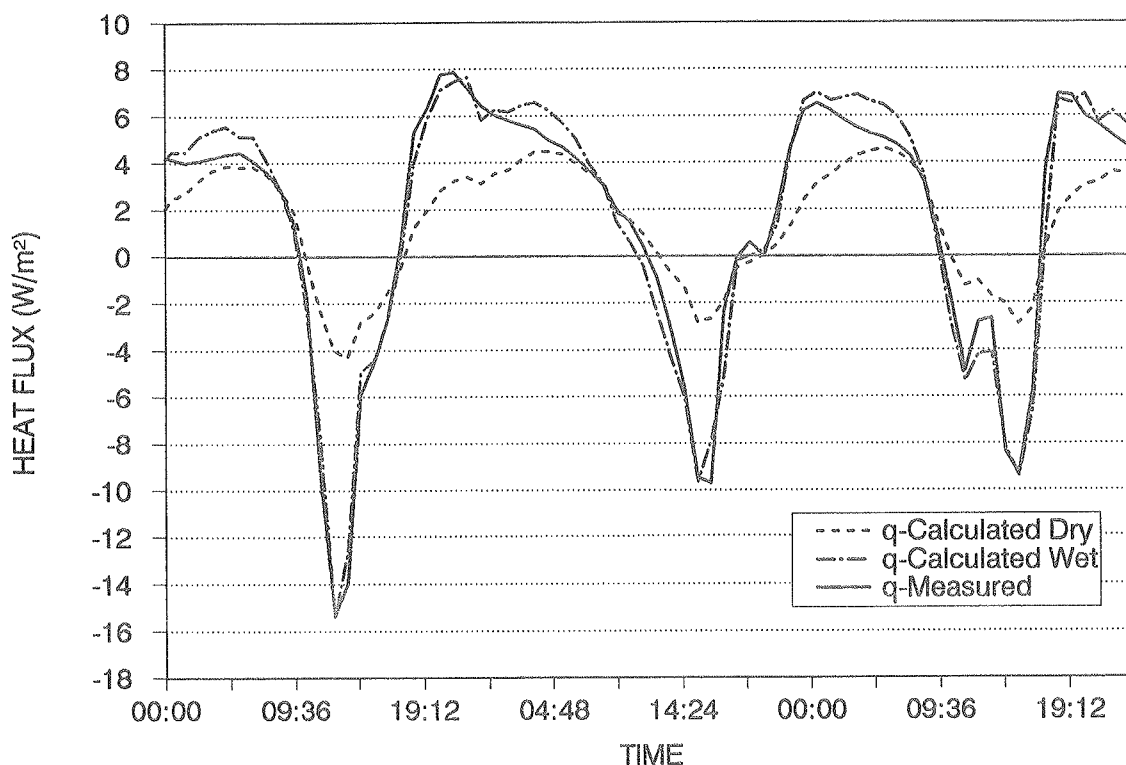
Figure 3.29   Measured wet and calculated wet and dry heat flows for the construction with 0.25 vol–% moisture. Inward heat flows are negative.

The calculations of summed outwards and inwards heat flows were also used to calculate the increase from dry to wet constructions. The results are shown in table 3.3. It is seen that there is some effect already at 0.10 vol–% moisture, while almost the full effect is seen from 0.25 vol–%. The results obtained at the different moisture contents are not quite comparable, however, because they were not obtained in the same periods and the boundary conditions and the duration of the experiments may therefore have been different. One can also tell that the effects are relatively larger for the inwards than for the outwards heat flow. This is because (1) most of the dry heat flux is outwards directed and (2) the moisture started from the top and may therefore, over the duration of each experiment, have migrated more down than up — on average.

TEST IN THE LABORATORY:

Heat fluxes were measured in the same panels that were tested for drying rates in the Large Scale Climate Simulator of Oak Ridge National Laboratory (see section

Moisture Content	Inwards	Outwards	Θ
0.10 vol-%	38	2	%
0.25 vol-%	163	53	%
0.50 vol-%	260	112	%
1.00 vol-%	117	138	%

Table 3.3   Increase of heat flows through differently wet constructions compared to those of dry constructions (calculated).

3.3.2). Figure 3.12 also shows the location of the heat flux transducers in the cold deck constructions that were tested.

One transducer, the one next to the vapor retarder, is assumed to register the sensible as well as the latent heat. The vapor condenses when it hits the heat flux transducer because the transducer is made of an impermeable material and is located almost in the same horizontal plane as the vapor retarder — where the moisture has to condense anyway. The other transducer is located between the top of the insulation and the plywood/blotting paper sandwich. At first the moisture will also condense on this transducer, but that makes the vapor pressure on the transducer equal to the saturation pressure at the transducer temperature. The bottom of the plywood/blotting paper sandwich has almost the same temperature but it absorbs the moisture at a hygroscopic vapor pressure being less than saturation (at this moisture content). Therefore, all the moisture that condenses on the transducer re-evaporates immediately, bypasses the transducer and is absorbed in the wood and paper. When the condensation and re-evaporation rates are equal, the latent heat effects are not felt at the transducer and therefore only the sensible heat is registered here. This hypothesis was confirmed by the readings of the transducer at the top being far less than those from the transducer at the bottom despite the fact that the temperature impulses were imposed from the top.

Figure 3.30 shows the measured heat flux at the top of the insulation plotted together with the calculated heat transfer by conduction at the same location. The two other curves in the same figure shows the measured heat flux at the bottom together with the calculated total heat flux at this place. The period shown is the one in the middle of figure 3.13 with the large temperature gradients that are varied in diurnal cycles. Heat flux results are shown for the panel with a punched

108

polyethylene membrane. The temperatures at the boundaries of this panel, quite similar to those from the panel with the hygrodiode (figure 3.13), were used as input to the calculations.

The panel with the ideal polyethylene also had a layer of blotting paper between the polyethylene and the bottom of the fiber glass. This, apparently, had the effect described above that some of the moisture was bypassed around the transducer, so it did not register all of the latent heat flow. The bottom transducer from this panel gave readings (not shown) that were somewhere between the expected sensible and total heat flows.
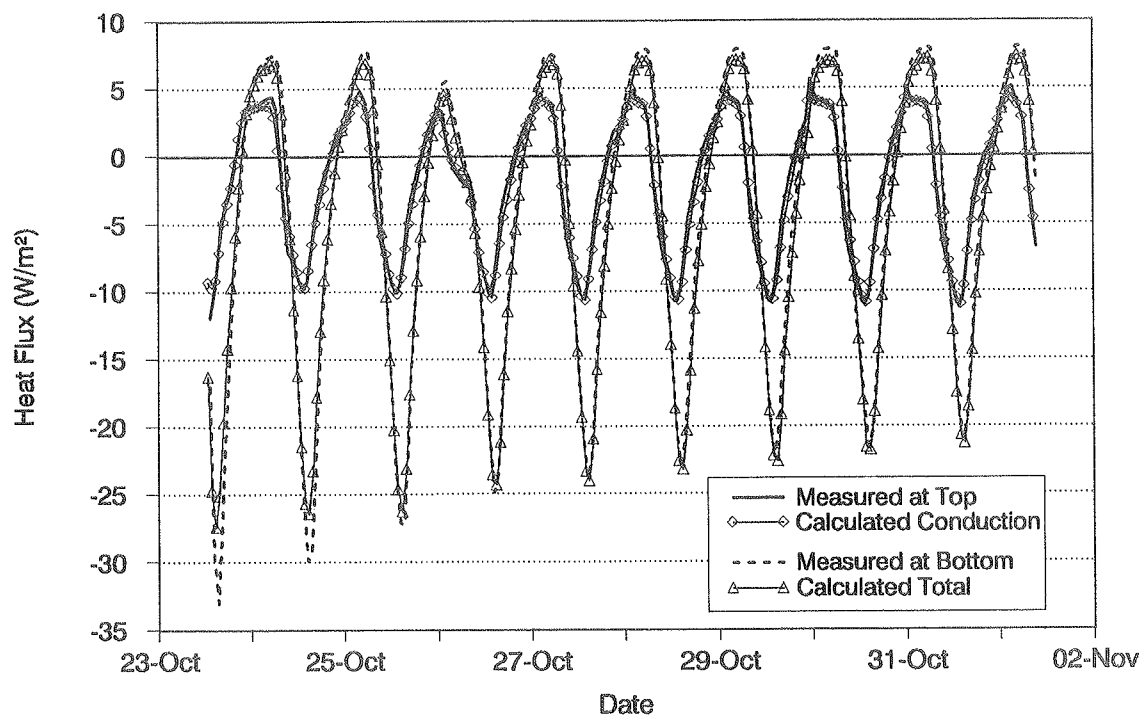
Figure 3.30   Measured and calculated heat flows for the panel with punched polyethylene. Conduction heat flow is shown for the top of the panel and total heat flow for the bottom.

There is some discrepancy between the negative peaks of the measured and calculated total heat flows the first two days of the period shown. Another discrepancy, which is seen throughout the whole period, is that the total calculated heat flows do not reach the same amplitude in the positive direction as the measured results. If the positive and the negative heat flux values are added separately for the whole period, except for the two first days, it is seen that the calculated total flow up (positive) is only 83% of the measured value while it is

106% of the measured value for downwards heat flow. The inclusion of the first two days in the sums actually gives better results because the error in the beginning counteracts the errors throughout the rest of the period.

These results are considered quite acceptable considering the number of thermal and hygric parameters for the materials included in the calculation. Some of the thermal parameters were determined in a separate part of this experiment while other parameters had to be estimated.

3.4.3 SIMULATIONS OF LATENT HEAT TRANSFER

This section takes advantage of the knowledge gained in steady state and transient experiments with latent heat transfer and uses this information to analyze the thermal balance of a construction for a whole year in different climates. The goal with analyses of this kind must be to incorporate the latent as well as the sensible heat flows through constructions with permeable materials into models that analyze whole building thermal loads (models like DOE–2 (US), BLAST (US), TSBI (DK), ESP (UK) etc.). The calculations shown here are to be regarded as another step in this direction.

The same type of construction that was calculated in section 3.3.3 for diffusion through EPDM is used here. This time, though, it has been assumed that the roofing membrane as well as the vapor retarder are perfectly vapor tight, i.e. all the moisture initially present stays in the roof cavity. The calculation assumes 1% moisture by volume to be present in the roof. Since the insulation thickness is 100 mm (of 120 kg/m^3 mineral wool) this corresponds to 1 kg moisture per square meter roof. The construction is, again, exposed to either the Danish Test Reference Year or the Test Meteorological Year for Miami, FL. The notes from section 3.3.3 about the probability of having such a construction in these two types of climate are of course still valid, i.e. insulation thickness, presence of vapor retarder and composition of materials may not be according to local standard these two places.

The calculations assume an effect from the presence of moisture on type I heat transfer. This effect is quite small because the moisture content is not very high and because most of the moisture will be located in a thin layer next to one of the

110

vapor–tight materials. The results shown compare the conducted heat (sensible heat) and the latent heat. Calculations of dry constructions will probably not give the same results as obtained here for sensible heat alone. The reason is not as much the inclusion of the small moisture effects on the thermal conductivity as it is the change of the thermal pattern when the latent heat is being transferred. It gives smaller temperature gradients across the insulation and the sensible heat flows shown will therefore be less than those that would have been obtained across similar dry constructions.

The calculations start in July of one year and run all through the next year. Results are shown for this second year only.

Figures 3.31 and 3.32 give the location of moisture in the insulation for the constructions located in Denmark and Miami, respectively. These graphs are shown to give an initial idea of how the moisture migrates within the insulation. The values shown are daily averages. The variations within each day should be added to these seasonal variations. These hourly variations are, of course, included in the calculations.
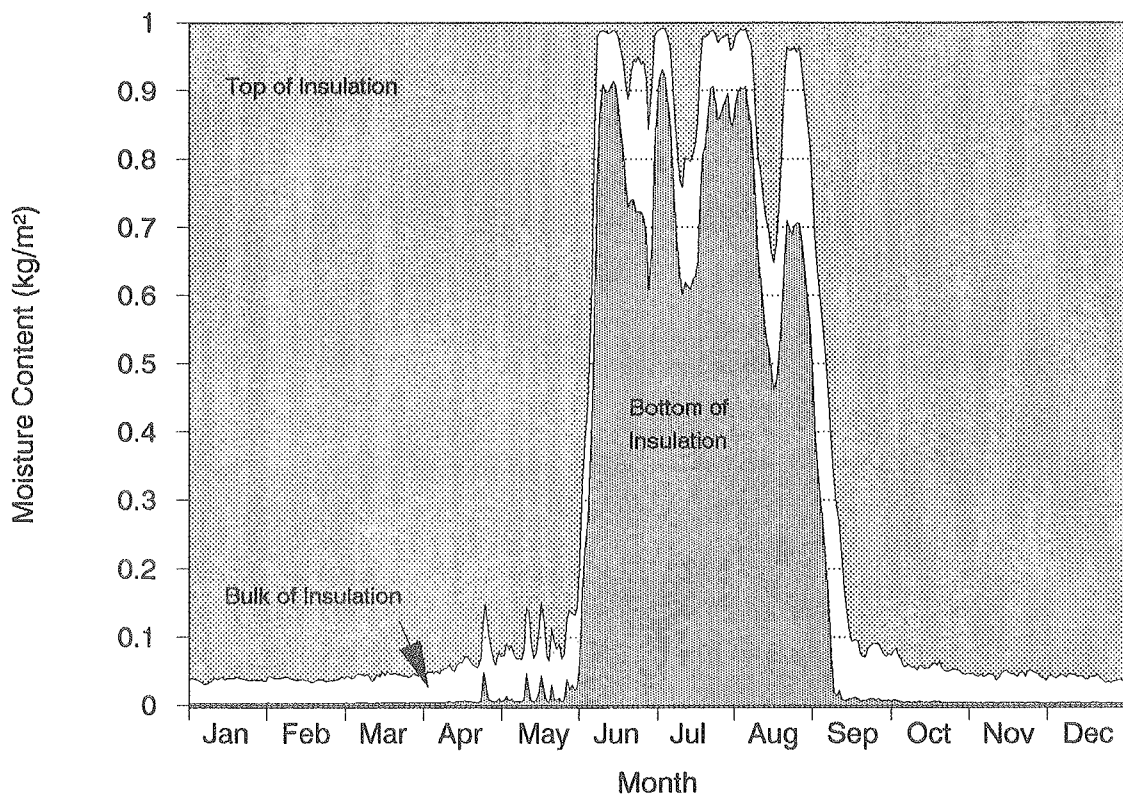
Figure 3.31   Annual variation of the location of moisture within the construction exposed to the Danish climate.
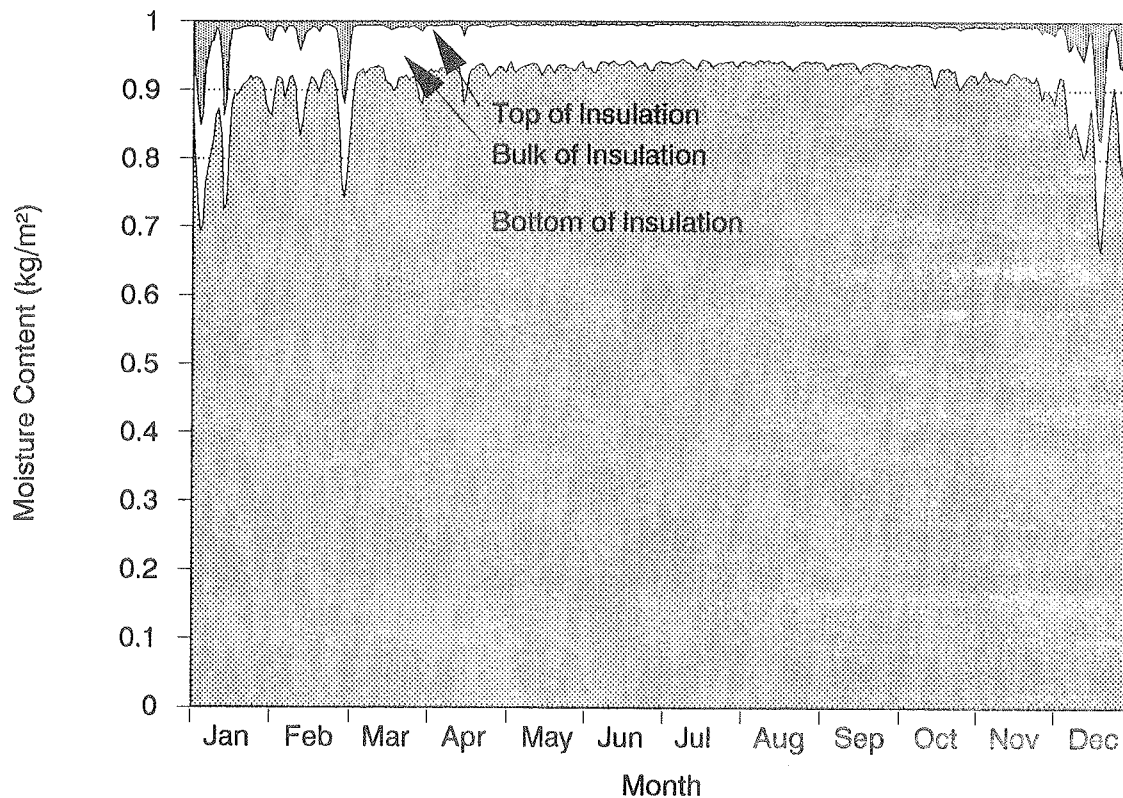
Figure 3.32   Annual variation of the location of moisture within the
construction exposed to the climate in Miami, FL.

The moisture stays in the top of the insulation for about three quarters of the year
in the Danish construction. It has been calculated as if it were absorbed by the
outmost insulation layer (1 cm), but most is probably accumulated in an
approximately 1 mm thick layer of condensate immediately under the membrane
(and similarly with the summer condensate at the bottom). Most of the moisture
stays at the bottom of the insulation in a few summer months. The central part of
the insulation (8 cm) holds an almost constant amount of hygroscopic moisture all
the time. It does, however, absorb a little more in the periods when the moisture
migrates a lot.

In Miami, most of the moisture is accumulated at the bottom of the insulation
throughout most of the year. Only small amounts migrate to the top for shorter
periods in the winter.

Figure 3.33 shows the daily sums of positive and negative heat flows for conduction
alone as well as for the added amount from latent heat (the shaded area) for the
Danish construction. The heat flows are registered at the bottom of the insulation.

112

In the winter, the moisture stays permanently at its location in the top of the roof and, therefore, there is no contribution from latent heat in this period. Only between May and September does the moisture migrate in diurnal cycles — driven down by the sun in the daytime and up in the nighttime when the roof surface is cooled by the outdoor air and by radiation to the sky. The magnitude of the latent heat depends more on the amount of moisture involved in the diurnal cycles than on the location of the bulk of the moisture. An investigation of a period in the summer shows that the migrating amount is around 0.065 kg/m² per day (i.e. 0.065 vol–% moisture). This amount is often determined by the smallest of the potentials for driving the moisture either up or down. If, for instance, in a period with many warm and sunny summer days the bulk of the moisture is located at the bottom, the limiting factor becomes the cooling of the roof surface in the night, as it determines how much moisture is driven to the top for re–evaporation the next day.
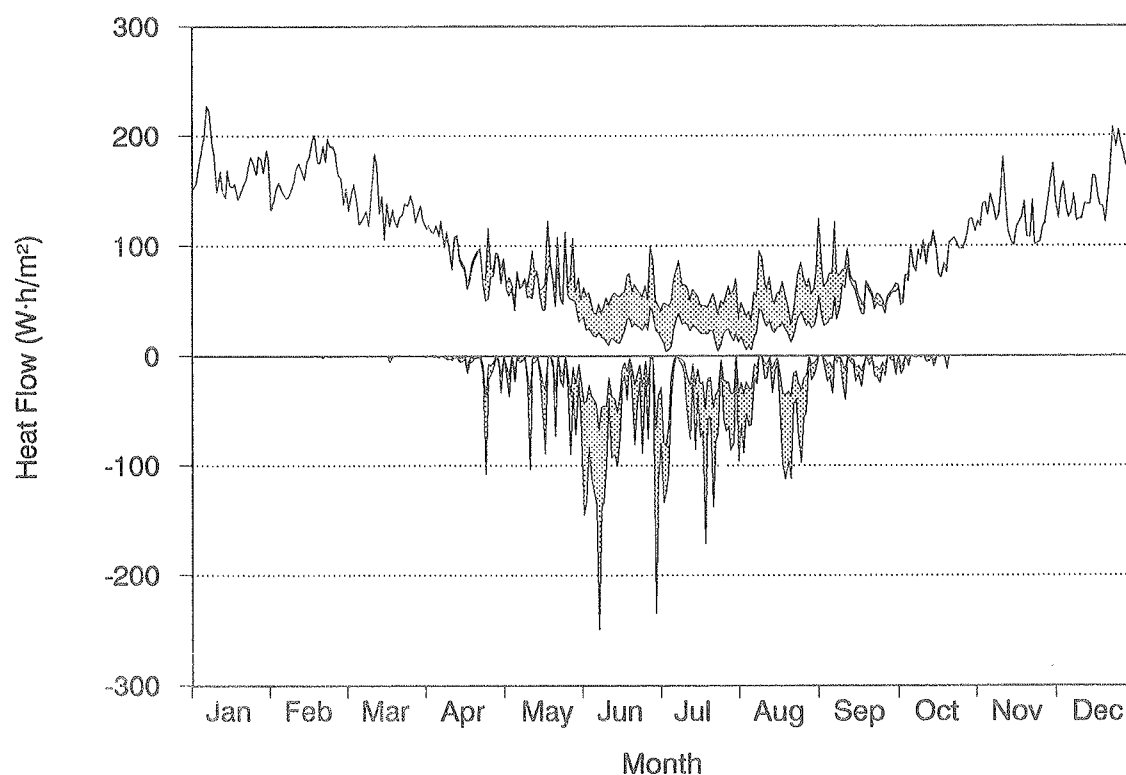
Figure 3.33   Daily sums for Denmark of heat flow up (positive) or down by conduction alone and by latent heat transfer (shaded area).

The numerical value of the latent heat transfer is about the same for the upwards as for the downwards heat flow since the same amount of moisture is driven back and forth. Table 3.4 summarizes the added heat flows up and down through the

113

roof for the whole year (in kWh/m²). The relative impact is largest on the heat flow into the building since this figure is quite small when the latent heat is not considered.

Denmark	Sensible	Latent	Total	Increase
Up	33.8	4.5	38.3	13 %
Down	2.9	4.5	7.4	153 %

Table 3.4   One year sums for Denmark of heat flows up and down by sensible and latent heat transfer (kWh/m²).

Figure 3.34 shows a curve similar to figure 3.33 for conditions in Miami. Heat flow is downwards directed most of the year. The latent heat effect is there all the year. In the summer, it is because the top of the insulation gets quite warm in the daytime and therefore dries to a very low hygroscopic moisture content. This moisture (around 0.03–0.04 kg/m²) returns to the top layers of the insulation in the night, even if the temperature gradients are not upwards directed. It is only driven by differences in hygroscopic vapor pressures. Diurnal temperature fluctuations of the roof surface in the winter cause the latent heat effect seen here. The annual sums of heat flows are shown in table 3.5.

Miami	Sensible	Latent	Total	Increase
Up	1.4	8.9	10.3	643 %
Down	21.7	8.9	30.6	41 %

Table 3.5   One year sums for Miami over heat flows up and down by sensible and latent heat transfer (kWh/m²).

The numerical value of the latent heat transfer is larger in the climate of Miami than it is in the Danish climate. Usually, the most important determining factor is the number and magnitude of diurnal variations of roof surface temperature around the indoor temperature. Thus, latent heat becomes important in the summer in northern climates and in the winter in southern climates. Most climates will therefore have seasons with important transfer of latent heat.
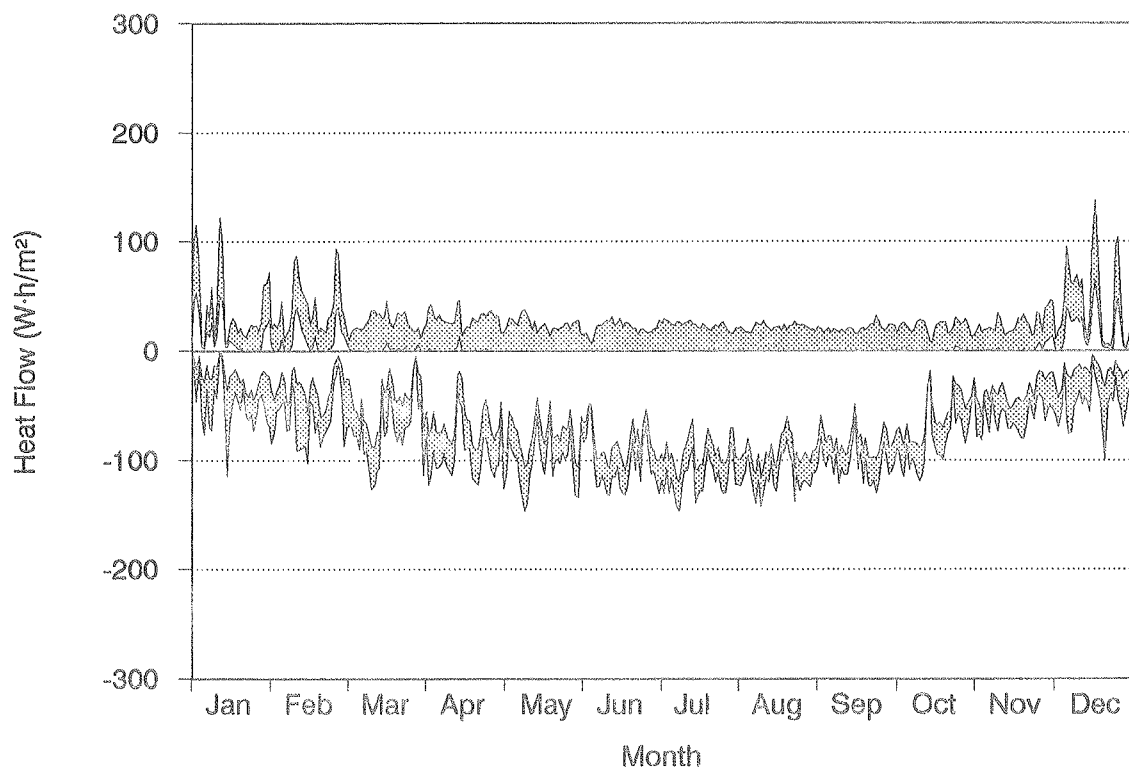
Figure 3.34   Daily sums for Miami of heat flow up (positive) or down by
conduction alone and by latent heat transfer (shaded area).

The effect on the fuel bill for running the HVAC or heating system must be determined by models for building loads analysis, as the capability of the underlying rooms to absorb the calculated extra loads must be considered. It seems, that the effect on the heating requirements is limited because the latent heat becomes important in weather situations where the heating requirements are vanishing (i.e. summer in Denmark and all the year in Miami). It is possible in both climates though, that buildings that require cooling because of high internal thermal loads may suffer from this extra contribution of heat. The extra thermal load appears in the daytime where it coincides with the peaks of activities in for instance office buildings.

The effect may become less if the insulation is more hygroscopic (by using foam insulation or increasing the binder content of mineral wool) or if the insulation has facers that separate the boards. Calculations have been shown by Courville and Pedersen, 1990 for constructions that were insulated with faced mineral wool or with polystyrene boards. Using two layers of mineral wool with a facer in between the boards approximately halved the latent heat effect, while the use of polystyrene

115

instead of mineral wool reduced the latent heat flows to approximately 20%.

Reducing the moisture content is of course another solution. Courville and Pedersen showed that the moisture content must be less than approximately 0.25 vol–% before this helps. From this moisture content and up there is enough moisture available for the diurnal cycles of vapor transfer to take place. Changing the moisture content above this limit practically does not influence the latent heat effect. As soon as there is over–hygroscopic moisture present — as there usually is in warm deck roofs — this moisture will participate in the latent heat transfer.

DISCUSSION

The theory for combined heat and moisture transport can be found in several textbooks. Quite often, these books describe the combined phenomena by two partial differential equations where the temperature and moisture content are used as the driving potentials for both heat and moisture transfer. Material parameters are the moisture and thermal diffusivities together with coefficients which describe the mutual interference between the transport of heat and moisture. Such parameters combine both the transport and storage capabilities of a material in a single figure. A major drawback of this type of model is that one of the driving potentials, the moisture content, undergoes abrupt changes at material interfaces, thus requiring special treatment of these.

The theory given in this work differs as to the way in which the transport phenomena for heat, vapor and liquid moisture are described. The equations needed to characterize the transport of heat and matter are shown when there is no cross interference. These are equations of similar types. Required in a transient description are:

-     Transport equations. Fourier's, Fick's and Darcy's laws.
-     Balance equations for enthalpy, water vapor and liquid moisture.
-     "Equations of state" which give the relation between the driving potentials, temperature, vapor and liquid pressures, and their corresponding quantities from the balance equations. These relations are given by the heat capacity, the sorption and the suction curves for the material.

The similarity in description of moisture and heat transfer demystifies the matter of subject. It makes it easy to tell when and where the cross coupling effects become important. For instance, the most important effect of temperature on moisture transport is usually the way the saturation vapor pressure is affected. This is an effect in the "equation of state" for vapor. An important effect of moisture on the thermal balance is the release or uptake of enthalpy when moisture condenses or evaporates. This effect is incorporated in the balance equation for enthalpy.

117

Another advantage of the equations used is that the driving potentials are closer to those used in irreversible thermodynamics. This implies that they change in a continuous way across material interfaces.

A numerical model, called MATCH – Moisture and Temperature Calculations for Constructions of Hygroscopic Materials, has been developed for analysis of composite building constructions according to the theory outlined. This model applies a finite control volume method as the solution technique. A special solution scheme, called "API" (Alternating Parameter Implicit method), has been used that calculates one parameter implicitly at a time with an explicit influence from the secondary parameter, i.e. the temperature takes part in the determination of new temperatures implicitly, while the moisture effect is taken into account explicitly. This has proven to be a fast method that gives sufficient accuracy – considering the uncertainty in material parameters. The philosophy has been to avoid iterative optimization of each time step as this is a time consuming process and the accuracy gained is not found to be justified.

The model uses analytical expressions for how the material parameters vary with primarily the levels of moisture content, and with temperature. Variables in these equations have been implemented in a simple materials library – thus making it easy to perform calculations of new constructions by simply assigning the material parameters by means of the name of the material. A small preprocessor eases the generation of input and a graphical display of some of the important variables in the calculation has been developed to further improve the user interface.

The model was validated against well defined data for the drying of aerated concrete. The results simulated for moisture distributions and drying rates came fairly close to those found in measurements with gamma ray equipment. The large number of parameters involved in the definition of the problem gave reason, however, to emphasize the importance of knowing the value of these as accurately as possible.

Several other applications have been analyzed with the model. Some of them are of a kind that mainly will be of interest for the researcher, while others involve quite practical problems that may be of interest for the building designer in finding the optimal solution of a design problem.

118

The way the model was constructed made it easy, in an empirical way, to include the effect of hysteresis in the sorption and suction curves. The calculations appeared to describe the hysteresis well when a specimen that was subjected to extended periods of wetting and drying was simulated. The hysteresis turned out, however, not to be important in the analysis of a "real" construction subjected to a naturally varying climate. The use of a middle curve, between the drying and wetting curves in the diagrams for moisture retention, gave practically the same results.

Condensation of moisture has been a traditional problem in low slope roofs. Years of research and practical knowledge have shown that the moisture cannot be removed by non–mechanical ventilation of the roof cavity with outdoor air. Such ventilation may cause even more humid indoor air to penetrate into the cavity and give rise to further condensation. New ideas are based on a concept in which the exterior parts of the roof are made perfectly air tight combined with the use of a new sort of vapor retarder.

The recently developed vapor retarder called the Hygro Diode has a large vapor resistance when it is dry, as in the winter, but it has the ability to let liquid moisture pass through easily. Thus, summer condensate formed on the vapor retarder in sunny weather will be removed from the roof cavity rapidly, while the diffusion into the cavity in the winter is quite slow. Experiments in a climate simulator and in the field showed, along with predictions by MATCH, that the new vapor retarder is indeed able to dry out considerable amounts of excessive moisture in roofs.

MATCH was also used to determine if, as often stated, the use of permeable roof membranes would cause moisture accumulation in roofs in hot humid climates, especially when the temperature dependence on the vapor permeability of such membranes is considered. Though some parameters were not considered, especially the probability of water ponding, the calculations performed by means of a weather tape for Miami, FL, did not indicate that such accumulation would take place.

Finally, after it was validated against heat flux data from the field and the laboratory, the model was used to analyze the increase of heat flows caused by latent heat transfer. The transfer of such heat by evaporation of moisture from the warm side of the construction, migration of vapor through permeable insulation

and condensation on the colder side, becomes important in weather situations where the temperature of the outer surfaces fluctuates diurnally around the indoor temperature. The process is poorly described by simply increasing the "apparent" thermal conductivity, as was common practice when tools for simultaneous calculation of heat and moisture transfer were not available.

For shorter periods of time, heat flows may be more than doubled due to the increase by latent heat compared with the heat transferred by conduction. Over whole-year periods this process could cause significant additional thermal loads on buildings — in a calculation for Miami for instance, the annual heat flow into the building was increased by approximately 40% of the conducted heat when the latent heat was taken into account.

CONCLUSION

A numerical model has been developed for combined heat and moisture transport in composite building constructions, using the basic transport equations, Fourier's, Fick's and Darcy's laws and usual descriptions for moisture retention and heat storage. The mutual interference between the transport of heat and moisture is easily taken into account in these equations.

The model runs on a personal computer. The aim has been to make the user interface a friendly one in order to give designers of buildings and building components easy access to an advanced tool for modeling of hygrothermal problems.

The power of the model is shown by its application on several building physical problems. Of interest for the researcher are calculations where the hysteresis in the moisture retention curves is investigated and calculations that simulate and help explain measurements in the laboratory. But the model has also been used for more practical applications such as the analysis of the moisture behavior of building components, for example flat roofs, or the analysis of the thermal performance of wet constructions.

The availability of such models presents a further step towards incorporating improved building physical principles in buildings and building codes of the future.

☺ ☺ ☺

REFERENCES

Ahlgren, L., "Fuktfixering i porösa byggnadsmaterial", ("Moisture Fixation in Porous Building Materials", in Swedish with English summary), Division of Building Technology, The Lund Institute of Technology, Report 36, 1972.

Andersson, A–C., "Verification of Calculation Methods for Moisture Transport in Porous Building Materials", Swedish Council for Building Research, Document D6:1985, 1985.

ASHRAE, "ASHRAE Handbook: 1989 Fundamentals", American Society of Heating, Refrigerating and Air Conditioning Engineers, Atlanta, 1989.

Bisgaard, N.F., "Opvarmning og ventilation 1, Varmetransmission", ("Heating and Ventilation 1, Heat Transmission", in Danish), Akademisk Forlag, 1974.

Bomberg, M., "Moisture Flow Through Porous Building Materials", Division of Building Technology, Lund Institute of Technology, Report 52, 1974.

Byggestyrelsen, "Bygningsreglementet 1982", ("The Danish Building Code", in Danish), Copenhagen, 1982.

Childs, P.W., Courville, G.E., Pedersen, C.R. & Petrie, T.W., Report on moisture tests in the Large Scale Climate Simulator – to be published, 1990.

Christensen, G., Prebensen, K. & Vesterløkke, M., "Sammenligning mellem retvendt og omvendt merisolering af flade tage", ("Comparison Between Conventional and Inversed Roofing with Additional Insulation of Flat Roofs", in Danish with English Summary), COWIconsult, Publ. nr. 492, 1986.

Cohan, L.H., "Hysteresis and the Capillary Theory of Adsorption of Vapors", Journal of the American Chemical Society, 66, pp. 98–105, 1944.

Courville, G.E. & Pedersen, C.R., Paper on latent heat transfer to be published, 1990.

Dansk Ingeniørforening, "Dansk Ingeniørforenings regler for beregning af bygningers varmetab, Dansk Standard DS 418", ("Rules for the Calculation of Heat Loss from Buildings", in Danish), Teknisk Forlag, 1986.

Danvak, "Varme– og Klimateknik, Grundbog", ("Heat and Indoor Climate, Fundamentals", in Danish), DANVAK, 1988.

Duffie, J.A. & Beckman, W.A., "Solar Engineering of Thermal Processes", Wiley, 1980.

Dupuis, R.M., "Field Survey of Moisture Gain Behavior Within Single–Ply Roof Systems", Proceedings – Second International Symposium on Roofing Technology, September 1985.

Fick, A., "Ueber Diffusion", Pogg. Ann. (Annalen der Physik und Chemie), 94, pp. 59–86, 1855.

Freeman, A., "Analytical Theory of Heat", Dover Publications, New York, 1955.
Glaser, H., "Graphisches Verfahren zur Untersuchung von Diffusionsvorgängen", Kältetechnik, heft 10, pp. 345–349, 1959.

Hansen, K.K., "Sorption Isotherms. A Catalogue", Building Materials Laboratory, Technical University of Denmark, Technical Report 162/86, 1986.

Hansen, P.F., "Koblet fugt/varmetransport i konstruktionstværsnit af beton", ("Combined Heat and Moisture transport in Cross Sections of Concrete Structures", in Danish), Beton– og Konstruktionsinstituttet, Arbejdsnotat, 1985.

Hartley, J.G., "Coupled Heat and Moisture Transfer in Soils: A Review", Advances in Drying, 4, 1987

Hedlin, C.P., "Effect of Moisture on Thermal Resistance of Some Insulations in a Flat Roof under Field–Type Conditions", Thermal Insulation, Materials, and Systems for Energy Conservation in the '80s, ASTM STP 789, American Society for Testing and Materials, pp. 602–625, 1983.

Hedlin, C.P., "Seasonal Variations in the Modes of Heat Transfer in a Moist Porous Thermal Insulation in a Flat Roof", Journal of Thermal Insulation, 11, pp. 54–66, 1987.

Hedlin, C.P., "Heat Transfer in a Wet Porous Thermal Insulation in a Flat Roof", Journal of Thermal Insulation, 11, pp. 165–188, 1988 (a).

Hedlin, C.P., "Heat Flow Through a Roof Insulation Having Moisture Contents between 0 and 1% by Volume, in Summer", ASHRAE Transactions, 94, pp. 1579–1594, 1988 (b).

Korsgaard, V., Prebensen, K. & Bunch–Nielsen, T., "Ventilation af flade tage", ("Ventilation of Flat Roofs", in Danish with English summary), COWIconsult, Publ. nr. 472, 1984.

Korsgaard, V., "Hygro Diode Membrane: A New Vapor Barrier", ASHRAE/DOE/BTECC Conference: "Thermal Performance of the Exterior Envelopes", Clearwater Beach, Florida, December 2–5, 1985.

Krischer, O., "Die wissenschaftlichen Grundlagen der Trocknungstechnik", Springer–Verlag, 1978.

Kumaran, M.K., "Moisture Transport Through Glass–Fibre Insulation in the Presence of a Thermal Gradient", Journal of Thermal Insulation, 10, pp. 243–255, 1987.

Kumaran, M.K., "Comparison of Simultaneous Heat and Moisture Transport through Glass–Fibre and Spray Cellulose Insulations", Journal of Thermal Insulation, 12, pp. 6–16, 1988.

Langlais, C., Hyrien, M. & Klarsfeld, S., "Influence of Moisture on Heat Transfer Through Fibrous–Insulating Materials", Thermal Insulation, Materials, and Systems for Energy Conservation in the '80s, ASTM STP 789, American Society for Testing and Materials, pp. 563–581, 1983.

124

Luikov, A.V., "Heat and Mass Transfer in Capillary–porous Bodies", Pergamon Press, 1966.

Lund–Hansen, P., "Fugttransport i byggematerialer", ("Moisture Transfer in Building Materials", in Danish with English summary), Thermal Insulation Laboratory, Technical University of Denmark, meddelelse nr. 15, 1967.

Nicolajsen, A., "Trykforhold i flade tage", ("Pressure Conditions in Flat Roofs", in Danish with English summary), Statens Byggeforskningsinstitut, Rapport 153, 1983.

Nielsen, A.F., "Fugtfordelinger i gasbeton under varme– og fugttransport", ("Moisture Distributions in Cellular Concrete During Heat– and Moisture Transfer", in Danish with English summary), Thermal Insulation Laboratory, Technical University of Denmark, meddelelse nr. 29, 1974.

Pedersen, C.R. & Rasmussen, M.H., "Kombineret fugt– og varmetransport i bygningsmaterialer", ("Coupled Heat and Moisture Transport in Building Materials", in Danish), Building Materials Laboratory & Thermal Insulation Laboratory, Technical University of Denmark, Masters Thesis, 1986.

Pedersen, C.R., "Koblet fugt og varmetransport i bygningskonstruktioner – fugtfysik", ("Combined Heat and Moisture Transport in Building Constructions – Moisture Physics", in Danish), Thermal Insulation Laboratory, Technical University of Denmark, Report 89–2, 1989 (a).

Pedersen, C.R., "MATCH – A Computer Program for Transient Calculation of Combined Heat and Moisture Transfer", Contribution to CIB W–40 meeting: "Reducing Moisture–Related Damage in the World's Buildings", Victoria, Canada, September 11–14, 1989 (b).

Philip, J.R., & de Vries, D.A., "Moisture Movement in Porous Materials under Temperature Gradients", Transactions American Geophysical Union, 38, No. 2, pp. 222–232, 1957.

Sandberg, P.I., "Byggnadsdelars fuktbalans i naturligt klimat", ("Moisture Balance in Building Elements Exposed to Natural Climatic Conditions", in Swedish with English Summary), Division of Building Technology, Lund Institute of Technology, Report 43, 1973.

Sandberg, P.I., "Thermal Resistance of Wet Insulation Materials", Nordtest Technical Report 063, Swedish National Testing Institute, SP–RAPP 1986:29, 1986.

Statens Byggeforskningsinsitut, "Bygningers fugtisolering", (National Building Research Institute, "Moisture Insulation of Buildings", in Danish), SBI–anvisning 139, 1984.

Tagpapbranchens Oplysningsråd, "Tagdækning med bitumenprodukter, Teknik, Økonomi", ("Roofing with Bituminous Materials, Technique, Economics", in Danish), TOR–Anvisning nr. 14, 1985.

Thomas, W.C., Bal, G.P. & Onega, R.J, "Heat and Moisture Transfer in a Glass Fiber Roof–Insulating Material", Thermal Insulation, Materials, and Systems for Energy Conservation in the '80s, ASTM STP 789, American Society for Testing and Materials, pp. 582–601, 1983.

Tobiasson, W., Korhonen, C., Coutermarsh, B. & Greatorex, A., "Can Wet Roof Insulation Be Dried Out?", Thermal Insulation, Materials and Systems for Energy Conservation in the '80s, ASTM STP 789, American Society of Testing and Materials, pp. 626–639, 1983.

Tobiasson, W., "Wetting of Polystyrene and Urethane Roof Insulations in the Laboratory and on a Protected Membrane Roof", Thermal Insulation: Materials and Systems, ASTM STP 922, American Society for Testing and Materials, pp. 421–430, 1987.

Tobiasson, W., "Wood–Frame Roofs and Moisture", Custom Builder, pp. 33–37, March 1988.

Tveit, A., "Measurement of Moisture Sorption and Moisture Permeability of Porous Materials", Norwegian Building Research Institute, Report 45, Oslo, 1966.

The following references have not been available for this work in their original print:

Darcy, H., "Les fontaines publiques de la ville de Dijon", Dalmont, Paris.

Fourier, J., "Théorie analytique de la chaleur", 1822. Available in English translation, see Freeman, 1955.

Knudsen, M., "The Kinetic Theory of Gases", Methuen, London, 1934.

BIBLIOGRAPHY

Pedersen, C.R. & Rasmussen, M.H., "Kombineret fugt— og varmetransport i bygningsmaterialer", ("Coupled Heat and Moisture Transport in Building Materials", in Danish), Building Materials Laboratory & Thermal Insulation Laboratory, Technical University of Denmark, Masters Thesis, 1986. 139 pages + appendices.

Hansen, M.H. & Pedersen, C.R., "Irreversibel termodynamik for koblet fugt— og varmetransport i porøse bygningsmaterialer", ("Irreversible Thermodynamics for Combined Heat and Moisture Transport in Porous Building Materials", in Danish), Thermal Insulation Laboratory, Technical University of Denmark, Report 88—17, 1988. 33 pages.

Pedersen, C.R., "Instationære diffusionsberegninger", ("Non—stationary Calculations of Diffusion", in Danish), Thermal Insulation Laboratory, Technical University of Denmark, Report 88—6, 1988. 62 pages.

Pedersen, C.R., "Matematiske modeller til simulering af fugtforhold under umættede tilstande i afsvovlingsprodukter", ("Mathematical Models for Simulation of Moisture under Unsaturated Conditions in Desulphurization Products", in Danish), Thermal Insulation Laboratory, Technical University of Denmark, Report 88—8, 1988. 16 pages.

Pedersen, C.R., "Stabile eksplicitte differensmetoder", ("Stable Explicit Finite Difference Methods", in Danish), Thermal Insulation Laboratory, Technical University of Denmark, Report 88—13, 1988. 20 pages.

Dytczak, M., Hansen, P.N. & Pedersen, C.R., "Characterization of the Thermal and Economical Performance of Thermal Seasonal Storage", Contribution to JIGASTOCK 1988, Versailles, France, Oct. 17—20, 1988,. 6 pages.

Pedersen, C.R., "Hvad er diffusivitet?", ("What is Diffusivity?", in Danish), Thermal Insulation Laboratory, Technical University of Denmark, Report 88—20, 1988. 11 pages.

Hansen, K.K. & Pedersen, C.R. (Editors), "Report from the Nordic Symposium — Numerical Methods for Combined Moisture and Heat Transfer in Building Materials and in Structural Elements", Building Materials Laboratory & Thermal Insulation Laboratory, Technical University of Denmark, 1989. 184 pages.

Pedersen, C.R., "Koblet fugt— og varmetransport i bygningskonstruktioner — Fugtfysik", ("Coupled Heat and Moisture Transport in Building Constructions", in Danish), Thermal Insulation Laboratory, Technical University of Denmark, Report 89—2, 1989. 129 pages.

Pedersen, C.R., "En sammenligning mellem differensmetoder og elementmetoder med henblik på beregning af koblet fugt— og varmetransport", ("A Comparison between Finite Difference and Finite Element Methods for Calculation of Combined Heat and Moisture Transport", in Danish), Thermal Insulation Laboratory, Technical University of Denmark, Report 89—5, 1989. 38 pages.

Pedersen, C.R., "MATCH – Moisture and Temperature Calculations for Constructions of Hygroscopic Materials – Users Guide", Thermal Insulation Laboratory, Technical University of Denmark, 1989. 23 pages.

Korsgaard, V. & Pedersen, C.R., "Evaluation of the Moisture Content in Heavily Insulated Flat Roofs in Scandinavia. Integral Part of the Design Work", VIIth International Roofing Congress, München, June 1989. 9 pages.

Pedersen, C.R., "Users Guide for Computer Program MAC, Moist Air Unit Conversions", Thermal Insulation Laboratory, Technical University of Denmark, 1989. 7 pages.

Pedersen, C.R., "MATCH – A Computer Program for Transient Calculation of Combined Heat and Moisture Transfer", Contribution to the CIB W40 meeting: "Reducing Moisture–Related Damage in the World's Buildings", Victoria, Canada, Sep. 11–14, 1989. 14 pages.

Korsgaard, V. & Pedersen, C.R., "Transient Moisture Distribution in Flat Roofs with Hygro Diode Vapor Retarder", Thermal Performance of the Exterior Envelopes of Buildings IV, ASHRAE/DOE/BTECC/CIBSE, Orlando, FL, USA, Dec. 4–7, 1989. 10 pages.

128

APPENDIX

The following is a print of the file for material data used by MATCH. Material data used in the calculations are taken from this library when nothing else has been mentioned in the text. The first few lines declare the names of the variables in the same order as they come in the list for each material. The names of the variables are approximately the same as those used in the report (see chapter 2) and should therefore be comprehensible.

File MATLIB.DAT

Material	delx
	m

{ Thermal parameters }

ro	cp	dtfreez	lambda	lambdauw	lambdaui
kg/m3	J/(kgK)	K	W/(mK)	W/(mK)	W/mK

{ Diffusional parameters }

deltadry	deltawet	usdes	us1des	us2des	usabs	us1abs	us2abs
kg/msPa	kg/msPa	kg/kg	- (1/n)	- (A)	kg/kg	- (1/n)	- (A)

{ Suctional parameters }

akliq	bkliq	ucr	ucap	uvac	plim1	plim2
kg/msPa	-	kg/kg	kg/kg	kg/kg	ln(Pa)	ln(Pa)

a-ipt	b-ipt	u0	a-dry	b-dry	lnp0
kg/kg	1/ln(Pa)	kg/kg	kg/kg*	-	ln(Pa)

AIRCONC		0.05					
500	900	7.0	0.15	0.3	0.62		
3.00e-11	6.00e-11	0.927	0.806	1.20e-02	1.60	0.641	5.72e-04
2.78e-16	20.956	0.4	0.70	1.50	7.50	12.50	
3.874	0.3794	133.553	132.662	9.028e-04	7.1833		

EPDM		0.0015					
1000.0	1000.0	3.0	0.20	0.6	1.8		
4.00e-14	4.00e-14	0.01141	8.33	7.21	0.0114	8.33	7.21
1.0e-50	0.0	0.03	0.02	0.03	1	1	
1	1	1	1	1	1		

Vapor permeability for EPDM based on thickness 0.0015 m (=60 mil).

```
BLOTPAP              0.002
220.0     1340.0     3.0       0.07      0.054     0.162
1.35e-10  1.35e-10   0.117     1.695     1.110     0.116     1.695     1.110
1.0e-50   0.0        0.3       0.3       10.6      1         1
1         1          1         1         1         1


BRICK                0.055
1700.0    800.0      5.0       0.8       4.4       9.4
2.30e-11  2.30e-11   0.0113    0.541     0.0748    0.0182    0.191     2.79e-05
2.66e-13  71.73      0.02      0.18      0.25      12.7      14.5
0.896     0.06711    0.009538  -1451.158 -8.43022  9.159994


BUR                  0.006
1050.0    1000.0     3.0       0.20      0.63      1.89
1.20e-15  1.20e-15   0.1391    0.543     0.235     0.139     0.543     0.235
1.0e-50   0.0        0.3       0.15      0.30      1         1
1         1          1         1         1         1
Vapor permeability for Built Up Roofing based on thickness 0.006 m.


CONCRETE             0.05
2400.0    800.0      15.0      2.0       36.0      108.0
2.5e-12   10.0e-12   0.04966   0.8475    0.4924    0.04631   0.9479    0.2566
7.156e-18 183.5      0.04      0.062     0.085     7.50      12.50
0.1389    0.008889   0.04524   -47149.0  -5.212    -8.277


CONC48               0.05
2400.0    880.0      15.0      1.0       35.0      108.0
2.5e-12   3.42e-12   0.04966   0.8475    0.4924    0.04631   0.9479    0.2566
4.107e-28 533.4      0.04      0.062     0.085     7.50      12.50
0.1389    0.008889   0.04524   -47149.0  -5.212    -8.277


EPS                  0.05
20.0      1400.0     5.0       0.034     0.004     0.054
5.00e-12  5.00e-12   0.09976   0.2068    0.01104   0.05848   0.09434   0.004770
1.0e-50   0.0        32.0      0.10      32.0      0.95      12.0
40.0      40.0       0.08688   -0.1118   -0.9042   0.9068


FELT                 0.005
90.0      1000.0     3.0       0.1       0.054     0.162
1.35e-10  1.35e-10   0.2121    0.719     0.149     0.212     0.719     0.149
1.0e-50   0.0        0.3       0.3       10.6      1         1
20        1          1         1         1         1


FIBGLASS             0.0127
52.0      964.0      3.0       0.036     0.016     0.048
1.46e-10  1.46e-10   0.01295   0.6680    9.252e-02 0.01294   0.6680    9.252e-02
1.0e-50   0.0        19.0      0.2       19.0      1         1
1         1          1         1         1         1


GYPSUM               0.012
950.0     820.0      7.0       0.16      0.57      1.71
2.10e-11  1.05e-10   0.0881    0.943     0.105     0.0397    0.917     0.203
1.0e-50   0.0        0.1       0.2       0.79      1         1
1         1          1         1         1         1
```

```
GLSWOOL              0.10
50.0      800.0      3.0        0.036      0.03       0.09
1.35e-10  1.35e-10   0.140      0.318      5.11e-04   0.0545     0.211      5.48e-04
1.0e-50   0.0        19.0       0.2        19.0       1          1
20        1          1          1          1          1


HDM150               0.001
500.0     1000.0     3.0        0.1        0.3        0.9
1.40e-14  2.00e-13   0.0951     1.56       0.751      0.095      1.56       0.751
1.0e-50   0.0        1.9        1.00       1.90       0.95       12.0
40.0      40.0       0.08688    -0.1118    -0.9042    0.9068
```
Vapor permeability for Hygro Diode based on thickness 0.001 m. Z_{wet}=5 GPam^{2}s/kg
```
PIR                  0.05
30.0      1300.0     5.0        0.032      0.018      0.054
3.10e-12  3.10e-12   0.0802     0.617      0.280      0.0532     0.132      0.0439
1.0e-50   0.0        16.7       3.0        16.7       1          1
20        1          1          1          1          1


PLYWOOD              0.0125
600.0     2500.0     7.0        0.14       0.17       0.21
2.50e-12  1.00e-11   0.3247     0.6849     0.2193     0.2802     0.5889     0.1509
1.42e-14  1.24       0.35       0.45       2.35       13.0       14.5
9.61      0.696      0.303041   -2.8e+45   -38.7739   -2.39527


PSTYR                0.05
30.0      1000.0     5.0        0.030      0.018      0.054
8.80e-12  8.80e-12   0.09976    0.2068     0.01104    0.05848    0.09434    0.004770
1.0e-30   0.0        16.7       3.00       16.7       0.95       12.0
40.0      40.0       0.08688    -0.1118    -0.9042    0.9068


PUR                  0.05
20.0      1400.0     5.0        0.030      0.004      0.054
5.00e-12  5.00e-12   0.09976    0.2068     0.01104    0.05848    0.09434    0.004770
1.0e-50   0.0        32.0       0.10       32.0       0.95       12.0
40.0      40.0       0.08688    -0.1118    -0.9042    0.9068


ROCKHARD             0.1
80.0      800.0      3.0        0.04       0.048      0.144
1.35e-10  1.35e-10   0.0442     0.290      5.58e-04   0.0273     0.113      5.91e-07
1.0e-50   0.0        12.0       0.10       12.0       0.95       12.0
40.0      40.0       0.08688    -0.1118    -0.9042    0.9068


ROCKWOOL             0.1
30.0      800.0      3.0        0.036      0.018      0.054
1.35e-10  1.35e-10   0.0442     0.290      5.58e-04   0.0273     0.113      5.91e-07
1.0e-50   0.0        32.0       0.1        32.0       0.95       12.0
40.0      40.0       0.08688    -0.1118    -0.9042    0.9068


ROOFMATE             0.025
40.0      1000.0     5.0        0.030      0.024      0.072
2.10e-12  2.10e-12   0.0802     0.617      0.280      0.0532     0.132      0.0439
1.0e-50   0.0        12.5       1.0        12.5       1          1
20        1          1          1          1          1
```

```
SARNAFIL            0.003
1000.0    1000.0    3.0       0.20      0.6       1.8
4.00e-14  4.00e-14  0.01141   8.33      7.21      0.0114    8.33      7.21
1.0e-50   0.0       0.03      0.02      0.03      1         1
1         1         1         1         1         1
Vapor permeability for Sarnafil based on thickness 0.003 m.


SINGLPLY            0.003
1000.0    1000.0    3.0       0.20      0.6       1.8
4.00e-14  4.00e-14  0.01141   8.33      7.21      0.0114    8.33      7.21
1.0e-50   0.0       0.03      0.02      0.03      1         1
1         1         1         1         1         1
Vapor permeabilty for single ply based on thickness 0.003 m.


STEEL               0.002
7850.0    540.0     3.0       68.0      10.0      10.0
1.0e-20   1.0e-20   0.000011  1.0       1.0       0.00001   1.0       1.0
1.0e-50   0.0       0.00001   0.00001   0.00001   1         1
1         1         1         1         1         1


WOOD                0.0125
450.0     2500.0    7.0       0.12      0.17      0.21
1.50e-12  1.50e-11  0.310     0.725     0.267     0.317     0.485     0.0720
1.0e-50   0.0       0.35      0.75      1.25      1         1
2         1         1         1         1         1


WOODFB              0.0125
274.0     1300.0    4.0       0.055     0.17      0.21
3.29e-11  3.29e-11  1.12      0.493     0.0058    0.485     0.457     0.0171
1.0e-50   0.0       0.35      0.75      1.25      1         1
2         1         1         1         1         1


WOODCONC            0.025
350.0     1500.0    7.0       0.09      0.21      0.63
2.50e-11  5.00e-11  0.2771    0.99      0.371     0.277     0.99      0.371
1.0e-50   0.0       0.5       0.75      2.7       1         1
3         1         1         1         1         1


WOOD-IN             0.0125
696.0     2500.0    7.0       0.17      0.17      0.21
6.50e-13  6.55e-12  0.310     0.725     0.267     0.317     0.485     0.0720
1.0e-50   0.0       0.35      0.75      1.25      1         1
2         1         1         1         1         1


WOOD-OUT            0.0125
696.0     2500.0    7.0       0.17      0.17      0.21
3.20e-12  3.20e-12  0.310     0.725     0.267     0.317     0.485     0.0720
1.0e-50   0.0       0.35      0.75      1.25      1         1
2         1         1         1         1         1
```